DOE/PC/92550--T2

EVALUATION OF HYPERBARIC FILTRATION FOR FINE COAL DEWATERING

Final Report

DOE Grant No. DE-FG22-92PC92520

By

B.K. Parekh (PI)
University of Kentucky

R. Hogg (Co-PI)
The Pennsylvania State University

A. Fonseca (Co-PI)
CONSOL Inc.

Submitted to

U.S. Department of Energy
Pittsburgh Energy Technology Center
P.O. Box 10940
Pittsburgh, PA 15236

15 August 1996

DISCLAIMER

LEGAL NOTICE

THIS REPORT WAS PREPARED BY THE UNIVERSITY OF KENTUCKY CENTER FOR APPLIED ENERGY RESEARCH AS AN ACCOUNT OF WORK SPONSORED BY THE PITTSBURGH ENERGY TECHNOLOGY CENTER. NEITHER THE UNIVERSITY OF KENTUCKY NOR ANY PERSON ACTING ON ITS BEHALF:

(A) MAKES ANY WARRANTY, EXPRESSED OR IMPLIED, WITH RESPECT TO THE USE OF ANY INFORMATION, APPARATUS, METHOD, OR PROCESS DISCLOSED IN THIS REPORT OR THAT SUCH USE MAY NOT INFRINGE PRIVATELY OWNED RIGHTS; OR

(B) ASSUMES ANY LIABILITIES WITH RESPECT TO THE USE OF, OR FOR THE DAMAGES RESULTING FROM THE USE OF, ANY INFORMATION, APPARATUS, METHOD, OR PROCESS DISCLOSED IN THIS REPORT.

TABLE OF CONTENTS

LIST OF TABLES

LIST OF FIGURES

ACKNOWLEDGEMENT

The authors would like to acknowledge assistance of the following personnel; without their help, it would have been difficult to complete the project in time.

University of Kentucky: J.W. Leonard, J.G. Groppo, D.J. Sung, X.H. Wang, J. Yang, J. Wiseman and D. McLean.

Pennsylvania State University: S. Ranjan

CONSOL Inc.: R. Kosky and G. Meenan

Andritz Ruthner Inc.: G. Evans, J. Hughes, H. Riemer and G. Hähling

The guidance and assistance provided by the project monitor, Ms. Patricia Rawls and funding by U.S. DOE under Grant No. DE-FG22-92PC92550 is acknowledged.

EXECUTIVE SUMMARY

This report describes the work performed under the U.S. Department of Energy University Coal Research Program Contract No. DE-FG22-92PC92550. This was the first university-industry joint collaboration project funded by the USDOE under the University Coal Research (UCR) program. The University of Kentucky's Center for Applied Energy Research along with The Pennsylvania State University and CONSOL Inc. participated in the program. In addition, Andritz Ruthner Inc. provided and operated the hyperbaric filter pilot plant unit under a sub-contract to CONSOL Inc. The research program was cost shared by all the participants.

Program Objectives and Major Tasks

The main objectives of the project are to investigate the fundamental aspects of particle-liquid interaction in fine coal dewatering, to conduct laboratory and pilot plant studies on the applicability of hyperbaric filter systems and to develop process conditions for dewatering of fine clean coal to less than 20 percent moisture.

The program consisted of three tasks, namely, Task 1 - Model Development, Task 2 - Laboratory Dewatering Studies, and Task 3 - Pilot Plant Testing. The Pennsylvania State University led the efforts in Task 1, the University of Kentucky in Task 2, and CONSOL Inc. in Task 3 of the program. All three organizations were involved in all the three tasks of the program. The Pennsylvania State University developed a theoretical model for the hyperbaric filtration systems, whereas the University of Kentucky Center for Applied Energy Research conducted laboratory experiments to identify the best operating conditions of the high pressure filter in fine clean coal dewatering. The best conditions identified in Task 1 and Task 2 were

then tested at two of the CONSOL Inc. preparation plants using an Andritz Ruthner portable hyperbaric filtration unit.

Results

Generalized models for continuous hyperbaric filtration have been developed using the classical model for constant pressure filtration as a starting point. Specific models have been developed and evaluated for:

- cake formation and filter capacity
- cake dewatering: residual saturation and air consumption

Emphasis has been placed on the role of cake structure in the filtration process. Since detailed analysis of cake structure is only possible *post priori*, and by no means simple even then, we have concentrated primarily on the use of simplified structure models in which the pore structure in the cake is predicted from a knowledge of the characteristics of the feed particles.

It has been shown that the simplest structure model, in which pores are treated as a set of uniform capillaries with a single effective circular radius, cannot uniquely represent a pore size distribution. The distribution of pore sizes has a dominant effect on fluid (water or air) flow through the cake and on residual moisture content. Pore shape is also important but its effects appear to be less significant than those of size distribution. Our evaluation of shape effects suggest that it is probably reasonable, in most cases, to combine size and shape effects into a single distribution of effective pore radii.

Materials such as clean coal do not generally form compressible filter cakes, yet measured flow resistances show some attributes (e.g., pressure effects) of compressible cakes. We have proposed a binary packing model in which the finest particles in the ~~feed~~ (which

may often be subject to agglomeration) form an inner, open-structured and potentially compressible layer within the main cake structure. Pressure effects and the role of flocculants, etc., can be ascribed to modifications of this layer.

While the major objective of this research program has been to investigate mechanical dewatering by hyperbaric filtration, the possible role of evaporation has also been evaluated. Based on a simplified model for evaporative dewatering, it has been concluded that this mechanism probably plays a negligible role under normal (i.e., ambient temperature) conditions. It could, however, be a principal mechanism at elevated temperatures, e.g., in steam filtration.

The laboratory dewatering studies indicated that for Illinois No. 6 clean coal slurry containing coarse particles (50 weight percent more than 100 mesh or 150 micron), vacuum filtration provided 24.8 percent moisture filter cake, whereas use of high pressure (4 bar or 60 psi) filter provided 21.8 percent filter cake moisture. Addition of an anionic flocculant (115 g/t) or a cationic surfactant (1.5 Kg/t) provided 17 percent filter cake moisture using the high pressure filtration. It was observed that to obtain meaningful dewatering data for commercial application, the slurry should be stirred during filtration cycle, which provides uniform distribution of particles. A modified filteration cell was developed which provided continuous agitation of slurry during filtration cycle.

For the ultra-fine size (40 weight percent finer than 500 mesh or 25 micron) Pittsburgh No. 8 clean coal slurry, it was difficult to dewater the slurry using vacuum filter. Hyperbaric filter provided 24.5 percent using 4 bar (60 psi) pressure. Use of non-ionic surfactant (500 g/t) lowered the filter cake moisture to 17.5 percent. Split size filtration using 500 mesh (25 micron) cut point and filtering the plus 500 mesh and minus 500 mesh -

separately and then combining provided 15.9 percent filter cake moisture. Addition of 100 g/t of Al^{+3} ions lowered filter cake moisture to 19.5 percent. Heating the slurry to 80°C lowered the moisture content to 15 percent. Using a combination of split size, a modified filtration support system and using a non-ionic flocculant (60 g/t) provided a 10.5 percent moisture product compared to 24.5 percent obtained using baseline operating conditions. This represents about 60 percent reduction in moisture content of the filter cake.

The Pocahontas No. 3 flotation product contained about 26 weight percent minus 325 mesh (44 microns) material. Vacuum filtration provided a 24 percent moisture filter cake, whereas high pressure (6 bar or 80 psi) filtration provided 11 percent moisture filter cake. Addition of non-ionic surfactant (800 g/t) or flocculant (50 g/t) lowered the filter cake moisture to 7.4 percent. A combination of split size filtration and anionic flocculant (50 g/t) using the modified filtration support system provided 4.85 percent filter cake moisture which was about 56 percent moisture reduction improvement over the baseline data. Addition of metal ion alone or with surfactant did not provide any significant reduction in the filter cake moisture.

For the pilot plant testing, two types of feed material produced at the mine processing Pittsburgh No. 8 coal were used. The currently produced filter feed, which consisted of froth flotation product and classifying cyclone underflow and the second feed material was flotation product alone. Table A, given below, summarizes the test results on both the Pittsburgh No. 8 material.

The dewatered product obtained with the filter feed was about 4 to 7 percent lower in absolute moisture content than currently obtained using 23 percent moisture vacuum filter.

Table A. Summary of Pilot Scale Hyperbaric Filter Test Results for the Pittsburgh No. 8 Clean Coal Slurries.

Material	Filter Cake Moisture %	Solids Throughput lb/ft^2-h	Solids Throughput Kg/m^2-h	Air Consumption cfm/t	Air Consumption Nm^3/t	Applied Pressure bar	Applied Pressure psi
Filter Feed	16-19	4-13	20-61	60-200	112-376	3.5	50.7
Flotation Product	21-25	4-6	20-30	100-250	188-470	3.5	50.7
Classified Flotation Product	21-25	5-6.6	26-32	100-150	188-280	3.5	50.7

For the flotation product the moisture content of the filter cake obtained with the hyperbaric filter was 21 to 25 percent, which is significant, as this product can not be filtered by vacuum filter. Addition of 800 g/t of a cationic surfactant lowered filter cake moisture from 24 to 21 percent. Classifying (desliming) the flotation product did not improve its dewatering.

The pilot scale data obtained with the Pocahontas No. 3 flotation product are summarized in Table B given below.

The hyperbaric filter was effective for the Pocahontas No. 3 coal in lowering the moisture of the filter by 6 to 10 percent absolute over the 23 percent moisture currently obtained at the plant using the vacuum filter. Addition of a cationic surfactant (380 g/t) lowered filter cake moisture from the 13.4 to 12.4 percent. Classifying the flotation product did not improve dewatering of the classified product.

Table B. Summary of Pilot Scale Hyperbaric Filter Test Results for the Pocahontas No. 3 Flotation Product.

Material	Filter Cake Moisture %	Solids Throughput		Air Consumption		Applied Pressure	
		lb/ft^2-h	Kg/m^2-h	cfm/t	Nm^3/t	bar	psi
Flotation Product	13-17	7-17	31-82	40-80	21-42	5	72.5
Classified Flotation Product	12-14	7-17	31-82	30-100	16-53	5	72.5

In summary, the hyperbaric filter provided 50 to 70 percent reduction in moisture content of filter cake compared to that obtained with the vacuum filtration. The applied pressure and cake formation angle are the most important parameters to control filter cake moisture. Addition of flocculants was detrimental to the filter cake moisture. However, addition of a cationic surfactant was effective in lowering the filter cake moisture by about 10 percent.

Recommendations

Based on the pilot scale test data, it is recommended that the Andritz Hyperbaric Unit should be tested on a continuous basis (7 to 15 days) at a plant to evaluate its effectiveness and obtain economic (operating) data. The coarse material required lower air consumption than fine size material; an attempt should be made to understand this unusual behavior of the hyperbaric filter. Tests should also be conducted using the column flotation product.

INTRODUCTION

For the United States of America, it is forecasted that coal will constitute a principal source of energy for the next several decades. A typical coal preparation plant produces about 20 percent of the mined coal as minus 0.5 mm (28 mesh). Generally, this fine fraction is discarded due to its high cost of processing. However, with the development of advanced coal cleaning technology, such as column flotation, cleaning of fine size coal to low ash and low pyritic sulfur is feasible at high recovery. One of the biggest hurdles in utilization of fine coal cleaning technology by the coal industry is the economic dewatering of the fine clean coal product. Until an economical and practical solution to dewatering of fine clean coal is achieved, the efforts put in developing fine clean coal technology will be wasted.

Most of the coal cleaning preparation plants utilizes water-based processes. In the U.S.A., about 40 percent of mined coal is cleaned. Water, while being the mainstay of coal washing, is also one of the least desirable components in the final product. Coarse coal (+3/4") is easily dewatered to a 3-5 percent moisture level using conventional vibrating screens and centrifuges. The degree of difficulty associated with dewatering increases as the particle size decreases or the surface area of particles to be dewatered increases. Aqueous suspension of particles finer than 0.5 mm are the most difficult to dewater. Even though in a coal preparation plant the fines (<0.5 mm) may constitute about 20 percent of plant feed, the high surface moisture retained by the fines offsets many of the benefits of coal cleaning and can seriously undercut utilization of advanced coal cleaning technologies which can provide an ultra-clean coal.

Even a one-percent increase in clean coal moisture can result in significant increase in transportation costs. A power plant using 3.0 million tpy of coal from a plant located 250 miles away might spend about $350,000 per year to transport the additional one percent moisture.[1] This situation clearly identifies the need for advanced dewatering technology and such technology could result in significant cost savings for the coal-using industry.

The degree of difficulty associated with dewatering increases as the particle size decreases or the surface area of particles to be dewatered increases. For particles larger than 0.5 mm (28 mesh) size no particular dewatering problem is encountered. These large size particles are usually dewatering using vibrating screens and centrifuge techniques. Particles finer than 0.5 mm are the most difficult to dewater. A wide variety of equipment such as solid bowl centrifuge, screen bowl centrifuge and vacuum disk are used for fine particles dewatering. However, moisture content in the final product is unacceptable. Moisture content of the fine coal could be lowered using thermal dryer. However, high operating cost as well as air pollution and fire hazard associated with fine coal makes thermal drying very unattractive.

Generally, water is removed from coal by mechanical or thermal methods. The thermal method, though efficient, is less desirable because of high energy consumption and associated emission concerns. The mechanical method includes sedimentation and filtration techniques. The sedimentation process involves the separation of solids and water using the force of gravity, for example; a thickener where fine solids are flocculated to increase the sizes of particles which settle, leaving clear water at the top.

Filtration is the most common method used for dewatering fine coal (minus 28 mesh) slurries. Vacuum and hyperbaric (pressure) filtration techniques are generally utilized. Currently, most coal preparation plants utilize vacuum filtration technology for dewatering fine clean coal, providing a dewatered product containing about 25 to 30 percent moisture. However, hyperbaric filtration can produce a 4 to 10 percent lower cake moisture with higher throughput. While the hyperbaric filter is becoming popular in Europe, no such filters have been installed in the U.S. coal industry.

It is common practice to dewater fine coal slurries using vacuum filtration followed by thermal drying to meet the final product moisture specifications. Because of its ability to produce a lower moisture product, the hyperbaric filtration has a potential to replace the thermal drying. The cost savings, due to replacement of vacuum filter-thermal drier systems with hyperbaric filters, would be approximately $1 to $2 per ton of dry solids.

This research has been undertaken to understand and optimize fundamentals parameters for fine coal dewatering using high pressure filtration and also to test the optimized parameters on a pilot scale at two of the CONSOL Inc. preparation plants.

OBJECTIVES AND SCOPE OF WORK

The main objectives of the project were to investigate the fundamental aspects of particle-liquid interaction in fine coal dewatering, to conduct laboratory and pilot plant studies on the applicability of hyperbaric filter systems and to develop process conditions for dewatering of fine clean coal to less than 20 percent moisture.

The program consisted of three phases, namely

Phase I - Model Development

Phase II - Laboratory Studies

Phase III - Pilot Plant Testing

The Pennsylvania State University led efforts in Phase I, the University of Kentucky in Phase II, and CONSOL Inc. in Phase III of the program. All three organizations were involved in all the three phases of the program. The Pennsylvania State University developed a theoretical model for hyperbaric filtration systems, whereas the University of Kentucky conducted experimental studies to investigate fundamental aspects of particle-liquid interaction and application of high pressure filter in fine coal dewatering. The optimum filtration conditions identified in Phase I and II were tested in two of the CONSOL Inc. coal preparation plants using an Andritz Ruthner portable hyperbaric filtration unit.

BACKGROUND

Although the term "dewatering" refers to removal of water, researchers have used different terms and descriptions to define water associated with particles. Tschamler and Ruiten[2] classified five types of water associated with coal, including interior adsorption, surface adsorption, capillary, interparticle and adhesion water. The last three types of water are termed as "free" water and are potentially removable by mechanical techniques. However, the first two types of water, known as "inherent" moisture, can only be removed by energy-intensive techniques such as thermal drying.

A variety of techniques are now used in contemporary practice for dewatering coal. The type and efficiency of various dewatering equipment varies as a function of particle size. The degree of difficulty associated with mechanical dewatering increases as the surface area of the particles increases. Particles finer than 0.5 mm (28 mesh) present the greatest

dewatering difficulty. Table I lists the theoretical amount of water present on various size coal particles. Note that 5 to 10 μm particles carry a significant amount of surface moisture.

There has been a rapid increase in research and technology involving developments to improve fine-coal dewatering. Parekh et al.[3] have published a review on fine coal and refuse dewatering which also included new dewatering technologies being developed in dewatering of fine coal. Methods for improving filtration of fine coal can be divided into two groups: those involving equipment modification and those involving process modifications.

Table I. Effect of Particle Size on Amount of Surface Moisture Present on Coal Particles

Particle Size	External Surface Area	Surface Moisture* (wt. %)
2"	0.9	0.009
3/4"	2.4	0.024
28 mesh	90.2	0.90
200 mesh	601	6.18
10 microns	4511	54.7
5 microns	9023	131

*Assuming a 1 micron thick film of water

In equipment modification, Ama pressure filters have been shown to be capable of achieving a low clean coal moisture level.[4] High 'g' centrifuges capable of creating forces up to 2,000 times gravity have been reported to be successful in dewatering a froth flotation product to less than 12-percent moisture.[1] Coal Technology Corp. has developed a super 'g' centrifuge capable of achieving forces up to 4,000 times the force of gravity.[5] Other new

equipment includes The Shoe Rotary Press,[6], membrane pressure filter[7], and electro-acoustic dewatering[8] techniques.

Perhaps a more promising avenue to improved dewatering of fine coal lies in the category of process modifications. The dewatering of fine-coal particles has been shown to be improved through process modifications that involve viscosity reduction, flocculation and surfactant additions.

Enhanced Dewatering

Two important aspects of dewatering fine coal are the dewatering rate and the final moisture content of the product produced; the most desirable conditions would be to have a fast dewatering or filtration rate and a low product moisture. Filtrate clarity is not of primary importance in coal applications because filtrate water and any solids in it are generally recirculated within the dewatering circuit. Theoretical treatment of the dewatering process has concluded that product moisture, or residual moisture as it is sometimes termed, is reduced while the dewatering rate is increased with:

Increasing

- driving force (gravity, vacuum or pressure)
- permeability of the medium (filter cloth and filter cake)
- contact angle or hydrophobicity
- filter area, and

Decreasing

- viscosity of the filtrate
- cake thickness, and
- filtrate surface tension.

When considering these factors, the driving force, medium permeability and filter area will be determined by the dewatering device used. The other parameters are properties of the slurry to be dewatered and can be controlled by the use of chemical additives.

The interconnected voids or pores in filter cakes form irregular capillary tubes. This analogy is frequently used in soil mechanics to describe the pore structure of soils. If one considers the cake structure to simplistically be a bundle of capillary tubes, residual saturation can be related to capillary rise or the level of water within a capillary tube.[9] The capillary rise formula is:

$$h = \frac{2\gamma\cos\theta}{g\rho R}$$

where h is the capillary rise, γ is the liquid/air surface tension, θ is the liquid/solid contact angle, R is the capillary radius, g is the acceleration due to gravity, vacuum or pressure and ρ is the liquid density. The primary mechanisms responsible for the improved dewatering achieved in laboratory studies with the surface modification treatment can be related to reducing the capillary rise.

Effect of Capillary Radius

Maximizing the radii of the capillaries within the filter cake structure can be accomplished in several ways. The most obvious is to blend coarser material to effectively increase the average particle size and reduce the surface area of the solids to be dewatered. While this would decrease the filter cake moisture, the coarser material could be more effectively dewatered with equipment other than filters and the net moisture reduction would be minimal.

Flocculants can be used to increase the effective particle size by agglomerating fines which increases permeability and results in a faster filtration rate. However, during floc formation, water can be entrained within the floc structure which ultimately limits the amount of water that can be removed and results in higher cake moisture. To reduce the floc size, surface chemical modification can be used to induce agglomeration if filtration is conducted at or near the zero point of charge (ZPC).

Effect of Contact Angle

The contact angle, θ, is a measurement of the hydrophobicity of the solid particles to be filtered. The adsorption of surfactants onto solids can increase the contact angle and make the surface more hydrophobic.[10,11] Increasing the contact angle can significantly lower the capillary rise as shown in the capillary rise equation. The extent to which surfactants can increase hydrophobicity is related to their structure. Dewatering efficiency of surfactants has been related to the HLB index, a calculated, dimensionless number related to the hydrophobicity of the surfactant. The HLB (Hydrophile-Lipophile Balance) System was developed by Atlas Chemical Industries in the late 1940's to choose an emulsifier for one or more ingredients. It is determined by quantification of the solubility in oil (low HLB) or water (high HLB) of the ingredients to be blended. With the assigned HLB of the ingredients and the relative amount of each, the HLB of the mixture can be calculated. Although originally conceived as a method to select appropriate emulsifiers, the HLB is frequently used to describe the hydrophobic/hydrophilic properties of surfactants. Better dewatering performance has been obtained with low HLB surfactants (HLB <14) which are more hydrophobic.

Effect of Surface Tension, γ

Numerous studies have shown that surfactants can indeed lower the moisture content of coal filter cake during dewatering. The general mechanism is that surfactants reduce the interfacial tension at the liquid/air interface which reduces capillary retention forces.[12,13] Reduction of interfacial surface tension at the liquid/air interface will lower the capillary rise, hence reducing the moisture contained in the capillaries.

Literature evidence challenges the importance of surface tension in dewatering. Silverblatt and Dahlstrom[15] reported that the moisture content obtained at surface tensions of 72 and 32 dynes per centimeter were essentially equal, however, moisture content was significantly decreased between 32 and 36 dynes per centimeter. The conclusion was that the improvement was due to surface reactions between the coal and the surfactants rather than a change in the liquid/air interfacial tension. Others have also shown that dewatering is more closely related to surfactant adsorption than to surface tension reduction.[10,11,14] Dewatering aids have been developed claiming increased adsorption on solids, and measurements of the filtrate have shown very little decrease in surface tension but significant decrease in cake moisture.[15,16,17]

Gray[18] used flocculants, oil and surfactants and reported that each improved dewatering. The benefit of the oils may have been due to impurities of surface active components in the oils, while evidence of surfactant adsorption onto the coal was reported even though his work assumed that surfactants only lowered the liquid/air interfacial tension. Dolina and Kominski[19] used several surfactants during vacuum filtration and found that the residual moisture content of the filter cake decreased or increased depending on which

surfactant was used. This is not surprising because solution pH and electrolyte content have a significant influence on surfactant adsorption.[20] Nicol[13] reported improvements in dewatering of coal using anionic surfactants while Brooks and Bethell[21] found that a cationic surfactant also improved dewatering. Keller et al.[10] showed that surfactants added during the washing period of the filtration cycle improved dewatering by i) changing the pressure differential required for dewatering and ii) lowering the residual water content of the filter cake. The pressure differential required was correlated with a decrease in surface tension while the residual moisture content was related to surfactant adsorption at the solid/air interface. Cationic, anionic and non-ionic surfactants showed similar effectiveness at different dosages.

The use of surfactants as filtration aids shows potential benefits for lowering cake moisture, particularly in longer filtration cycles. There is contradictory evidence in literature pertaining to the mechanism responsible for this improvement. Some evidence exists for surfactant adsorption increasing the hydrophobicity of the substrate. Additional research suggests that lowering the surface tension at the solid/liquid interface is the primary mechanism. Regardless of the mechanism responsible, removal of "free" or "surface" water is the primary objective and the addition of agglomerating as well as surface tension modifying reagents can indeed reduce the moisture content of fine coal.

Effect of Gravity, g

In the capillary rise formula given above, increased gravitational forces minimize the capillary rise. In filtration processes, for fluid to flow through the medium (filter cake and filter medium), it is necessary that a pressure drop be applied across the medium. The driving

force to achieve the pressure drop can be gravity, vacuum or pressure. Increasing the driving force will increase moisture removal from the capillary network in the filter cake. Gravity filters are not used in the mineral industry, rather a similar principle is employed by high speed centrifuges where forces are several hundred times greater than gravity are generated. Pressure, and much more frequently, vacuum are commonly used as driving forces in the mineral industry. The basic principle remains essentially the same.

Industrial Practice

Vacuum filtration is by far the most commonly practiced dewatering technique in the U.S. coal industry. Vacuum disc filters are generally chosen over rotary drum filters because of the higher capacity. The production rate is approximately 60 to 70 lb/hr/ft^2 for clean coal and 20 to 30 lb/hr/ft^2 for coal refuse.

Centrifuges are also used for dewatering minus 0.5 mm (28 mesh) coal and refuse. The centrifuges are mounted horizontally and a high speed of rotation forces a particle bed to form at the centrifuge wall so that most of the water can be decanted. For a screen bowl centrifuge, the solids are then conveyed to a chamber where the walls are perforated and further dewatering takes place through the walls. For a solid bowl centrifuge, the solids are advanced to the discharge point by a scroll-conveyor and additional water drains back into the decantation zone. Screen bowl centrifuges have a much higher throughput, however solid bowls produce a lower moisture product for capacities of 2 to 30 tons per hour.

Pressure filtration is widely practiced in Europe and has been attempted at several preparation plants in the U.S. Most applications are for refuse dewatering, although some clean coal applications have been reported. Plate and frame filters are the most common and

employ high pressure to force water through a filter medium while retaining the solids as a cake. While pressure filters produce very dry cakes, their application in the coal industry is limited because it is a batch process. To dewater slurry continuously requires two filters and/or a surge tank which significantly increases capital costs. Continuous pressure filtration devices such as hyperbaric have recently been developed but have not been used use in the U.S. coal industry. Several European installations report low moisture and high throughput for fine coal applications. The Andritz-Ruthner Hyperbaric Filter (HBF) is one example and consists of a high specification vacuum disc filter installed in a pressure vessel and applies dewatering pressures up to 90 psi. Commercial units vary in size from 260 to 1300 ft^2 of filter area and under plant operating conditions with fine coal has produced 17.9 percent moisture versus 25.7 percent on a vacuum filter at Ruhrkohr mines in Germany.[22]

Several other dewatering devices such as the belt filter press or vacuum belt filter press are also used, but their primary application is for refuse dewatering. Despite relatively high capacities, high chemical consumption and high product moisture limit their use.

Dewatering of ultrafine clean coal ($D_{50} \sim 25$ μm) produced in advanced flotation technology are difficult to dewater to a low (less than 20 percent) moisture due to large surface area. Table II list dewatering test data obtained on a column flotation product using various types of equipment.[3] Note, that only pressure filters were able to provide a low moisture product.

In-Situ Dewatering/Hardening

Recently, Wen et al.[23] have investigated an in-situ cake hardening process for fine coal slurry. They reported that addition of 2 to 8 percent of asphalt emulsion lowered the

moisture as well as reduce the dust formation. Wilson et al.[24] have reported success in a single stage dewatering and briquetting process in which oriemulsion is used as dewatering and binding agent.

In summary, there is an immediate need to reduce the moisture content of fine coal filter cakes to about or below 20 percent level. Treatment of coal slurry prior to filtration by flocculant and surfactant can provide some benefits but may not be cost effective. The use of steam can be effective in dewatering but may not be economical. High pressure dewatering of coal may be effective in lowering filter cake moisture of the fine coal slurry. However,

Table II. Dewatering Test Data on Clean Coal Slurry Using Various Types of Equipment

Equipment	Rate	Moisture %
Vacuum Disc Filter	4.9 lb/hr/ft^2	25
Horizontal Belt Vacuum Filter	15 lb/hr/ft^2	25
Belt Press Filter	2.8 tph/m	40
Belt Press Filter*	10 tph	30
Belt Press Filter*	20 tph	38
Plate and Frame Pressure Filter	-	22.7
Ama Filter (Continuous Pressure Filter)	21 tph	21.0

*Organic polymeric flocculant used

systematic research on the optimization of the process and pilot scale studies have not been conducted. This project report emphasizes the hyperbaric filtration of fine coal.

RESULTS AND DISCUSSION

This project was divided into three tasks. Details on results and discussion of each phase is given below.

Task I - Model Development:

Hyperbaric filtration for the dewatering of fine coal is a complex process involving numerous material and system variables. The objectives of the modeling phase of this research program have been to provide a realistic framework for the analysis of laboratory and pilot-scale experimental data and to develop procedures which can be used for mathematical simulation of industrial-scale, hyperbaric filtration systems. Existing models, developed primarily for vacuum filtration, have provided a useful starting point for the modeling effort. Since hyperbaric filtration is, in effect, a simple extension of vacuum filtration, involving the same physical processes, the existing models should be generally valid. Extrapolation of "typical" results, however, may be suspect. These models are also somewhat limited, especially with regard to the role of feed characteristics (size distribution, etc.). As a consequence, while they are useful for data evaluation and for system design and scale-up, they generally lack predictive capability.

The typical filter cycle involves three stages:

- cake formation, characterized by particle deposition and single-phase flow of water through the cake
- initial dewatering in which there is two-phase flow of air and water
- final dewatering where flow is again primarily single-phase (air)

Cake structure plays a critical role in each of the above stages in the process as well as in the limiting residual cake saturation (final moisture content) which can be achieved by pressure filtration. Water and air flowrates which, respectively, determine filter capacity (throughput) and air consumption both depend on cake structure. For incompressible cakes, the physical arrangement of particles does not change significantly

during the filter cycle and should be essentially the same in each of the stages indicated above. However, there can be very substantial changes in pore structure. During cake formation, the entire pore network is available for fluid while, in final dewatering, residual saturation reduces effective porosity and also changes effective pore geometry.

In the classical treatment of cake filtration the effects of cake structure are accounted for using a macroscopic characteristic known as the specific cake resistance (25). Theories of flow through porous media can be used to relate the specific cake resistance to structural characteristics of the pore system such as the effective pore size distribution and overall porosity. However, characterization of pore structures in packed beds is a difficult undertaking and the relationships between pore structure and particle characteristics such as size distribution are not generally known. As a consequence, reliable procedures for predicting the effects on filter performance of changes in feed characteristics have not been established.

In this study, emphasis has been placed on the role of cake/pore structure in the different stages of pressure filtration as applied to fine coal dewatering.

CAKE FORMATION

Filtration Kinetics

In cake filtration, slurry is forced through a membrane - the filter medium, typically cloth or paper - which retains the particles forming a filter cake. The liquid passes through the medium and the cake into the filtrate. This is the stage in the process when filtration actually occurs. Analysis of the process is based on the assumption that flow through the medium and the cake can be described using a form of Darcy's law:

$$\frac{Q_w}{A}=\frac{K}{\mu_w}\frac{dp}{dz} \tag{1}$$

where Q_w is the volumetric flow rate through area A, μ_w is the liquid viscosity, dp/dz is the applied pressure gradient and K is the permeability. Combined with a mass balance on the solids and liquid, Equation 1 can be used to derive the classical filtration rate expression:

$$\frac{t}{V_w}=\frac{\mu_w}{A\Delta p}\left(\frac{\overline{\alpha} c_v V_w}{2A}+\alpha_m\right) \tag{2}$$

where V_w is the volume of liquid flowing in time t across area A with an applied pressure drop Δp. c_v is the concentration of solids in the slurry (mass of solid per unit volume of liquid). $\overline{\alpha}$ is the average specific cake resistance given by

$$\overline{\alpha}=\frac{1}{\overline{K}\overline{\rho}_b} \tag{3}$$

where $\overline{K}$ is the average cake permeability and $\overline{\rho}_b$ is the average cake bulk density. α_m is the filter medium resistance such that

$$\alpha_m=\frac{\lambda_m}{K_m} \tag{4}$$

where λ_m is the medium thickness and K_m is its permeability.

Examples of the application of Equation 2 to the filtration of fine (-100 mesh) coal from the Pittsburgh seam are given in Figures 1 and 2. Generally consistent agreement can be seen; both α and α_m increase slightly with increasing applied pressure.

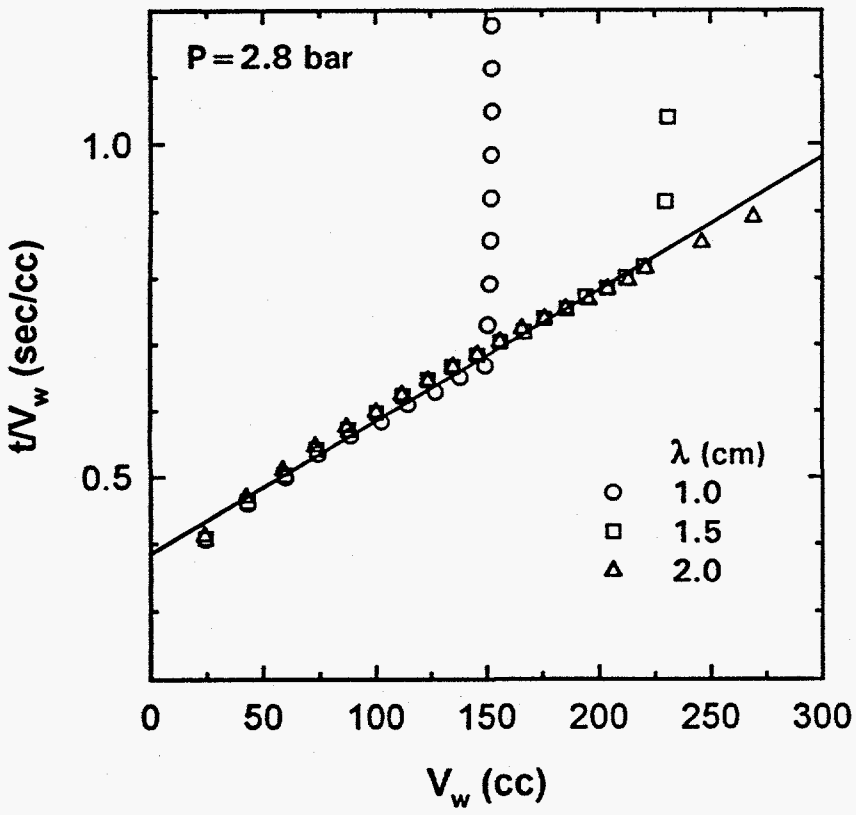

Figure 1. Cake formation kinetics for Pittsburgh seam coal at 2.8 bar (40 psi).

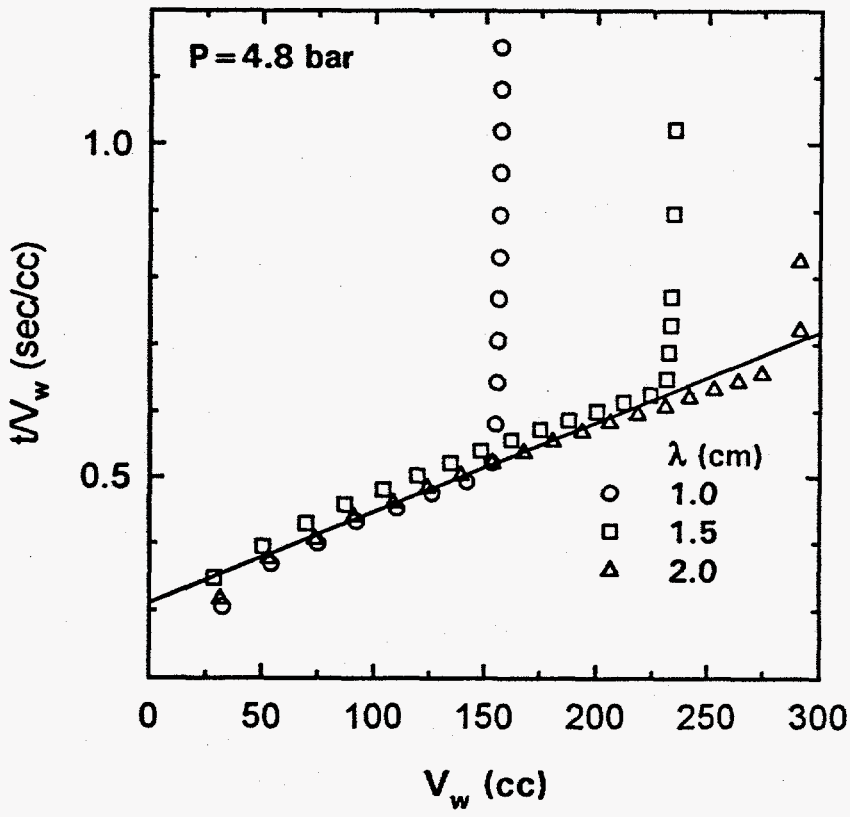

Figure 2. Cake formation kinetics for Pittsburgh seam coal at 4.8 bar (70 psi).

Cake Structure and filtration rate

In the filtration rate expression given by Equation 2, the characteristics of the feed solids are lumped into a single parameter, the specific cake resistance $\bar{\alpha}$, which must be determined empirically. An important objective of the research conducted under this grant has been to establish relationships between cake resistance, cake structure and, ultimately, feed solids characteristics.

Uniform pore model

One approach to the correlation of cake permeability with cake structure involves the application of the well-known Carman-Kozeny model for flow through porous media. In this treatment, a porous bed is regarded as a bundle of similar capillaries, each with an effective mean hydraulic radius r_h. The latter is defined, in the usual way as

$$r_h = \frac{2\ (\text{pore cross}-\text{sectional area})}{\text{pore perimeter}} \qquad (5)$$

Assuming that any cross-section of the bed is a two-dimensional representation of the overall bed, the pore area can be represented by the total pore volume and the perimeter by the pore surface area. For point contacts between particles in the bed, the total pore surface area is equal to the particle surface area. In this way, the mean hydraulic radius can be estimated from

$$r_h = \frac{2\,\varepsilon}{S_V(1-\varepsilon)} \qquad (6)$$

where ε is the average bed porosity and S_V is the volume specific surface area of the solids in the bed.

Flow in the individual pores is assumed to be laminar and the mean flow velocity in each can be described by Poiseuille's equation:

$$\overline{v}=\frac{\Delta p r_h^2}{8\mu_w \lambda_e} \tag{7}$$

with the effective pore radius given by Equation 6, and the effective pore length λ_e related to the bed thickness through a tortuosity factor. By combining Equations 6 and 7, one arrives at the Carman-Kozeny equation for the overall flowrate per unit area of bed. Thus,

$$\frac{Q_w}{A}=k_t \frac{\varepsilon^3}{(1-\varepsilon)^2}\frac{\Delta p}{\mu_w \lambda S_v^2} \tag{8}$$

in which k_t is the tortuosity factor.

The use of Equation 8 in place of Equation 1 leads to a more explicit expression for the specific cake resistance, i.e.,

$$\overline{\alpha}=\frac{(1-\varepsilon)S_V^2}{k_t \varepsilon^3 \rho_s} \tag{9}$$

where ρ_s is the density of the solid particles. Equation 9 provides a link between cake resistance and filter feed characteristics - as expressed by the specific surface area S_V. Since, for materials such as fine coal, cake porosities vary only over a relatively narrow range, typically between about 0.4 and 0.6, Equation 9 offers some predictive capability.

Effect of pore size distribution

The Carman-Kozeny model involves some implicit assumptions which impact on its value as a descriptor/predictor of filter performance. In particular, it is implied that:

- pores consist of discrete, uniform channels
- each pore has the same effective radius
- the effects of non-circular shape can be properly accounted for through the use of the mean hydraulic radius.

It is instructive to evaluate the consequences of each of these simplifications in more detail.

Obviously, the pores in a packed bed of particles such as a filter cake are not a set of identifiable, discrete, parallel channels. In reality, they form a continuous, highly connected, three-dimensional network whose cross-section varies widely in all directions. However, if the cake is relatively uniform in structure, such that any plane parallel to the filter medium is representative of the whole cake, the system can be treated as one of flow through a series of parallel thin sheets, each of which contains a set of discrete channels oriented perpendicular to the sheet. Each of the sheets would present the same resistance to flow and the interconnection between channels should compensate for misalignment of the channels in adjacent sheets. Thus, the representation by parallel channels should be mathematically equivalent to the actual pore system.

Even in a bed of uniform particles, a range of effective pore diameters can be expected. A broad range of particle sizes, as typically found in fine coal filter feeds, might be expected to be accompanied by a similarly wide range of pore sizes. To some extent, this might be offset by the pore-filling effect of fines but, at the same time, it could be enhanced due to non-uniform packing and by channeling during flow through the cake.

The effects of pore size distribution can be evaluated by comparing the relative flow rate through a single pore with that through a system of pores with the same overall mean hydraulic radius and the same total volume. Considering the simple case of parallel cylindrical pores of fixed length and a number distribution of radii $f_o(r)$, the total pore volume per unit length is

$$V_p = \pi N_p \int_{r_{min}}^{r_{max}} r^2 f_o(r) dr \tag{10}$$

where N_p is the total number of pores which would be equivalent to a single pore of radius r_h. For the latter,

$$V_p = \pi r_h^2 \tag{11}$$

so that, for the same volume in both cases

$$r_h^2 = N_p \int_{r_{min}}^{r_{max}} r^2 f_o(r) dr \tag{12}$$

In order that the distributed pore system have the same overall mean hydraulic radius, its total surface area must also be the same. Thus, per unit length

$$\pi r_h = \pi N_p \int_{r_{min}}^{r_{max}} r f_o(r) dr \tag{13}$$

It follows from Equations 12 and 13 that

$$r_h = \frac{\int_{r_{min}}^{r_{max}} r^2 f_o(r) dr}{\int_{r_{min}}^{r_{max}} r f_o(r) dr} \tag{14}$$

For laminar flow through a pore of radius r_h Poiseuille's equation states that

$$Q_s = Q_o r_h^4 \tag{15}$$

where Q_s is the volumetric flowrate through a single pore of radius r_h, and Q_o is the flowrate for a pore of unit radius. The total flowrate through the distributed pore system is

$$Q_d = Q_o N_p \int_{r_{min}}^{r_{max}} r^4 f_o(r) dr \tag{16}$$

By combining Equations 12, 14, 15, and 16, the relative flowrate can be expressed as

$$Q_{rel} = \frac{Q_d}{Q_s} = \frac{[\int_{r_{min}}^{r_{max}} r\, f_o(r)dr]^2 \int_{r_{min}}^{r_{max}} r^4 f_o(r)dr}{[\int_{r_{min}}^{r_{max}} r^2 f_o(r)dr]^3} \qquad (17)$$

The comparison can also be expressed as a relative "flow" resistance (equivalent to the specific cake resistance) α_{rel}. From the definition of α, it follows that

$$\alpha_{rel} = 1 / Q_{rel} \qquad (18)$$

The magnitude of the effect of pore size distribution can be seen by applying a specific functional form for $f_o(r)$ in Equation 17. An example, using the log normal distribution, is given in Table III. For this case, it can be shown that Equations 17 and 18 reduce to

$$\alpha_{rel} = e^{-3\ln^2\sigma} \qquad (19)$$

where σ is the log normal standard deviation. It can be seen that as the width of the distribution increases (increasing standard deviation, σ) the relative resistance decreases.

Table III. Illustration of the effect of (log normal) pore size distribution on relative flow resistance.

Standard Deviation, σ	1.0	1.5	2.0	3.0
Relative Resistance, α_{rel}	1.00	0.61	0.24	0.03

The effect becomes very significant for broad pore size distributions. For σ=3, the resistance is reduced to less than 3% of the value for uniform pores. It should be noted, however, that the result is especially sensitive to the presence of a few large pores; changes at the fine end of the distribution lead to less dramatic effects. At the same time,

it is clear that the existence of a distribution of pore sizes generally leads to lower resistance to flow.

Effect of pore shape

The role of pore shape is obviously important. Pores in a packed bed of particles are never circular in section and rarely even approach a circular form. An analysis of laminar flow through non-circular pores consisting of "arched triangles" has been presented by Klotz (26) and applied to filtration problems by Neesse and Fahland (27). The "arched triangle" is the shape of the space between three circular arcs (see Figure 3) in contact and is obviously relevant to packed beds. The analysis leads to a modified form of Poiseuille's equation:

$$Q_w = \frac{\Delta p}{\mu_w \lambda} G_{ijk} A_{ijk}^2 \tag{20}$$

where G_{ijk} is a shape factor defined by the radii of the touching arcs and A_{ijk} is the area of the "arched triangle". The specific expression for the shape factor G_{ijk} was given as

$$G_{ijk} = 3.442 (g_{ij} g_{jk} g_{ki} + g_{ik} g_{ji} g_{kj}) \tag{21}$$

where the functions g_{ij} are defined as

$$g_{ij} = \sqrt{y_{ij}^2 + 2y_{ij}} - \arccos\left(\frac{1}{1+y_{ij}}\right) - \frac{y_{ij}^2}{2} \arccos\left(1 - \frac{2}{(1+y_{ij})^2}\right) \tag{22}$$

with $y_{ij} = x_i/x_j$. From the geometry of the system, the area A_{ijk} is given by

$$A_{ijk} = \frac{1}{4}\left[\sqrt{x_i x_j x_k (x_i + x_j + x_k)} - (\phi_i x_i^2 + \phi_j x_j^2 + \phi_k x_k^2)\right] \tag{23}$$

in which

$$\phi_i = \frac{1}{2} \arccos\left(1 - \frac{2x_j x_k}{(x_i + x_j)(x_i + x_k)}\right) \tag{24}$$

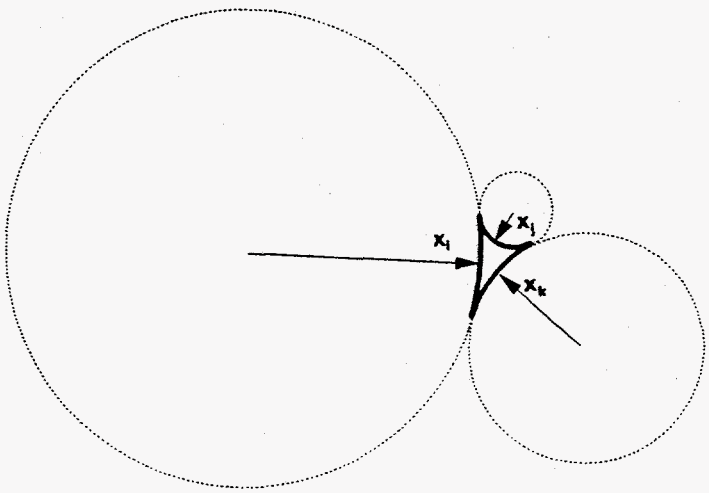

Figure 3. Irregular pore in the form of an "arched triangle" in the contact region between three solid particles (diameters x_i, x_j, x_k).

The mean hydraulic radius corresponding to the "triangular" pore is defined, in the usual way, by

$$r_h = \frac{2A_{ijk}}{p_{ijk}} \tag{25}$$

with the area A_{ijk} given by Equation 23 and the perimeter p_{ijk} by

$$p_{ijk} = x_i\phi_i + x_j\phi_j + x_k\phi_k \tag{26}$$

The effects of pore shape on flow can be evaluated as before by considering the case of a single circular pore of radius r_h and a set of identical "triangular" pores with the same overall mean hydraulic radius and the same total volume (porosity). It follows that the number of triangular pores must be

$$n = \pi r_h^2 / A_{ijk} \tag{27}$$

The flow through the set of pores is, from Equations 20, 25 and 27,

$$Q_w = \frac{4\pi\Delta p}{\mu_w \lambda} \frac{G_{ijk} A_{ijk}^3}{p_{ijk}^2} \tag{28}$$

By expressing the flow rate relative to that through a uniform cylindrical pore, the relative resistance, α_{rel} can be obtained. Thus

$$\alpha_{rel} = \frac{A_{ijk}}{2G_{ijk} p_{ijk}^2} \tag{29}$$

Some examples, for "triangular" pores between particles with various relative diameters are given in Table IV. For the four combinations of particle sizes considered, which include identical sizes and size ratios up to 10:1, the number of irregular pores required to give the same pore volume as a single circular pore with the same mean hydraulic radius is almost constant at about one fifth. Pores between identical particles give the largest

shape factor, G_{ijk} and the lowest relative flow resistance α_{rel}. Pores between particles which differ widely in size give smaller shape factors and lead to flow resistance quite close to that for the equivalent circular pore.

Table IV. Effect of pore shape on relative flow resistance.

Case	Relative Particle Size			Equivalent Circular Pore Radius	Number of Equivalent irregular pores	Shape Factor	Relative Flow Resistance
	x_1	x_2	x_3	r_h	n	G_{123}	α_{rel}
I	1	1	1	0.103	0.21	2.9×10^{-2}	0.28
II	3.3	3.3	0.33	0.103	0.18	7.1×10^{-3}	1.03
III	0.66	0.66	6.61	0.103	0.20	7.1×10^{-3}	1.15
IV	0.5	1	5	0.103	0.20	9.2×10^{-3}	0.87

The comparisons described above generally indicate that the approximation of pore structure by a set of hypothetical uniform pores with an effective mean radius does not provide a reliable description of resistance to flow during cake formation. The use of a conventional mean hydraulic radius appears to be inappropriate to account for the effects of either pore size distribution or pore shape.

CAPACITY OF CONTINUOUS FILTERS

The model for cake formation in batch filtration can be applied directly to continuous filter systems. It is useful, however, to make some minor modification in order to present the relationships in terms of directly measurable quantities. The basic expression for batch filtration can be rewritten:

$$\frac{t}{m_{wf}} = \frac{\mu_w \alpha c\, m_{wf}}{2A^2 \rho_w \Delta p} + \frac{\mu_w \alpha_m}{\rho_w A \Delta p} \qquad (30)$$

where m_{wf} is the mass of liquid collected in the filtrate in time t; α and α_m are defined, in the usual way, as the specific cake resistance and filter mechanism resistance,

respectively; μ_w and ρ_w are respectively the liquid viscosity and density, A is the filter area and Δp is the applied pressure. The concentration c is defined as the mass of solids in the cake per unit mass of liquid in the filtrate. For the general case where some liquid is retained in the cake and some solids pass into the filtrate, c can be related to the feed solids concentration through a simple mass balance which leads to:

$$c = \frac{(c_s - c_f)(1-M)}{(1-c_s-M)(1-c_f)} \tag{31}$$

where c_s is the mass fraction of solids in the feed, c_f is the mass fraction in the filtrate and M is the moisture content (mass fraction) in the filter cake.

In the case of continuous filtration, one complete cycle (revolution) is mathematically equivalent to batch filtration for time

$$t_f = \frac{\theta_f}{2\pi N} \tag{32}$$

where θ_f is the cake formation angle (radians) and N is the rotational speed (revolutions/time). Since the solid and liquid flows occur over the entire cycle, however, the flow rates refer to the cycle time.

$$T = 1/N \tag{33}$$

rather than to the apparent filtration time t_f. Thus the rate of liquid flow to the filtrate is

$$\frac{m_{wf}}{T} = m_{wf} N \tag{34}$$

The solids throughput can be expressed as

$$R_s = \frac{m_{sc}}{AT} = \frac{m_{sc} N}{A} \tag{35}$$

where R_s is the solids throughput per unit area (mass/area · time), m_{sc} is the mass of (dry) solids in the cake. From the definition of c,

$$m_{sc} = c\ m_{wf} \tag{36}$$

so that, from Equation 35,

$$\frac{m_{wf}}{A} = \frac{R_s}{cN} \tag{37}$$

Substitution from Equations 32 and 37 in Equation 30 leads to

$$\frac{\Delta p c \theta_f}{2\pi R_s} = \frac{\mu_w \alpha}{2\rho_w} \cdot \frac{R_s}{N} + \frac{\mu_w \alpha_m}{\rho_w} \tag{38}$$

Equation 38 provides a useful relationship between throughput R_s and the process variables Δp, c, θ_f and N.

Analysis of pilot-scale performance data for the tests on the Pittsburgh seam coal indicate reasonable agreement with the model using a constant value of 6.8×10^{10} m^{-1} for the medium resistance α_m and a specific cake resistance α which varies with feed size consist and applied pressure. Curve-fitting estimates of the specific cake resistance are summarized in Table V; their variation with pressure is shown in Figure 4. A direct comparison of the calculated and experimental values for solids throughput is shown in Figure 5.

Table V. Estimated specific cake resistance for hyperbaric filtration of Pittsburgh seam coal.

Medium resistance $\alpha_m = 6.8 \times 10^{10}$ m^{-1}

Pressure (bar)	Specific Cake Resistance α (m/kg)	
	-28 mesh	-100 mesh
2	8.4×10^{8}	2.1×10^{10}
3.5	2.2×10^{10}	2.6×10^{10}
5	4.0×10^{10}	3.1×10^{10}

The comparisons given in Figure 5 indicate that cake formation in the pilot-scale hyperbaric filter is in general accordance with the model. The scatter in the results

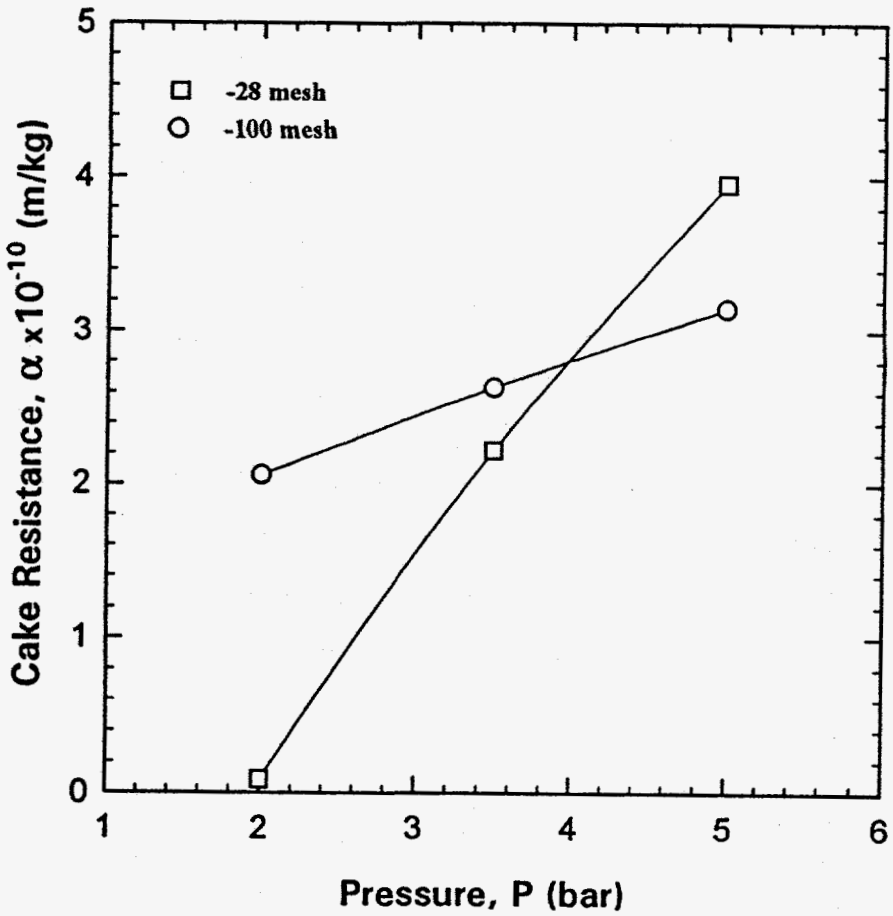

Figure 4. Effect of applied pressure on specific cake resistance in pilot-scale hyperbaric filtration of Pittsburgh seam coal.

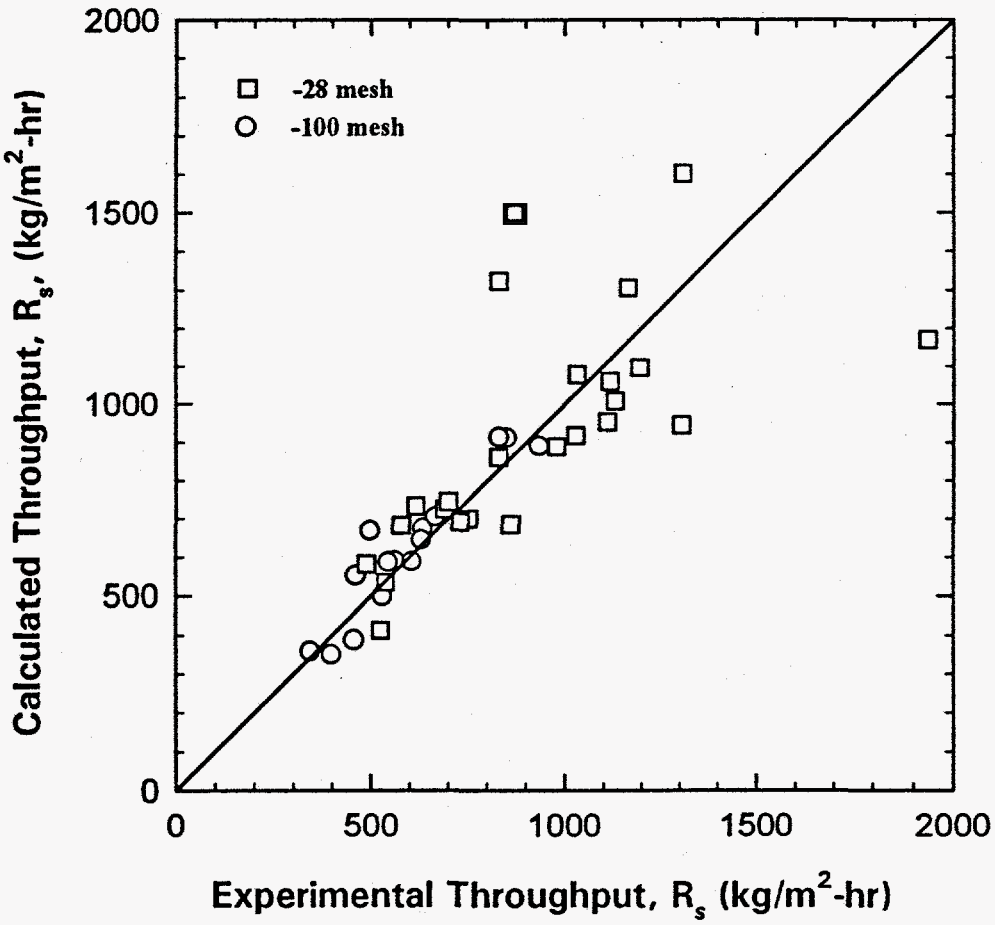

Figure 5. Comparison of calculated and observed throughput for hyperbaric filtration of Pittsburgh seam coal. Calculations based on Equation 38 with cake resistance values given in Table V.

reflects a combination of experimental error and non-idealities such as non-uniform cake structure. It should be noted that the results shown in the figure include only those tests conducted in the absence of chemical reagents such as surfactants or flocculants.

It is of interest to explore the effects of pressure and feed size distribution on the estimated cake resistances shown in Figure 4 and Table V. The results for the two feed size distributions at a pressure of 2 bar are in general agreement with Equation 9. The variation with pressure, for both cases, implies compression of the cake (i.e. reduced porosity with increasing pressure). Compressibility of the cake should be reflected in the relationship between solids throughput and cake thickness. According to Equation 35, the mass of cake per unit area should be:

$$\frac{m_{sc}}{A} = \frac{R_s}{N} \tag{39}$$

and, from simple geometry

$$m_{sc} = \lambda A \rho_s (1-\varepsilon) \tag{40}$$

It follows that

$$\lambda = \frac{R_s}{N\rho_s(1-\varepsilon)} \tag{41}$$

An example of results plotted according to Equation 41 is given in Figure 6. The essentially linear relationship indicates that the cake density is more or less constant. Based on the slope of the line and an assumed specific gravity of 1.4 for the coal, the cake porosity is about 47.4%.

Results for both filter feeds indicate similar cake densities, essentially independent of pressure. Such variations as may exist would not be sufficient to account for the variations in specific cake resistance.

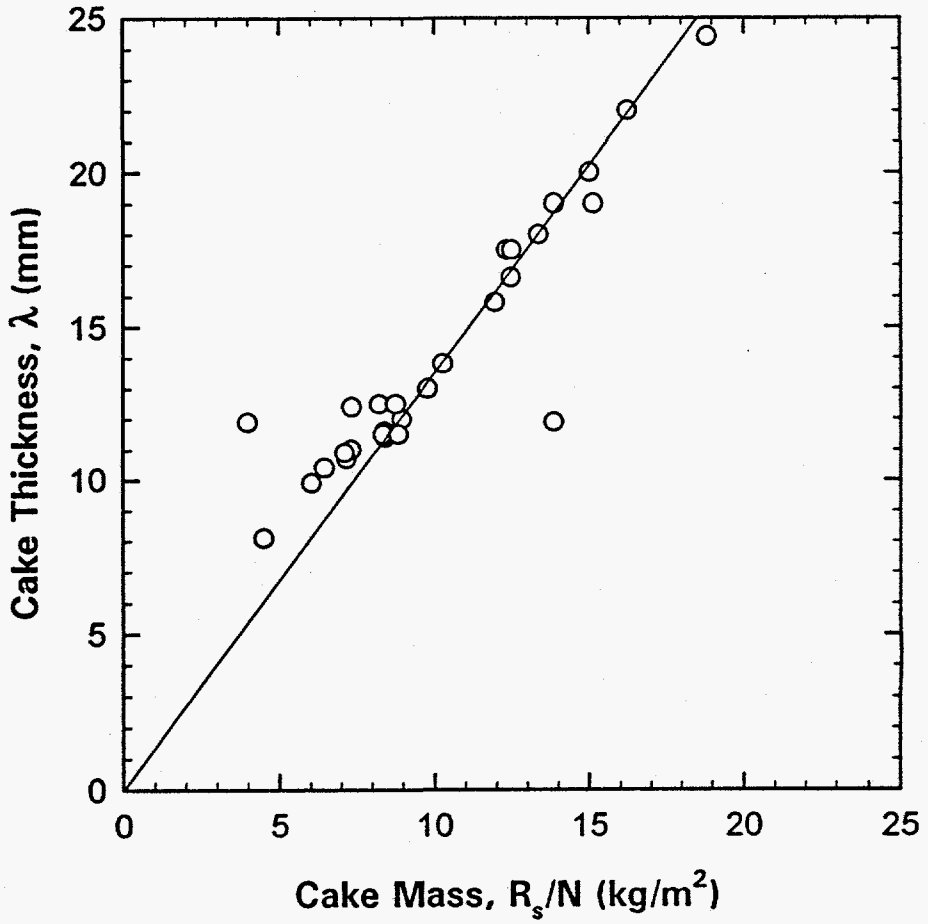

Figure 6. Relationship between cake thickness and solids throughput.

A more reasonable explanation for the apparent variations in cake resistance is that the cake structure is non-uniform. Flow of liquid during cake formation provides a driving force for the elutriation of fines through the relatively open structure formed from the coarser particles. Such material would accumulate at the inner surface of the cake, forming what amounts to a cake-within-a-cake. Since the inner "cake" would build-up in tandem with the total cake, the existence of such structures would not affect the applicability of the general model. The process could still be described using an overall, effective cake resistance. However, the inner cake could be compressible, leading to an increased resistance with pressure but will little or no effect on the overall cake porosity. The development of a "binary packing model" to describe non-uniform cakes is presented in the next section of this report.

The relatively large value for the medium resistance α_m is also somewhat surprising. The relative values of α and α_m imply that typically, about 25% of the pressure drop is across the filter medium with a considerably larger contribution for the coarser feed at low pressure. Partial blinding of the medium by penetration of fines during continuous operation may be responsible for this observation.

Non-Uniform Cakes: Binary Packing Model

Consider a particle bed in which the packing could be described by two distinct layers as follows (Figure 7):

- a uniform bed consisting of the coarser particles (> same size x_f)
- an inner layer, adjacent to the filter medium, consisting of the finer fraction (< x_f) occupying the voids in the coarse particle bed.

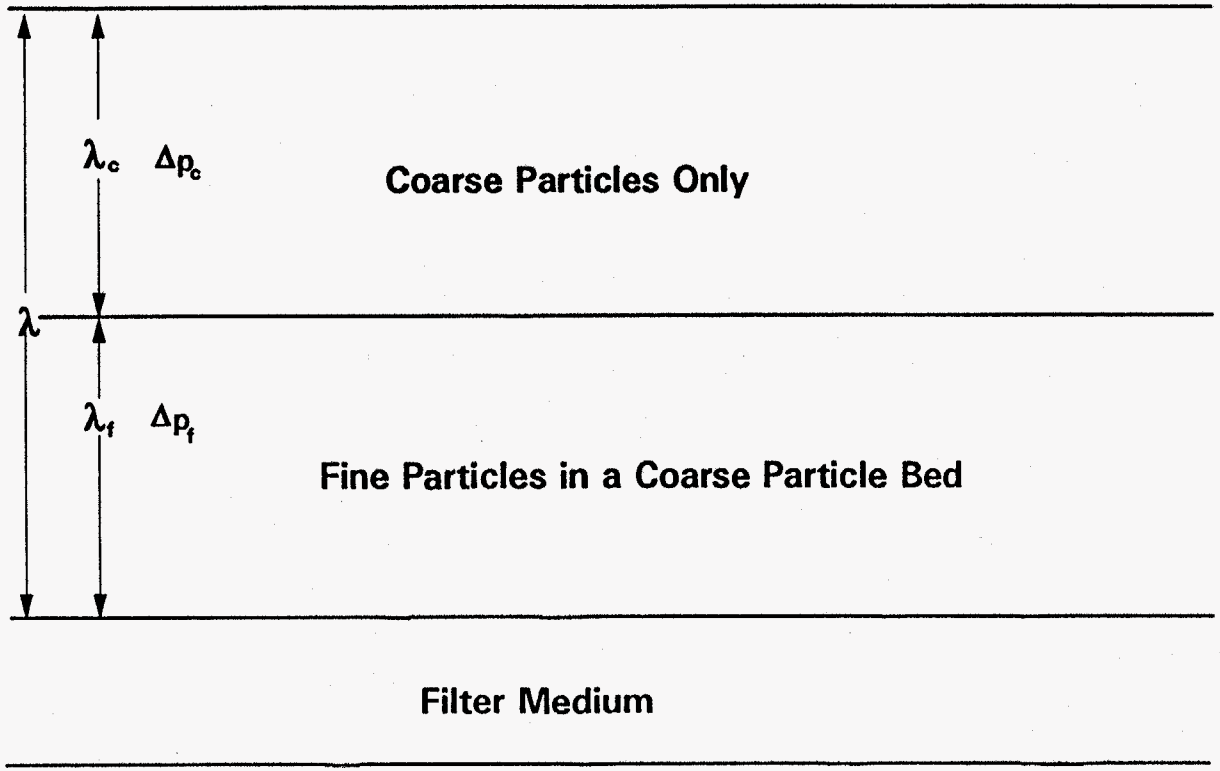

Figure 7. A schematic of a non-uniform cake as a binary packing structure.

The solid volume of fines,

$$V_{sf} = Q_f (1-\varepsilon) A\lambda \tag{42}$$

where Q_f = volume fraction of particles with $x < x_f$

ε = overall (bulk) bed porosity

Now the volume occupied by fines (including the associated pore volume), is given by

$$V_f = \frac{V_{sf}}{1-\varepsilon_f} = Q_f \frac{(1-\varepsilon)}{(1-\varepsilon_f)} A\lambda \tag{43}$$

Where ε_f = porosity of fine particle bed. In addition,

$$V_f = \varepsilon_c A\lambda_f \tag{44}$$

where ε_c = porosity (bulk) of the coarse particle bed

λ_f = thickness of the fines layer in the coarse bed

Then from Equations 43 and 42, we get

$$\lambda_f = \frac{Q_f (1-\varepsilon)\lambda}{\varepsilon_c (1-\varepsilon_f)} \tag{45}$$

Using Equation 45, the thickness of the coarse layer, λ_c is given by

$$\lambda_c = \lambda - \lambda_f = \lambda[1 - \frac{Q_f (1-\varepsilon)}{\varepsilon_c (1-\varepsilon_f)}] \tag{46}$$

The pressure drop across a bed of thickness λ with area of cross-section A can be obtained using Equation 8

$$\Delta p = \frac{\mu_w \lambda S_v^2}{k_t} (\frac{Q}{A}) \frac{(1-\varepsilon)^2}{\varepsilon^3} \tag{47}$$

The cake thickness, λ can be related to cake mass m_{sc} as follows

$$\lambda = \frac{m_{sc}}{A(1-\varepsilon)\rho_s} \tag{48}$$

Substitution of Equation 48 into Equation 47 gives

$$\Delta p = \frac{\mu_w m_{sc} S_v^2}{k_t \rho_s} \left(\frac{Q}{A^2}\right) \frac{(1-\varepsilon)}{\varepsilon^3} \tag{49}$$

where S_v is the specific surface area for the cake. Using Equations 46, 47, and 48, the pressure drop Δp_c across the coarse bed is

$$\Delta p_c = \frac{\mu_w m_{sc} S_{vc}^2}{k_t \rho_s} \left(\frac{Q}{A^2}\right) \frac{(1-\varepsilon_c)^2}{\varepsilon_c^3 (1-\varepsilon)} \left[1 - \frac{Q_f (1-\varepsilon)}{\varepsilon_c (1-\varepsilon_f)}\right] \tag{50}$$

where S_{vc} = specific surface area of the coarse particles in the cake.

For the fines/coarse bed, flow is across a reduced cross-section

$$A_f = \varepsilon_c A \tag{51}$$

Using Equations 45, 47 and 51, the pressure drop Δp_f across the fines/coarse particle bed is

$$\Delta p_f = \frac{\mu_w m_{sc} S_{vf}^2}{k_t \rho_s} \left(\frac{Q}{A^2}\right) \frac{Q_f (1-\varepsilon_f)}{\varepsilon_c^2 \varepsilon_f^3} \tag{52}$$

where S_{vf} = specific surface area of coarse/fine particles in the cake.

The cake resistance $\overline{\alpha}$ (using Equation 9) is

$$\overline{\alpha} = \frac{(1-\varepsilon) S_v^2}{k_t \varepsilon^3 \rho_s} = \frac{\Delta p}{\mu_w m_{sc}} \left(\frac{A^2}{Q}\right) \tag{53}$$

Using Equations 50, 52 and 53 overall cake resistance, α_b is

$$\alpha_b = \frac{S_{vc}^2}{k_t \rho_s} \frac{(1-\varepsilon_c)^2}{\varepsilon_c^3 (1-\varepsilon)} \left[1 - \frac{Q_f (1-\varepsilon)}{\varepsilon_c (1-\varepsilon_f)}\right] + \frac{S_{vf}^2}{k_t \rho_s} \frac{Q_f (1-\varepsilon_f)}{\varepsilon_c^2 \varepsilon_f^3} \tag{54}$$

The relative cake resistance based on a single uniformly packed bed is

$$\alpha_{rel}=\frac{\alpha_b}{\bar{\alpha}}=\left(\frac{S_{vc}}{S_v}\right)^2\left(\frac{1-\varepsilon_c}{1-\varepsilon}\right)^2\left(\frac{\varepsilon}{\varepsilon_c}\right)^3\left[1-\frac{Q_f(1-\varepsilon)}{\varepsilon_c(1-\varepsilon_f)}\right] \tag{55}$$

$$+\left(\frac{S_{vf}}{S_v}\right)^2\left(\frac{1-\varepsilon_f}{1-\varepsilon}\right)\left(\frac{\varepsilon}{\varepsilon_f}\right)^3\frac{1}{\varepsilon_c^2}Q_f$$

It should be noted that the quantities ε, ε_c and θ_f are not independent and are related as follows

$$A\lambda=\frac{m_{sc}}{\rho_s(1-\varepsilon)}=\frac{m_{sc}(1-\theta_f)}{\rho_s(1-\varepsilon_c)} \tag{56}$$

Equation 56 further simplifies to

$$\varepsilon_c=1-(1-\theta_f)(1-\varepsilon) \tag{57}$$

The effects of the binary packing arrangement on relative cake resistance can be seen in Table VI.

Table VI. Predicted relative cake resistance for fixed overall porosity $\varepsilon = 0.5$ and feed particle size distribution given by $F_3(x) = x/K_s$.

ε_f	Relative Cake Resistance, α_{rel}			
	K_s = 28 mesh		K_s = 100 mesh	
	x_f = 5 μm	x_f = 2 μm	x_f = 5 μm	x_f = 2 μm
0.95	2.31	4.19	0.71	1.37
0.9	5.25	9.54	1.66	3.07
0.8	14.64	26.71	4.59	8.44
0.7	32.55	59.49	10.17	18.68
0.6	68.73	125.67	21.43	39.35
0.5	148.24	271.15	46.17	84.79

If the fine particle bed porosity is a function of pressure, an increase in pressure translates to a decrease in ε_f. The form of the function is not known, but it can be inferred from the effect of increasing pressure on the specific cake resistance through comparison of Tables

V and VI. For example, the experimental cake resistances for the -28 mesh feed are consistent with a reduction in ε_f from 0.95 (at 2 bar) to about 0.55 (at 5 bar). The data for -100 mesh feed imply sunstantially lower compressibility of the inner cake, possibly due to the confining effect of the finer pore structure in the "coarse" part of the cake.

CAKE DEWATERING

Liquid Displacement

The dewatering step can be roughly divided into two stages: displacement of bulk liquid from the (initially) saturated cake followed by further, slow removal of residual moisture during airflow through the cake. The fraction of the cycle which is taken up by the initial displacement can be estimated from the liquid flow rate at the end of the cake formation stage. Thus, the displacement time t_d can be estimated from

$$t_d = V_{wc} / Q_{wd} \tag{58}$$

where V_{wc} is the volume of liquid in the saturated cake and Q_{wd} is the flowrate.

$$V_{wc} = \varepsilon V_c \tag{59}$$

where V_c is the cake volume. A solids mass balance leads to

$$V_c \rho_s (1-\varepsilon) = c \rho_w V_{wf} \tag{60}$$

where V_{wf} is the volume of liquid passing into the filtrate during the cake formation stage. Then,

$$V_{wc} = \frac{\varepsilon\ c\ \rho_w V_{wf}}{(1-\varepsilon)\rho_s} \tag{61}$$

The filtrate volume V_{wf} can be estimated from a simplified form of Equation 30 in which the medium resistance α_m is neglected. Thus,

$$V_{wf} = \frac{m_{wf}}{\rho_w} = A\sqrt{\frac{2\Delta pt}{\mu_w \alpha c \rho_w}} \tag{62}$$

Assuming the liquid flowrate to be the same as at the end of the cake formation stage,

$$Q_{wd} = Q_{wf} = \left.\frac{dV_{wf}}{dt}\right|_{t=t_f} \tag{63}$$

where t_f is the total cake formation time. Differentiating Equation 62,

$$Q_{wf} = A\sqrt{\frac{\Delta p}{2\mu_w \alpha c \rho_w t_f}} \tag{64}$$

Combining Equations 58, 61, 62 and 64.

$$t_d = \frac{2\varepsilon c \rho_w t_f}{(1-\varepsilon)\rho_s} \tag{65}$$

Expressed as a displacement angle, Equation 65 becomes

$$\theta_d = \frac{2\varepsilon c \rho_w \theta_f}{(1-\varepsilon)\rho_s} \tag{66}$$

Residual Moisture

Using typical values from the pilot-scale studies, i.e., ε=0.5, c=0.65, ρ_s =1.4, Equation 66 leads to $\theta_d \approx 0.93\theta_f$. In these tests, θ_f ranged from 55° to 165° while the overall dewatering angle was kept constant at 135°. Thus, in some cases with the larger cake formation angles, the dewatering times may not have been adequate. While there is some evidence that the higher cake formation angles lead to higher residual moisture content, no clear pattern emerges from the results.

The actual displacement time is larger than t_d because unlike the simple minded approach here, mechanical dewatering processes are, further, invariably limited by wetting phenomena and capillary forces. Liquids generally adhere to solids, even those

with hydrophobic surfaces. Wetting behavior is normally characterized by the contact angle; for pre-wetted solids, which is the case for dewatering systems, it is the so-called receding angle which is of interest (28). Receding angles for coals typically have values of around 30° but can be higher for high-rank and lower for low-rank coals.

Capillary forces are a manifestation of the pressure differential resulting from the effects of surface tension acting on a curved surface of a liquid confined in a pore. The capillary pressure across a curved interface can be calculated by means of the Laplace equation:

$$\Delta p_{cap} = 2\gamma / r_s \tag{67}$$

in which γ is the interfacial tension and r_s is the radius of curvature. For the simple case of a liquid in a cylindrical capillary the specific relationship becomes

$$\Delta p_{cap} = \frac{2\gamma \cos\theta}{r} \tag{68}$$

where θ is the contact angle and r is the radius of the capillary. In order to expel liquid from the capillary, the applied pressure must exceed the capillary pressure.

The situation is similar but considerably more complex in the voids and contact regions in a packed bed such as a filter cake. Whereas exceeding the capillary pressure is sufficient to eliminate liquid from a pore of circular section, liquid will generally be retained in the "corner" regions of irregular "triangular" pores such as those described previously. Thus it is not sufficient to exceed the average capillary pressure in the pore. For any applied pressure, liquid will remain in regions for which the radius of curvature of the meniscus is less than the critical value defined, using Equation 67, by

$$r_c = 2\gamma / \Delta p_{app}. \tag{69}$$

where Δp_{app} is the applied pressure.

It follows that the residual saturation in a filter cake subject to dewatering by air displacement consists of:

a) water trapped in filled pores whose effective overall radius is less than r_c

b) water remaining in "corner" regions of irregular pores.

The effects of pore size distribution and pore shape can be evaluated using the geometries described previously.

The controlling factor in establishing the limiting saturation in a pore system is a dimensionless pore radius R defined, following Equation 69 by

$$R=\frac{r\,\Delta p}{2\gamma} \tag{70}$$

Circular pores for which R<1 will remain saturated while those with R>1 will be completely empty. For a distribution of pore sizes defined, as before, by $f_o(R)$, the limiting saturation S is given by

$$S=\frac{\int_0^1 R^2 f_o(R)dR}{\int_0^\infty R^2 f_o(R)dR} \tag{71}$$

The effects of pore size distribution, for log normal systems with the same overall mean hydraulic radius, are illustrated in Figure 8. It can be seen that the distribution of sizes leads to lower saturation for systems with a small mean hydraulic radius but increased saturation for the coarser systems. In most cases, residual saturation in a filter cake with a distribution of pore sizes is less than would be predicted on the basis of a single, mean hydraulic radius.

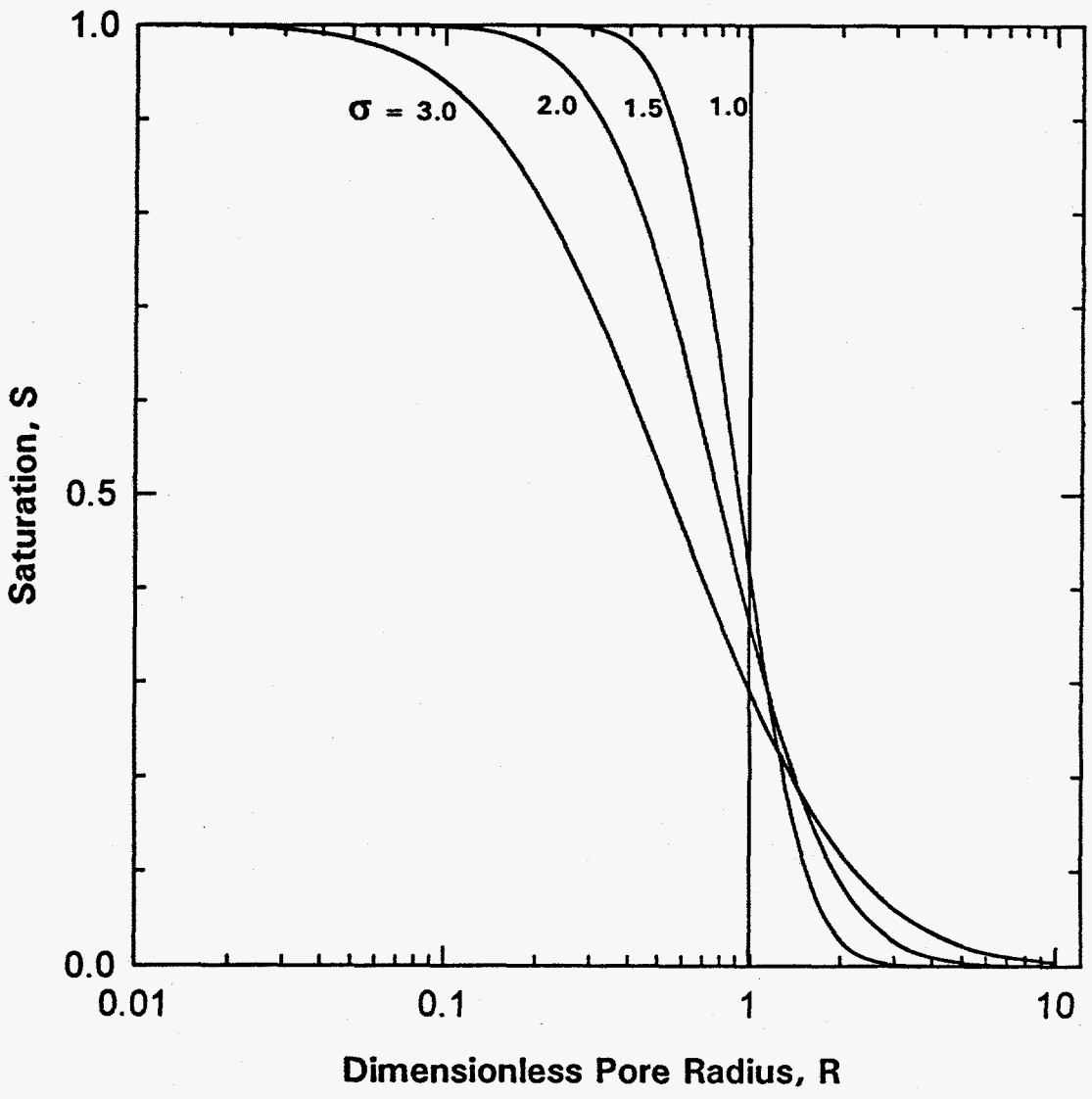

Figure 8. Effect of (log normal) pore size distrbution on residual saturation.

Shape Effect

A quantitative evaluation of the effects of pore shape on residual saturation can be obtained using the generalized "triangular" shapes described previously. The volume of liquid trapped in the contact region between two particles forming the "corner" of a triangular pore can be calculated using a form of Equation 23 with the third radius r_3 replaced by the capillary radius r_c defined by Equation 69. Thus, for the pore as a whole,

$$S=\frac{A_{ij}+A_{ik}A_{jk}}{A_{ijk}} \tag{72}$$

in which the A_{ij} are given by

$$A_{ij}=\frac{1}{4}[\sqrt{x_i x_j x_c (x_i+x_j+x_c)}-(\phi_i x_i^2+\phi_j x_j^2+\phi_c x_c^2] \tag{73}$$

and A_{ijk} is obtained directly from Equation 23.

Three specific geometries have been considered and are illustrated in Figure 9. These are: $x_1=x_2=x_3$; $x_1=x_2$, $x_3=x_1/10$, and $x_1=x_2$, $x_3=10x_1$. The calculated residual saturation is shown for each case, in Figure 10, as a function of the dimensionless mean hydraulic radius, defined by Equation 70. Noting that, for the equivalent circular pore, S=1 for $R_h<1$ and S=O for $R_h>1$, it can be seen that the irregular shape generally leads to an increase in residual saturation, for Rh>1, but a reduced saturation for $R_h<1$. The latter is a consequence of the fact that the mean hydraulic radius generally understates the "size" of an irregular pore. It is interesting to note that for the general pore shape considered here, residual saturation is relatively insensitive to the specific pore geometry. It can also be seen that, relative to residual saturation, the "triangular" pore shape is equivalent to a distribution of circular pores (see Figures 8 and 10).

CASE I

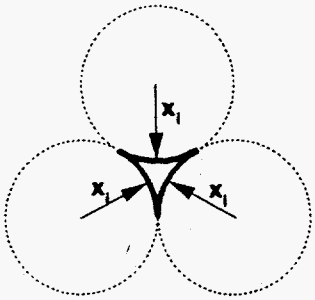

CASE II

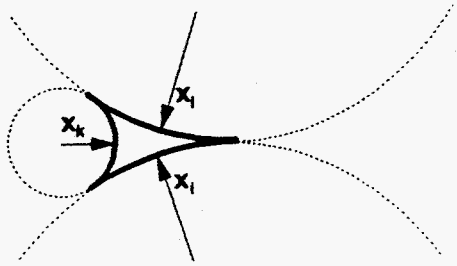

CASE III

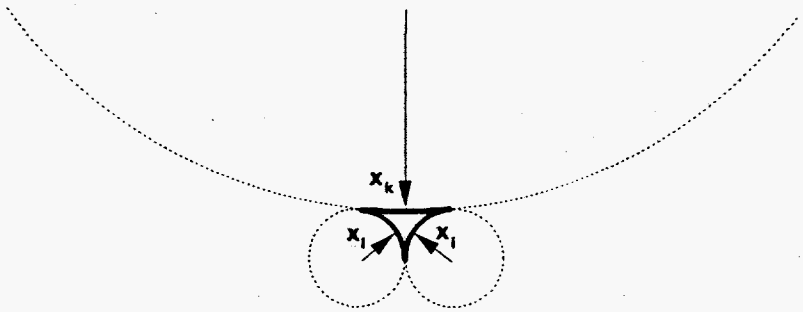

Set of equivalent circular pores

Figure 9. Pore geometries corresponding to the residual saturation curves shown in Figure 10.

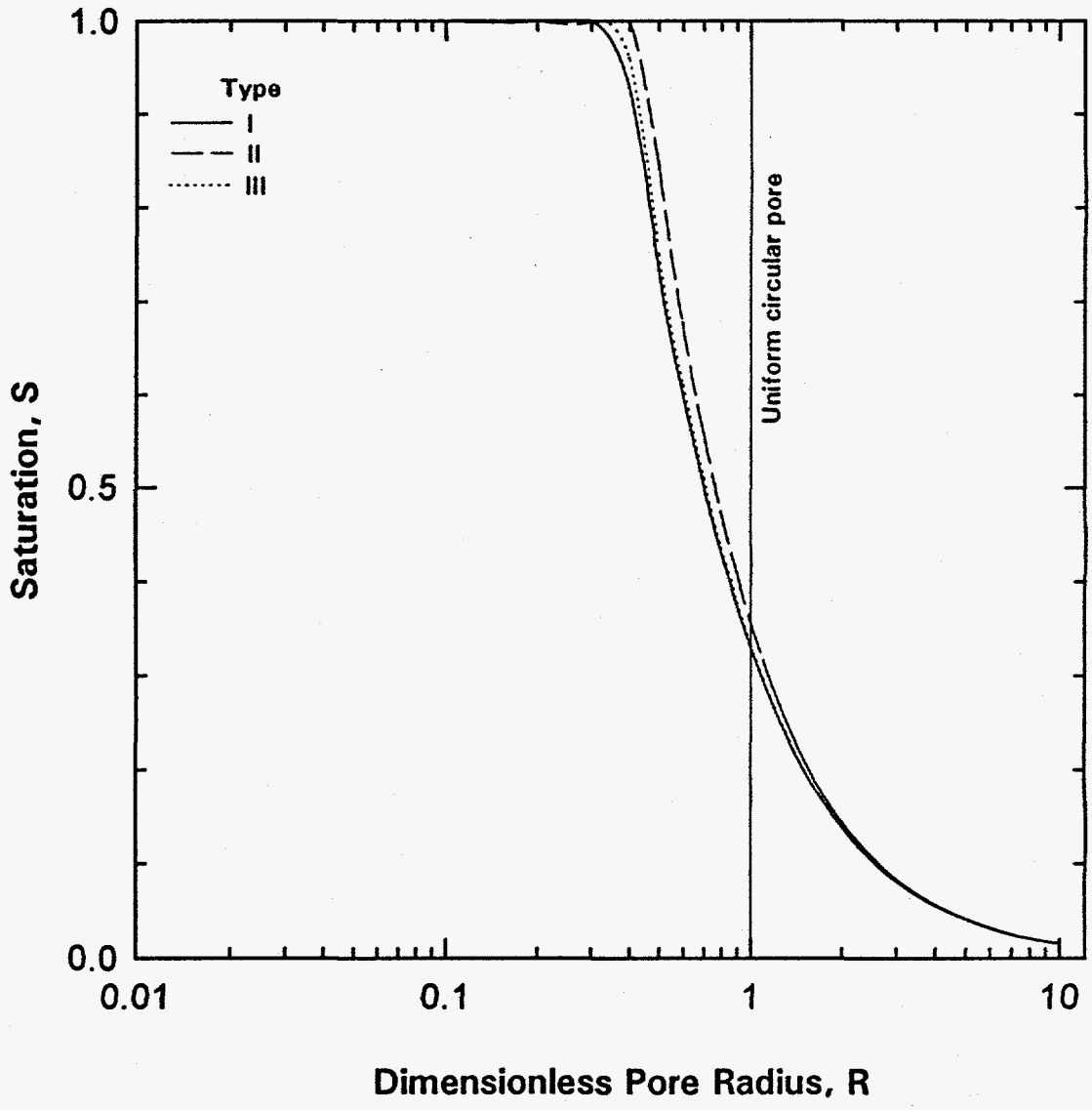

Figure 10. Effect of pore shape on residual saturation.

Application to Real Systems

Equations 65 or 72 can be used to estimate the residual saturation, but the pore size distribution or its shape are not known. The particle size distribution can be known through experimental measurements or predicted from some known distribution functions.

Rootare (29) showed that the pore size distribution follows the particle size distribution and the particle to pore ratios were of the order of 3-6.

$$x = k_p\, r \tag{74}$$

where x = particle diameter

r = pore radius

k_p = constant

Now from Equations 70 and 71, we get

$$S = \frac{\int_0^{\frac{2\gamma}{\Delta p}} r^2 f_o(r)dr}{\int_0^{\infty} r^2 f_o(r)dr} \tag{75}$$

Substitution of Equation 74 gives

$$S = \frac{\int_0^{\frac{2\gamma}{\Delta p}k_p} \frac{x^2}{k_p^2} f_o(x)dx}{\int_0^{\infty} \frac{x^2}{k_p^2} f_o(x)dx} \tag{76}$$

Now converting the number distribution, $f_o(r)$ into a volume distribution, $f_3(r)$ gives

$$S = \frac{\int_0^{\frac{2\gamma}{\Delta p}k_p} \frac{f_3(x)dx}{x}}{\int_0^{\infty} \frac{f_3(x)dx}{x}} \tag{77}$$

Some typical particle size data for a clean coal filter feed are given in Table VII. For an applied pressure of 3.5 bar, the experimental residual moisture content is 0.174 giving a saturation of 0.327 which gives a k_p value of 7.02 by interpolation from Table VII. Now based on an assumption of a constant k_p, residual moisture predictions have been made with changes in applied pressure, as shown in Table VIII. The experimental results in Table VIII show a much greater effect of the applied pressure on the residual saturation and moisture content. This could imply that the factor k_p is a function of applied pressure.

Table VII. Typical particle size distribution for clean coal (-28 mesh) filter feed.

Mean size $\bar{x}$ (μm)	Volume fraction f(x)	f(x) / x	cumulative $\frac{f(x)}{\bar{x}}$
460.43	0.1600	0.0003	0.0301
346.41	0.1400	0.0004	0.0298
244.95	0.1500	0.0006	0.0294
158.11	0.1822	0.0012	0.0288
104.88	0.0575	0.0005	0.0276
74.46	0.0460	0.0006	0.0271
52.65	0.0345	0.0007	0.0264
36.93	0.0478	0.0013	0.0258
26.12	0.0415	0.0016	0.0245
18.76	0.0376	0.0020	0.0229
13.27	0.0311	0.0023	0.0209
9.26	0.0194	0.0021	0.0186
6.55	0.0160	0.0024	0.0165
4.63	0.0124	0.0027	0.0140
3.30	0.0119	0.0036	0.0113
2.31	0.0068	0.0029	0.0077
1.63	0.0034	0.0021	0.0048
0.70	0.0019	0.0027	0.0027

Table VIII. Residual Saturation and Moisture Content

Δp (bar)	Residual Saturation	Predicted Moisture Content	Experimental Moisture Content
0.7	0.71	0.31	0.21
2	0.48	0.24	0.19
3.5	0.315	0.17	0.17
5	0.216	0.12	0.16

The k_p value has been estimated for varying pressures and plotted in Figure 11. There is a definite change in k_p with pressure, which can be explained by changes in the structure of the cake with pressure. Pilot-scale performance tests have also shown changes in the cake resistance (Figure 4) with changes in the applied pressure with an almost constant overall bed porosity. These trends also imply a change in the cake structure. The overall cake density does not change, but there is an internal rearrangement of the fines which, though, still maintaining the same bed porosity, changes the finer structure.

Air Consumption

Air consumption during the dewatering stage in the cycle is an important practical consideration. Since both cake formation and dewatering involve fluid flow through the porous cake, some correlation of throughput and air consumption is to be expected. Approximate relationships can be obtained by extension of the basic filtration model.

The volume flow rate of air through unit area of the cake can be expressed as:

$$\frac{Q_a}{A} = \frac{k_a \Delta p}{\mu_a \lambda} \tag{78}$$

where k_a is the permeability to air and μ_a is the viscosity of air. Expressed as a standard volumetric flow rate, Equation 78 becomes

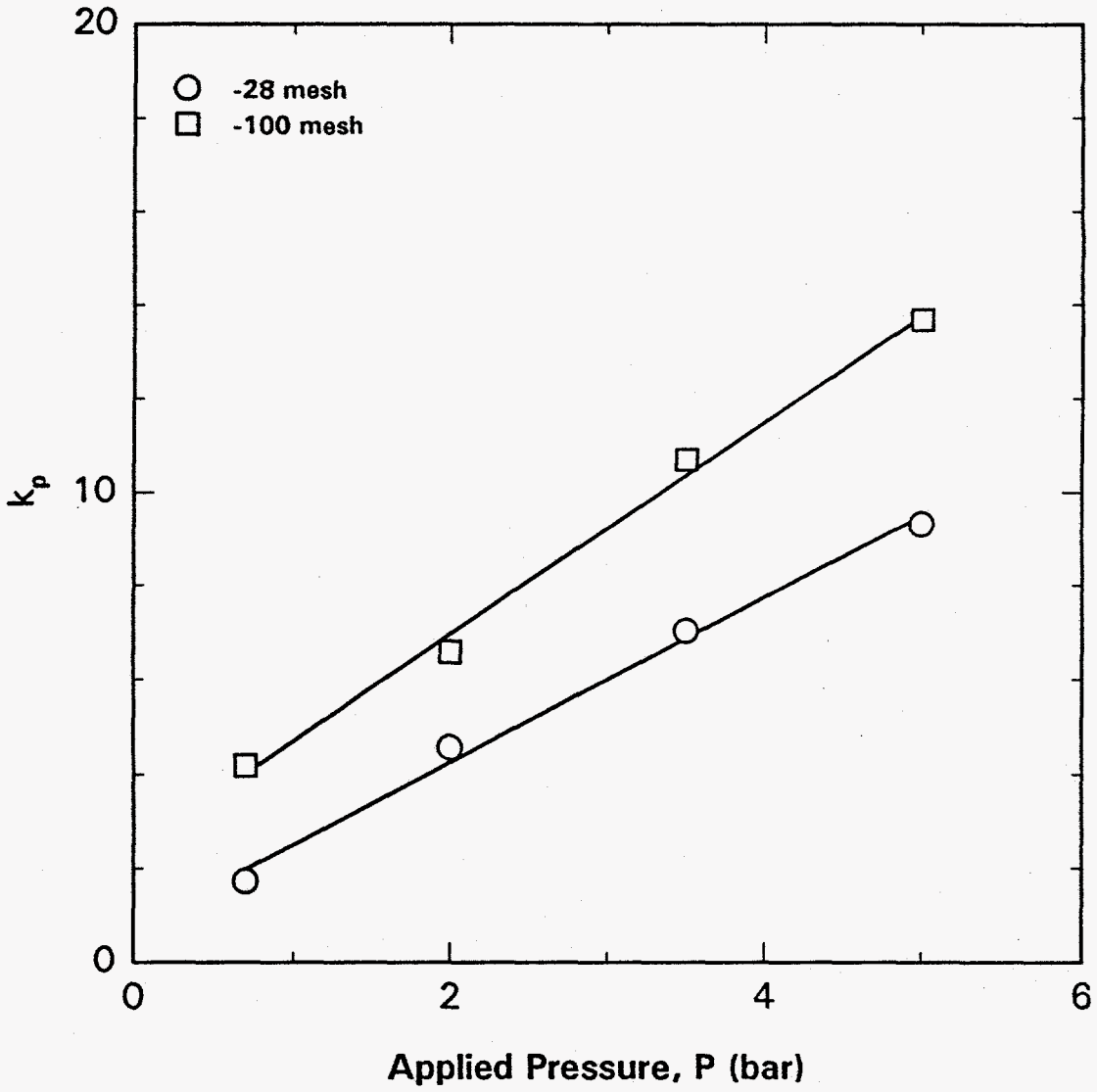

Figure 11. Effect of pressure on k_p, the pore size/particle size factor.

$$\frac{Q_{st}}{A} = k_a \frac{\overline{P}}{P_{st}} \frac{\Delta p}{\mu_a \lambda} \tag{79}$$

with

$$\frac{\overline{P}}{P_{st}} = \frac{\Delta p + 1}{2} \tag{80}$$

for hyperbaric filtration against an ambient pressure of one atmosphere.

At the end of the cake formation stage, the liquid flow can be similarly expressed as

$$\frac{Q_w}{A} = \frac{k_w \Delta p}{\mu_w \lambda} \tag{81}$$

so that, from Equations 79, 80 and 81

$$\frac{Q_{st}}{A} = K_r \frac{\mu_w}{\mu_a} \left(\frac{\Delta p + 1}{2}\right) \frac{Q_w}{A} \tag{82}$$

where K_r ($=k_a/k_w$) is a relative permeability factor whose value should be unity for an idealized dry cake and less than unity for cakes with residual moisture (which causes partial blockage of pores).

The flow velocity Q_w/A can be directly related to the rate of solids accumulation R_s through

$$\frac{Q_w}{A} = \frac{1}{\rho_w c N} \frac{dR_s}{dt} \Big|_{t=t_f} \tag{83}$$

or, in terms of angles

$$\frac{Q_w}{A} = \frac{2\pi}{\rho_w c} \frac{dR_s}{d\theta} \Big|_{\theta=\theta_f} \tag{84}$$

Differentiation of Equation 38 leads to

$$\frac{dR_s}{d\theta} = \frac{\rho_w \Delta p c N}{2\pi\mu_w(\alpha R_s + N\alpha_m)} \tag{85}$$

The pressure term in Equation 85 can be eliminated using Equation 38. The result is

$$\left.\frac{dR_s}{d\theta}\right|_{\theta=\theta_f} = \frac{R_s}{2\theta_f}\left(\frac{\alpha R_s + 2N\alpha_m}{\alpha R_s + N\alpha_m}\right) \tag{86}$$

It is convenient to express air consumption relative to solids throughput using

$$R_a = \frac{Q_{st}(\theta_a - \theta_d)}{2\pi A R_s} \tag{87}$$

where θ_a is the dewatering angle and θ_d is that part of the dewatering angle taken up by the expulsion of bulk liquid. Substitution of Equations 82, 84 and 86 in Equation 69 gives

$$R_a = \frac{K_r\mu_w(\theta_a - \theta_d)}{2\rho_w\mu_a c\theta_f}\left(\frac{\alpha R_s + 2N\alpha_m}{\alpha R_s + N\alpha_m}\right)\left(\frac{\Delta p + 1}{2}\right) \tag{88}$$

Using Equation 66, the final expression for relative air consumption is:

$$R_a = \frac{K_r\mu_w}{2\rho_w\mu_a}\left(\frac{\Delta p + 1}{2}\right)\left(\frac{\theta_a}{c\theta_f} - \frac{2\varepsilon\rho_w}{(1-\varepsilon)\rho_s}\right)\left(\frac{\alpha R_s + 2N\alpha_m}{\alpha R_s + N\alpha_m}\right) \tag{89}$$

By inspection, it is clear that the last term on the right hand-side is relatively invariant, ranging in value from about 1.1 to 1.3 for the results being analyzed here.

Experimental (pilot-scale) data on relative air consumption are compared with the predictions of Equation 89 in Figure 12. It can be seen that, typically, the air consumption is close to the predicted value. However, the results show considerable scatter. In some cases, the air consumption is as much as three times larger than predicted while for other conditions the observed value is substantially lower than the prediction. In addition to simple experimental error, a great many factors could lead to the discrepancies. These include the structure effects discussed previously and, perhaps

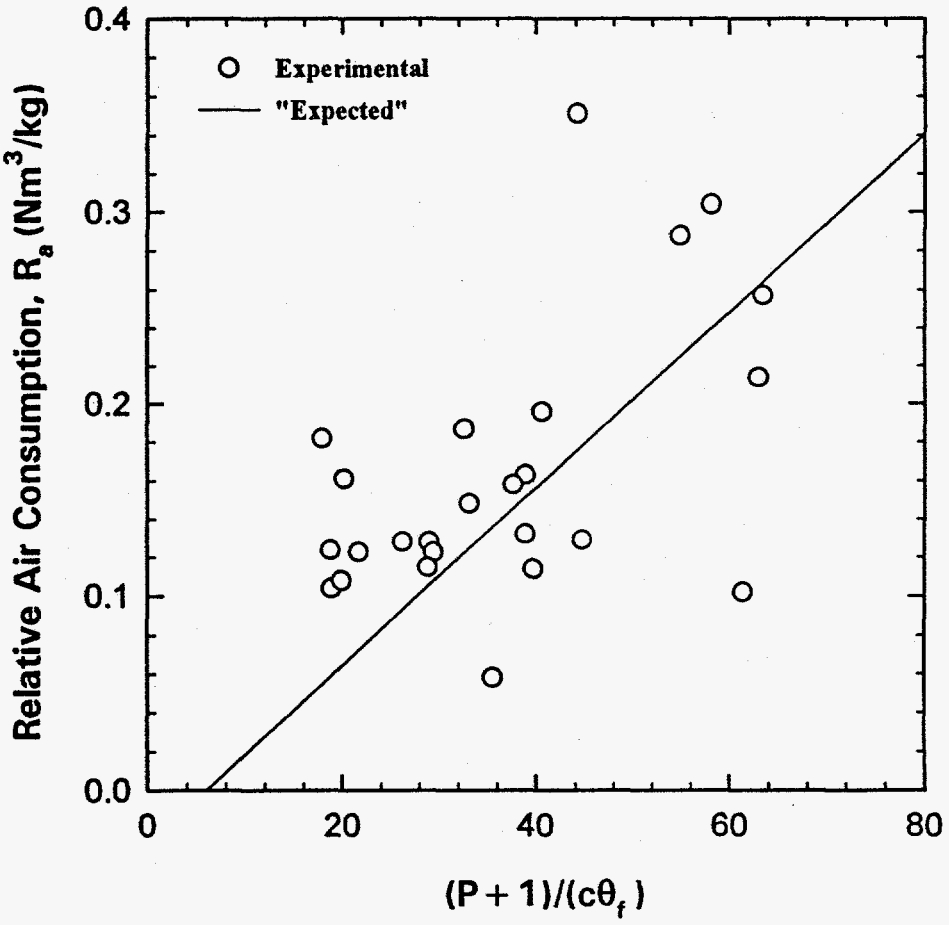

Figure 12. Relative air consumption in hyperbaric filtration of -28 mesh Pittsburgh seam coal.

most importantly, microcracking of the cake (or of any fine "inner layers") during the dewatering stage.

Evaporation

Contributions to the process by evaporation of the water during gas flow through the cake have generally been neglected in literature, so far. However, because of the high surface areas involved and potentially high mass transfer rates associated with high gas velocities, it is important to consider the effects of evaporation on the dewatering process.

Evaporation Model

For an element of cake, thickness dz, water vapor enters and leaves by convective transport in the gas phase. At the same time, evaporation in the layer leads to addition of vapor to the flowing gas. A mass balance on the vapor in the gas phase leads to

$$\frac{\partial n_m}{\partial t} = r_e A_l - \frac{\partial}{\partial z}(n_m u) \qquad (90)$$

where:

n_m = concentration of vapor in the gas (moles/cm^3)

u = superficial gas velocity (cm/sec)

r_e = evaporation rate (moles/cm^2 sec)

A_l = area of liquid surface per unit volume of the element (cm^{-1})

If the liquid water is present as a thin film on the particle surfaces, A_l will be approximately equal to the solid surface area , i.e.

$$A_l = S_v (1-\varepsilon) \qquad (91)$$

where S_v = solid specific surface area (cm^{-1})

ε = cake porosity.

It can be further assumed that

$$r_e = k_e (n_{mo} - n_m) \tag{92}$$

where

k_e = evaporation rate constant (cm/sec) (related to mass-transfer coefficient)

n_{mo} = equilibrium (saturation) vapor concentration (moles/cm^3)

Finally, if cake voidage, permeability, etc., do not vary significantly during gas flow, the velocity u will be approximately constant. The final expression then becomes

$$\frac{\partial n_m}{\partial t} = k_e S_v (1-\varepsilon)(n_{mo} - n_m) - u\frac{\partial n_m}{\partial z} \tag{93}$$

The solution to Equation 93 will provide a description of water vapor transport through the cake and of the dynamics of cake dewatering through the evaporation mechanism.

Considerable insight into evaporative dewatering can be obtained using a simplification to Equation 93 in which it is assumed that the vapor profile across the cake rapidly assumes an approximate steady state. In other words, the vapor concentration varies with position, but not significantly with time. Under such conditions, Equation 90 reduces to

$$\frac{dn_m}{dz} = \frac{k_e S_v (1-\varepsilon)}{u} (n_{mo} - n_m) \tag{94}$$

Using the boundary condition:

$$n_m = n_{ml} \text{ at } z = 0$$

where n_{ml} is the vapor concentration in the incoming gas, and $z = 0$ represents the exposed face of the cake, the solution is

$$n_m = n_{mo} - (n_{mo} - n_{ml}) \exp\left[\frac{-k_e S_v (1-\varepsilon) z}{u}\right] \qquad (95)$$

The rate of removal of water from the cake is given by the net flux out of the cake

$$J_n = u\,(n_m(\lambda) - n_{ml}) \qquad (96)$$

where $n_m(\lambda)$ is the vapor concentration in the effluent gas stream.

Substitution from Equation 95 (with $z = \lambda$) into Equation 96 leads to

$$J_n = u(n_{mo} - n_{ml})\left[1 - \exp\left(\frac{-k_e S_v (1-\varepsilon)\lambda}{u}\right)\right] \qquad (97)$$

Equation 97 describes the absolute rate of water removal (moles/cm^2 sec). The relative or fractional rate can be defined as the ratio of the absolute rate to the (molar) liquid content of the cake. For a given saturation S, the number of moles of water per unit cake area is $S\varepsilon\lambda\rho_w/M_w$ where M_w is the molecular weight (18 g/mole) and ρ_w is the density (1 g/cm^3) of water. The relative removal rate is then

$$J_r = \frac{J_n M_w}{S\varepsilon\lambda\rho_w} \quad (\text{sec}^{-1}) \qquad (98)$$

The superficial gas velocity is given, in standard units, by Equation 82 or, after substitution from Equations 84 and 86, by

$$u = \frac{Q_{st}}{A} = K_r \frac{\mu_w}{\mu_a}\left(\frac{\Delta p + 1}{2}\right) \frac{2\pi}{\rho_w c} \frac{R_s}{2\theta_f}\left(\frac{\alpha R_s + 2N\alpha_m}{\alpha R_s + N\alpha_m}\right) \tag{99}$$

The molar concentrations, n, can be replaced by the corresponding vapor pressures using

$$n_m = p/R_g T_o \tag{100}$$

where R_g is the gas constant (ergs/°K mole) and T_o is temperature (°K).

Combining Equations 97-100, the final expression for the relative dewatering rate becomes

$$J_r = \frac{K_1}{S\varepsilon\lambda}(p_o - p_l)K_2 \frac{\Delta p_o + 1}{2} \frac{R_s}{c\theta_f}\left[1 - \exp\left(-\frac{K_3}{K_2} \frac{2}{\Delta p_o + 1} \frac{c\theta_f}{R_s}\right)\right] \tag{101}$$

in which

$$K_1 = \frac{M_w}{\rho_w R_g T_o} \tag{102}$$

$$K_2 = \frac{K_r \mu_w \pi}{\mu_a \rho_w}\left(\frac{\alpha R_s + 2N\alpha_m}{\alpha R_s + N\alpha_m}\right) \tag{103}$$

$$K_3 = k_e \lambda S_v (1 - \varepsilon) \tag{104}$$

In order to apply Equation 101, it is necessary to evaluate the constants K_1, K_2 and K_3. The value of K_2 can be estimated from the air consumption data shown in Figure 12. The intercept of the line on the ordinate axis is R_a=-0.025, which leads to

$$38.84 = K_r \frac{\mu_w}{\mu_a}\left(\frac{\Delta p + 1}{2}\right)\left(\frac{\alpha R_s + 2N\alpha_m}{\alpha R_s + N\alpha_m}\right) \qquad (105)$$

from which K_2 can be calculated. The evaporation rate constant can be estimated from data on heat and mass transfer coefficients. Following McCabe et al., (30):

$$k_e \cong 0.0177\, u^{0.8} \qquad (106)$$

where u is given in cm/sec. Using Equation 106, and the test data given in Table IX, K_3 can be estimated.

The vapor pressure at 298 K is 2.4 kPa. Based on an assumption that air entering the filter is at 50% saturation, the relative moisture removal rate, J_r (from Equation 101) is 5.79×10^{-5} sec^{-1}.

Table IX. Test data for estimating contribution from evaporation.

Δp	5 bar
N	0.47 rpm
R_s	490 kg/m^2-hr
M	16.3%
λ	18 mm
θ_f	85°
c	0.65

The fraction of the cycle used for evaporation is given by

$$f_e = \frac{\theta_a - \theta_d}{2\pi} \qquad (107)$$

Under the present conditions, 18% of the cycle is available for evaporation. This translates to 22.66 seconds of evaporation time, which results in an additional 0.13% moisture removal.

Repeating these calculations for heated air (at 90°C) being blown in after the dewatering cycle (such that the cake is heated, theoretically, to 90°C instantaneously) shows that the relative moisture removal rate, J_r is 0.068 sec^{-1}. At this rate, the cake is dry in 15 seconds.

These calculations show that evaporation could be a significant factor in dewatering at high temperatures, but its effect is insignificant at room temperature.

Task II - Laboratory Studies:

For the laboratory studies, froth flotation product from three coal preparation processing plants, Illinois No. 6, Pittsburgh No. 8 and Pocahontas No. 3 coals were obtained in plastic lined fifty-five gallon drums. Representative samples of the clean coal slurries were characterized for percent solids, particle size and ash distribution. Tables X, XI and XII list characterization data for Illinois No. 6, Pittsburgh No. 8 and Pocahontas No. 3 froth samples, respectively. Note, that all the product had low ash content. However, the particle size distribution was significantly different from each other. Illinois and Pocahontas coal had more than 45 weight percent of particle in plus 100 mesh (150 micron) size, whereas, Pittsburgh coal had only 3 weight percent in plus 100 mesh and more than 42 weight percent in minus 500 mesh (25 micron) size. The solids content of Pittsburgh coal slurry was 11 percent, whereas the other two coal slurries had about 25 percent solids. As expected, the highest amount of the ash was present in the finest fractions of the coal slurries.

Dewatering Studies:

Laboratory dewatering studies were conducted using the test apparatus shown in Figure 13. For the present study, two types of filter media, namely, Whatman No. 1 filter paper and a fabric filter (manufactured by Tetko Inc., Lancaster, NY) were used. The fabric

Table X. Particle Size and Ash Distribution Data for Illinois No. 6 Clean Coal Froth Slurry

Size (Mesh)	Weight Percent	Ash Percent	Percent Ash Distribution
+100	45.84	4.28	34.2
100x200	14.72	4.77	12.2
200x325	7.72	5.43	7.3
325x500	11.85	3.71	7.7
-500	19.87	11.14	38.6
Feed (Calc)	100.00	5.73	100.0
(Actual)		6.43	

Percent Solids in Froth = 26

Table XI. Particle Size and Ash Distribution Data for Pittsburgh No. 8 Clean Coal Froth Slurry

Size (Mesh)	Weight Percent	Ash Percent	Percent Ash Distribution
+100	2.77	2.43	0.8
100x200	19.14	2.52	5.6
200x325	13.59	3.34	5.2
325x500	22.23	3.98	10.2
-500	42.27	15.92	78.2
Feed (Calc)	100.00	8.60	100.0
(Actual)		8.78	

Percent Solids in Froth = 11

Table XII. Particle Size and Ash Distribution Data for Pocahontas No. 3 Clean Coal Froth Slurry

Size (Mesh)	Weight Percent	Ash Percent	Percent Ash Distribution
+28	4.5	3.02	2.4
28x48	24.8	3.61	16.1
48x100	20.5	4.20	15.5
100x200	17.3	4.44	13.8
200x325	6.9	3.95	4.9
-325	26.0	10.00	47.3
Feed (Calc.)	100.0	5.53	
(Actual)		5.55	

% Solids in Froth = 25

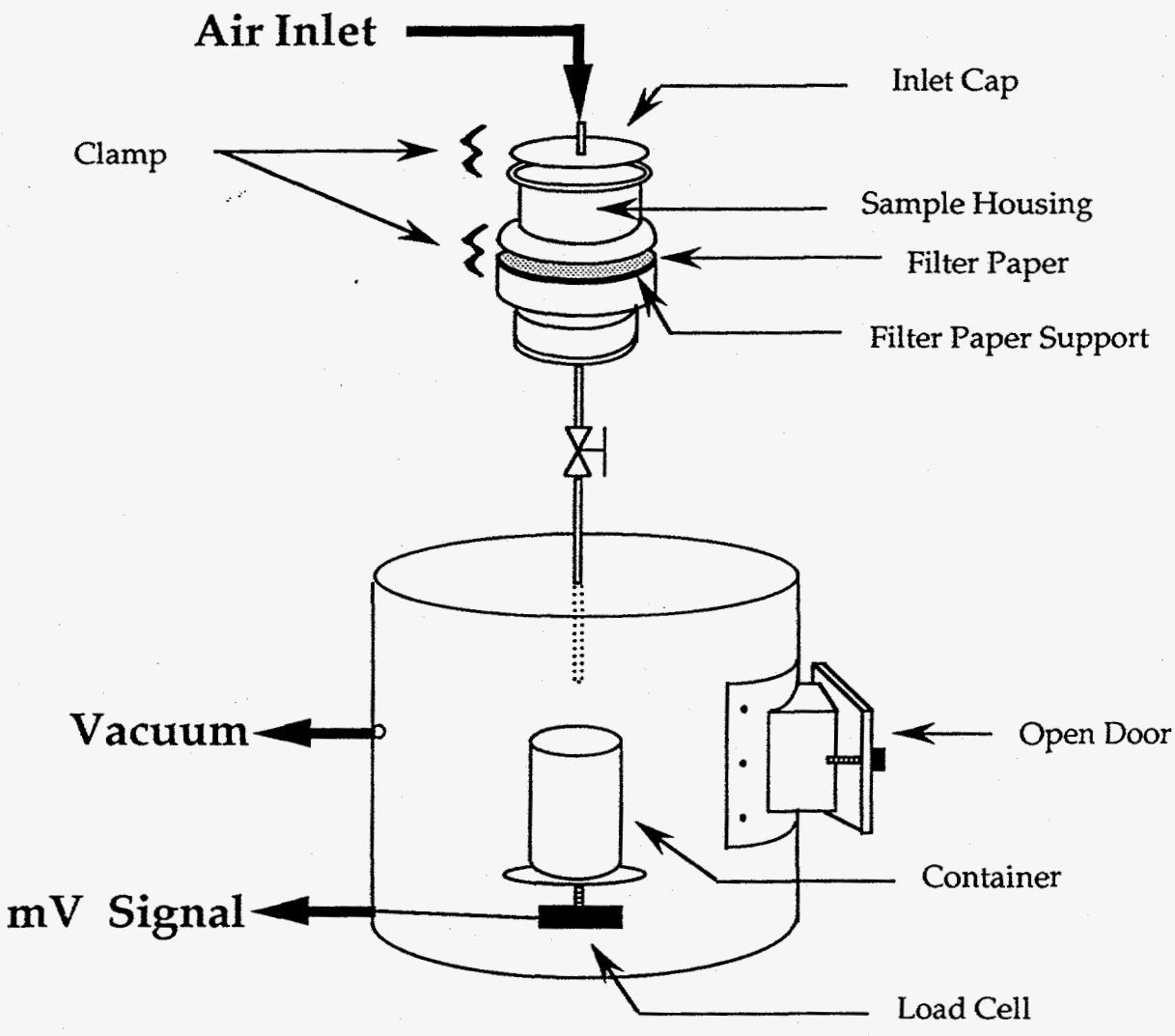

Figure 13. Laboratory equipment setup for high pressure and vacuum dewatering studies.

filter was selected based on the recommendation made by Andritz Ruthner Inc., manufacturer of the commercial scale hyperbaric filter system.

For the laboratory tests, a known volume of the slurry was obtained from a well-mixed suspension stored in a 5-gallon bucket. The slurry sample was conditioned in a 250 ml beaker for 3 minutes after the pH was stabilized. The volumes of reagents added were less than 5 ml, so that the solid concentrations of the slurries remained essentially unaffected by the addition of the reagents. The conditioned slurry was poured into the filtration cell and pressure was applied while simultaneously starting a digital timer and load cell-computer system. The filtration flow rate was recorded by the load cell-computer system and after the desired filtration time, the pressure was turned off. The filter cake was removed from the filtration cell, weighed and dried at 100°F for 24 hours and weighed again to determine the cake moisture using the following formula:

$$\%\ Cake\ Moisture = \frac{Weight\ of\ Wet\ Cake - Weight\ of\ Dry\ Cake}{Weight\ of\ Wet\ Cake} \times 100$$

In this investigation, three surfactants, five flocculants and two metal ions were studied as the enhancement additives in the fine coal dewatering. The choice of reagents was based on commercial availability and literature studies. The surfactants used are listed in Table XIII. One percent stock solution of each surfactant was prepared daily for the tests. The flocculants used are given in Table XIV. A 0.1 percent stock solution was prepared daily for filtration studies. Copper (Cu^{2+}) and aluminum (Al^{3+}) ions were obtained by dissolving their chloride salts into water.

Figure 14 shows vacuum (30-in Hg) dewatering data of all the three slurries. Note, that the Pittsburgh coal slurry because of its fine size particles did not dewater significantly.

Table XIII. List of Surfactants Used for the Study

	Sodium 2-Ethylhexyl Sulfate	Octyl Phenoxy Polyethoxy Ethanol	1-Hexadecyl Pyridinium Chloride
Type	Anionic	Nonionic	Cationic
Commercial Chloride Name	NAS 08	TRITON X-114	Cetyl Pridium Chloride
Active Ingredient (weight %)	40	100	100
Formula	$C_4H_6(C_2H_5)CH_2$-SO_4Na	C_8H_{17}-C_6H_4-$(OCH_2CH_2)_{7-8}OH$	$C_{16}H_{33}C_5H_5NCl$
Molecular Weight	232	536	340
Manufacturer	Niacet Corporation Niagara Falls, NY	Rohm and Haas Philadelphia, PA	Sigma Chemical Co. St. Louis, MO

Table XIV. List of the Flocculants Used for the Study

Name	Ionic Character	Mol. Wt.
Superfloc 204 Plus	Anionic	4-6
Superfloc 16	Non-ionic	4
Magnifloc 494C	Cationic	4

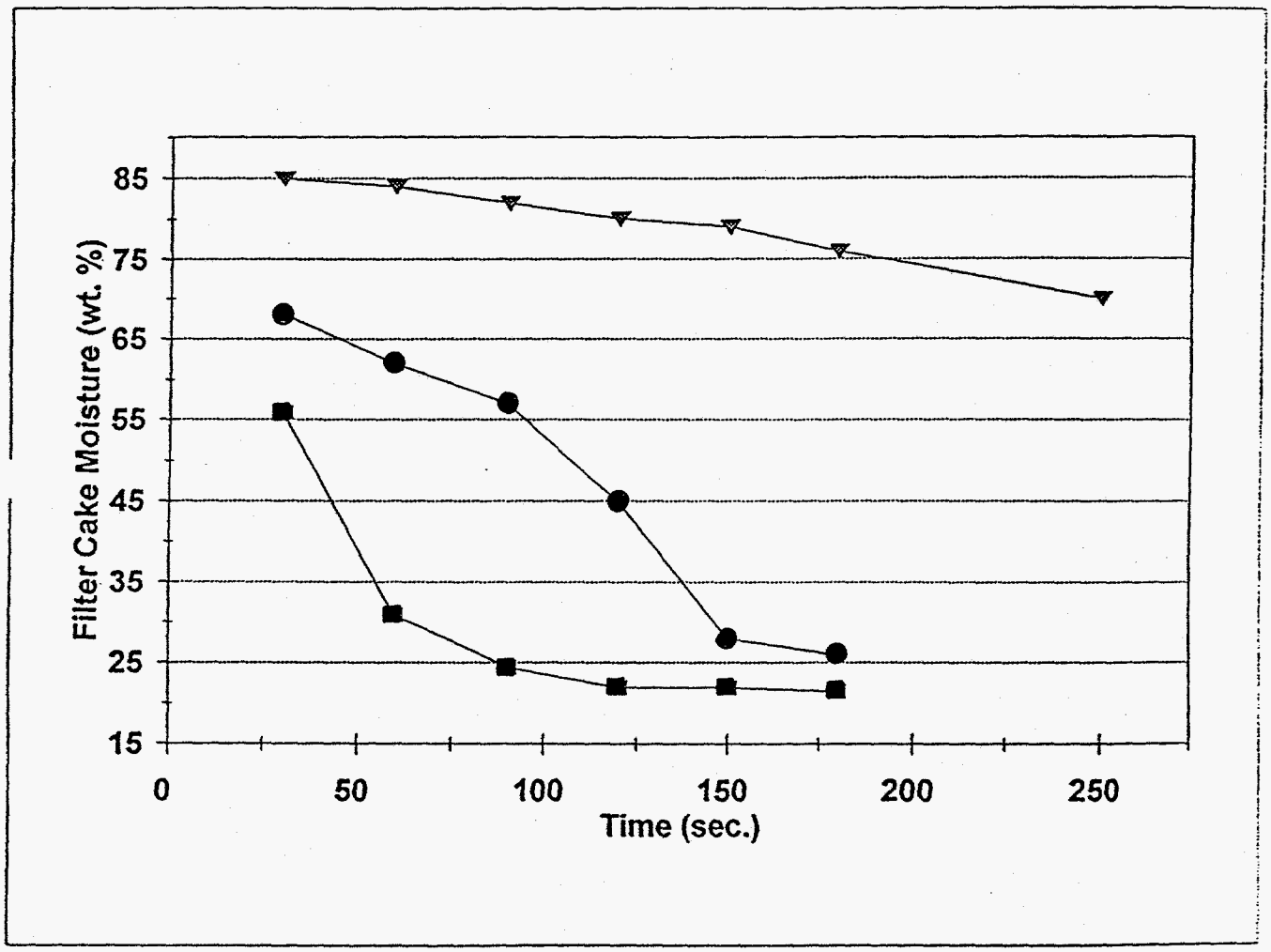

Figure 14. Vacuum filtration data of Illinois No. 6 (▼), Pittsburgh No. 8 (●) and Pocahontas No. 3 (■) clean coal slurries as a function of filter cake moisture and filtration time

Both Illinois and Pocahontas coal slurries dewater to about 25 percent moisture. This data clearly indicates that vacuum dewatering will not be applicable for ultra-fine coal particle slurries.

In the initial high pressure dewatering studies, it was observed that the filter cake obtained using the Illinois No. 6 was segregated; smaller size particles were at the top and larger particles were at the bottom of the filter cake. To avoid this problem and to obtain a uniform distribution of particles, a modified pressure filter cell which provided continuous agitation of slurry was developed. Figure 15 shows the modified filtration cell and the filtration setup used for the study.

The size analysis of the three different sections of the filter cake obtained without and with agitated during filtration is shown in Figure 16. Note, that the filter cake obtained with the modified system provided a more uniform cake structure. Morphology of the cake structure was studied using image analysis of the in-situ consolidated filter cake. A mixture of epoxy system consisting of a Buehler resin (20-8130), a hardener (20-8132), and acetone with volume ratio of 3:1:4, was used as a consolidating agent. After solidification, the filter cake was sectioned into various layers and polished for the image analysis. The photo-micrographs of the various layers of filter cake formed without and with agitation of the slurry are shown in Figure 17.

Figure 18 shows the comparison of high pressure dewatering data for the Illinois coal slurry obtained using the modified filter unit using agitated and non-agitated slurry. Note, that the slurry agitated while filtering provided much lower moisture compared to without agitation. The rest of the data reported hereafter were obtained using the agitated slurry in the modified filter unit.

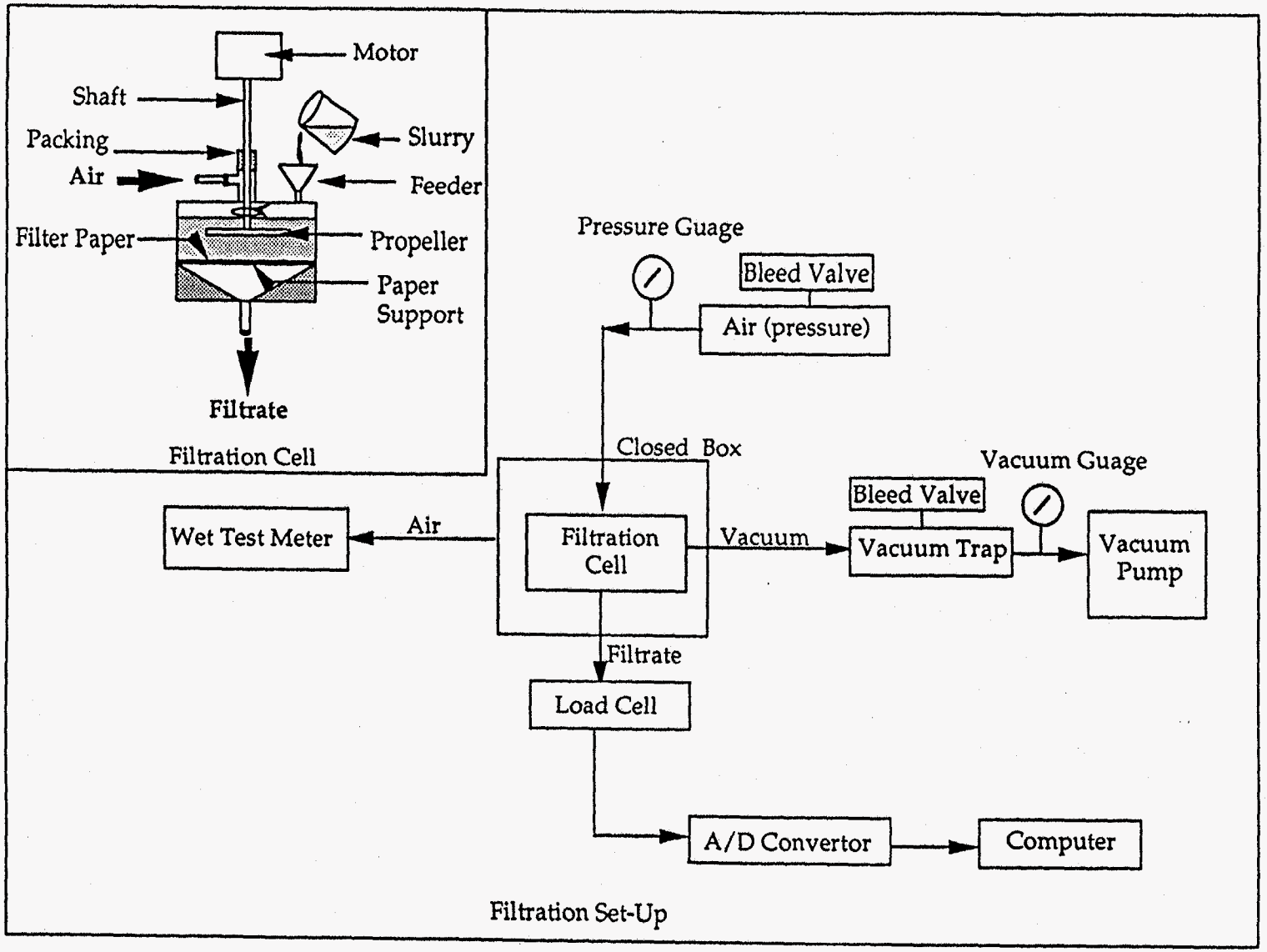

Figure 15. Modified laboratory filtration cell and dewatering equipment setup.

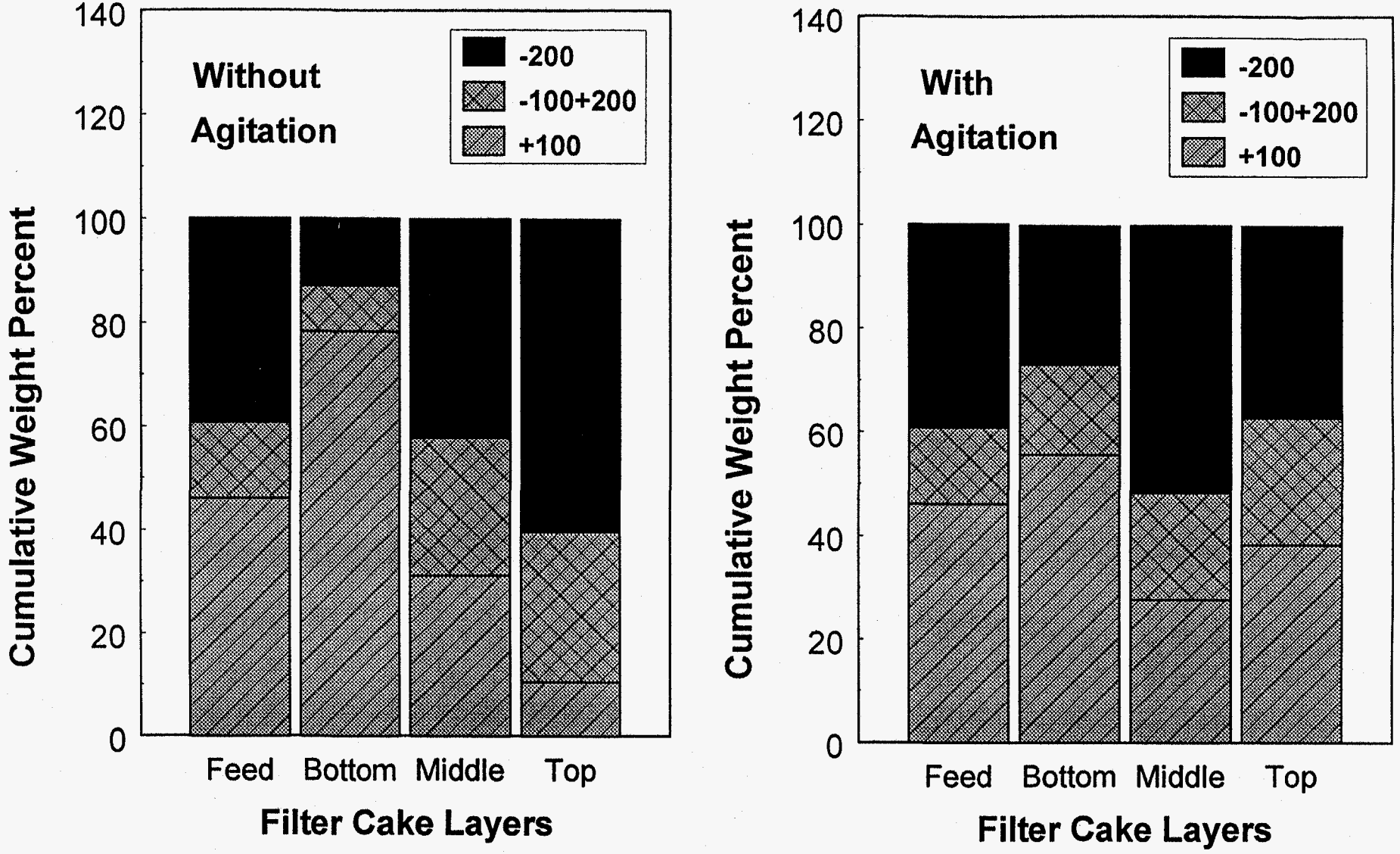

Figure 16. Particle size distribution in filter cake obtain without and with agitated (modified filtration cell) slurry.

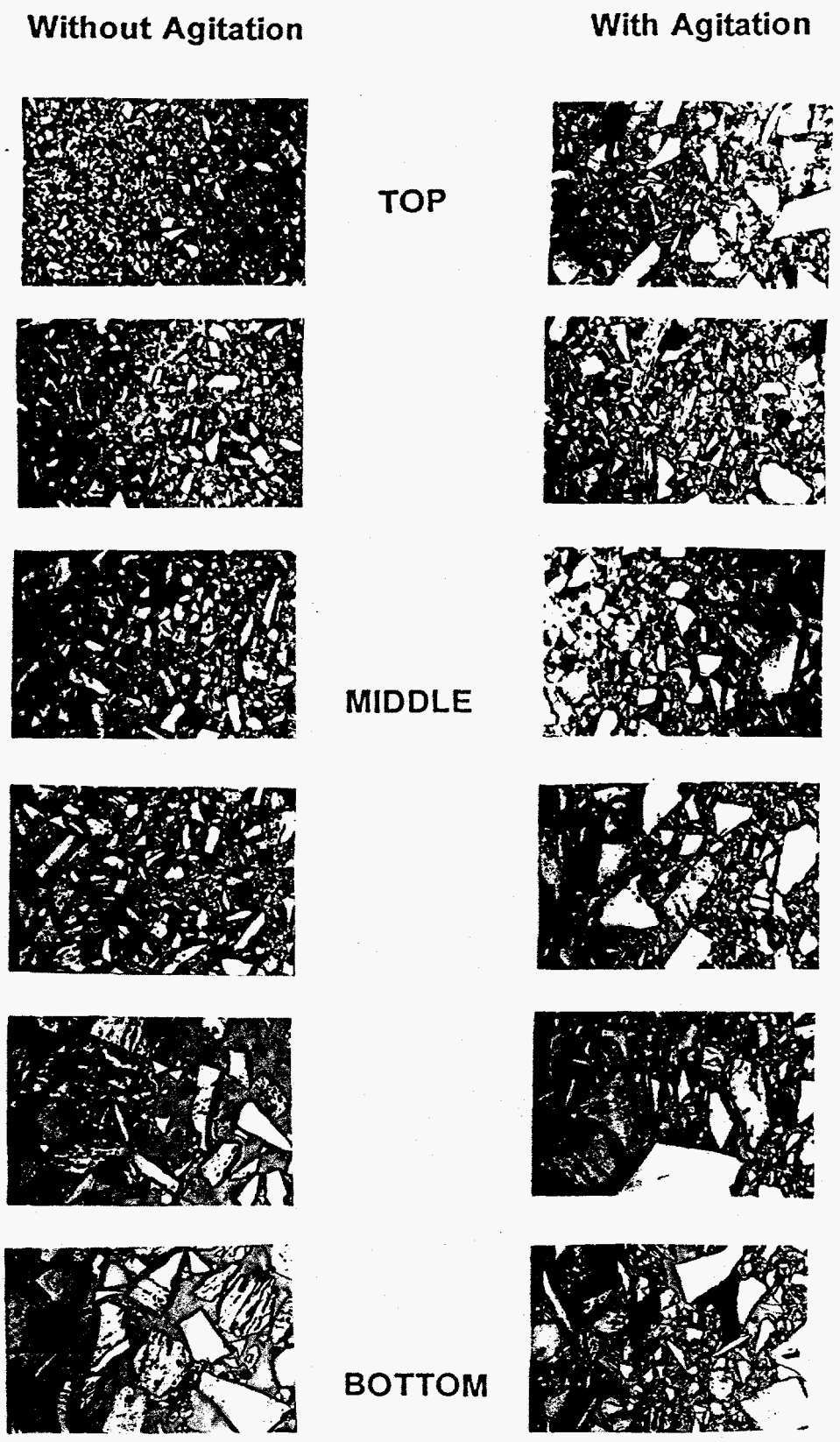

Figure 17. Photomicrographs of the various layers of filter cake obtained without and with agitation of the slurry during filtration.

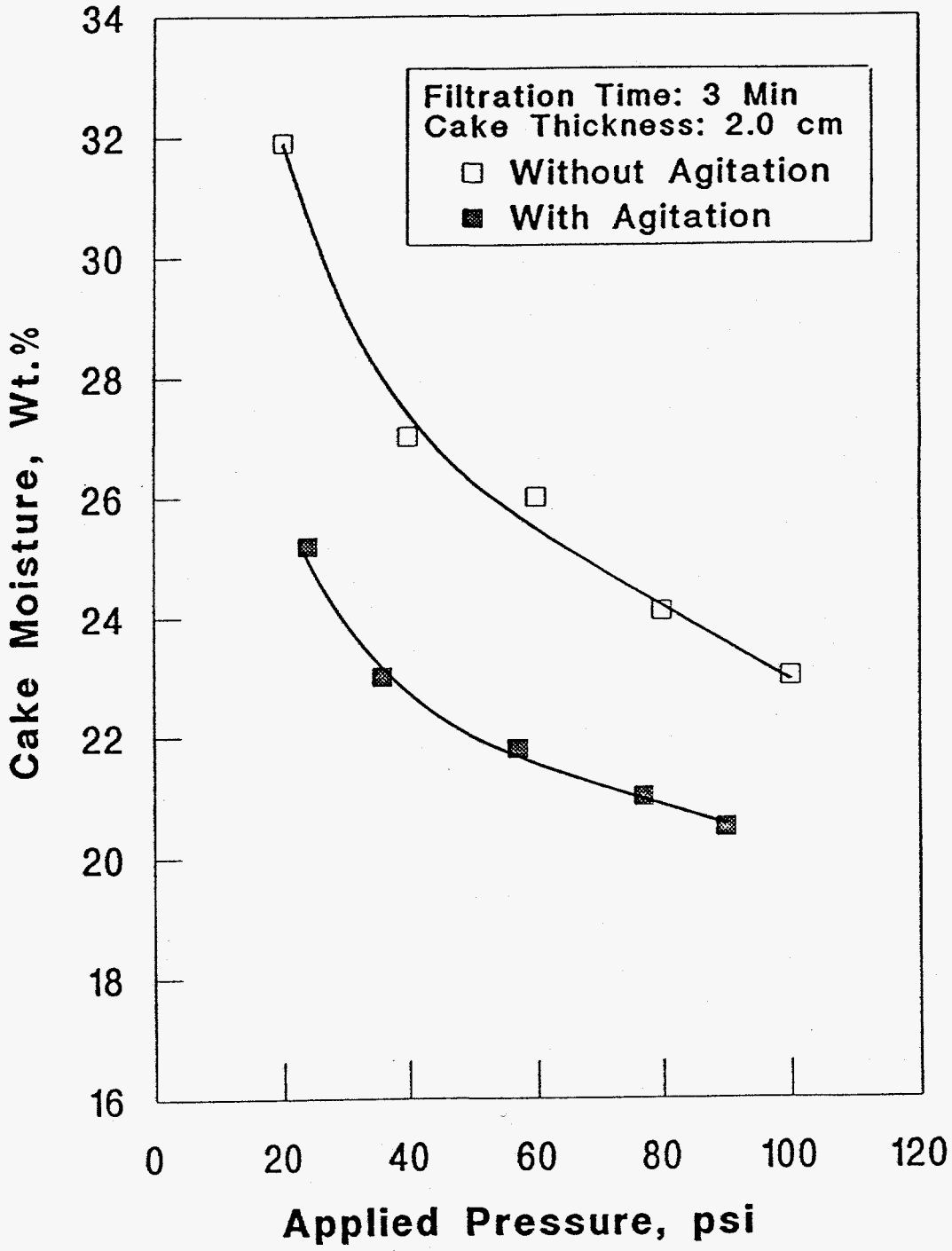

Figure 18. High pressure dewatering data of Illinois No. 6 clean coal slurry obtained with and without agitation of the slurry during filtration.

The effect of filtration time using two different pressures and cake thicknesses is shown in Figure 19. It shows that a cake thickness of 1.4 cm with about 3 minutes filtration time will be optimum for the dewatering of the slurry. A comparison of dewatering of all the three coal slurries with respect to pressure is shown in Figure 20. Note, that at about 60 psig (4 bar) pressure filter cakes with 25 percent, 22 percent, and 12 percent moisture are obtained for Pittsburgh, Illinois, and Pocahontas slurries, respectively.

Effect of Temperature:

The effect of increasing slurry temperature for all the three clean coal slurries is shown in Figure 21. In general, increasing slurry temperature lowered the filter cake moisture. The most significant filter cake moisture reduction was observed with the Pittsburgh coal slurry where increasing slurry temperature from 20° to 40°C lowered the filter cake moisture from 24 percent to 17.5 percent. The lowering of filter cake moisture using hot slurry could be attributed to a combination of lowering of surface tension and viscosity and also increasing the hydrophobicity of the coal particles. For example, the viscosity of the filtrate reduced from 1.00 to 0.28 cP when temperature was increased from 20°C to 100°C. Similarly, the surface tension of the slurry reduced from 70 dynes/cm to 40 dynes/cm and the contact angle on coal increased from 70° to 95°, as the slurry temperature was increased from 20° to 100°C.

Effect of pH:

The pH is an important parameter with respect to bulk chemistry and surface chemistry of solids suspended in an aqueous medium. In a solid/liquid/gas phase system, pH affects the chemical species distribution in bulk, zeta potential at the solid/liquid interface and other surface chemical properties. Figure 22 shows the effect of pH on zeta potential and

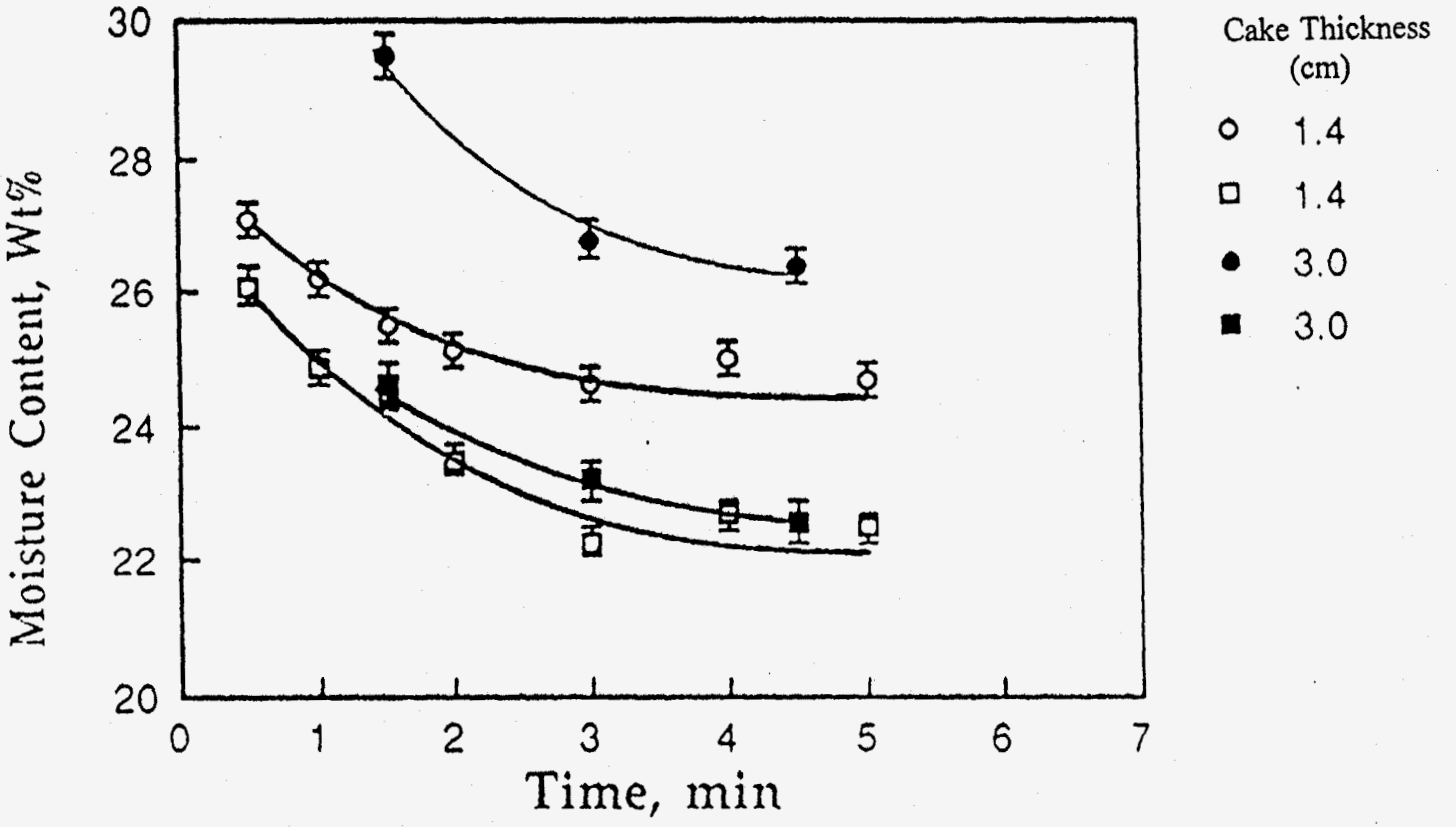

Figure 19. Effect of filtration time on filter cake moisture using 40 psig (O) and 80 psig (□) pressure with two different cake thickness.

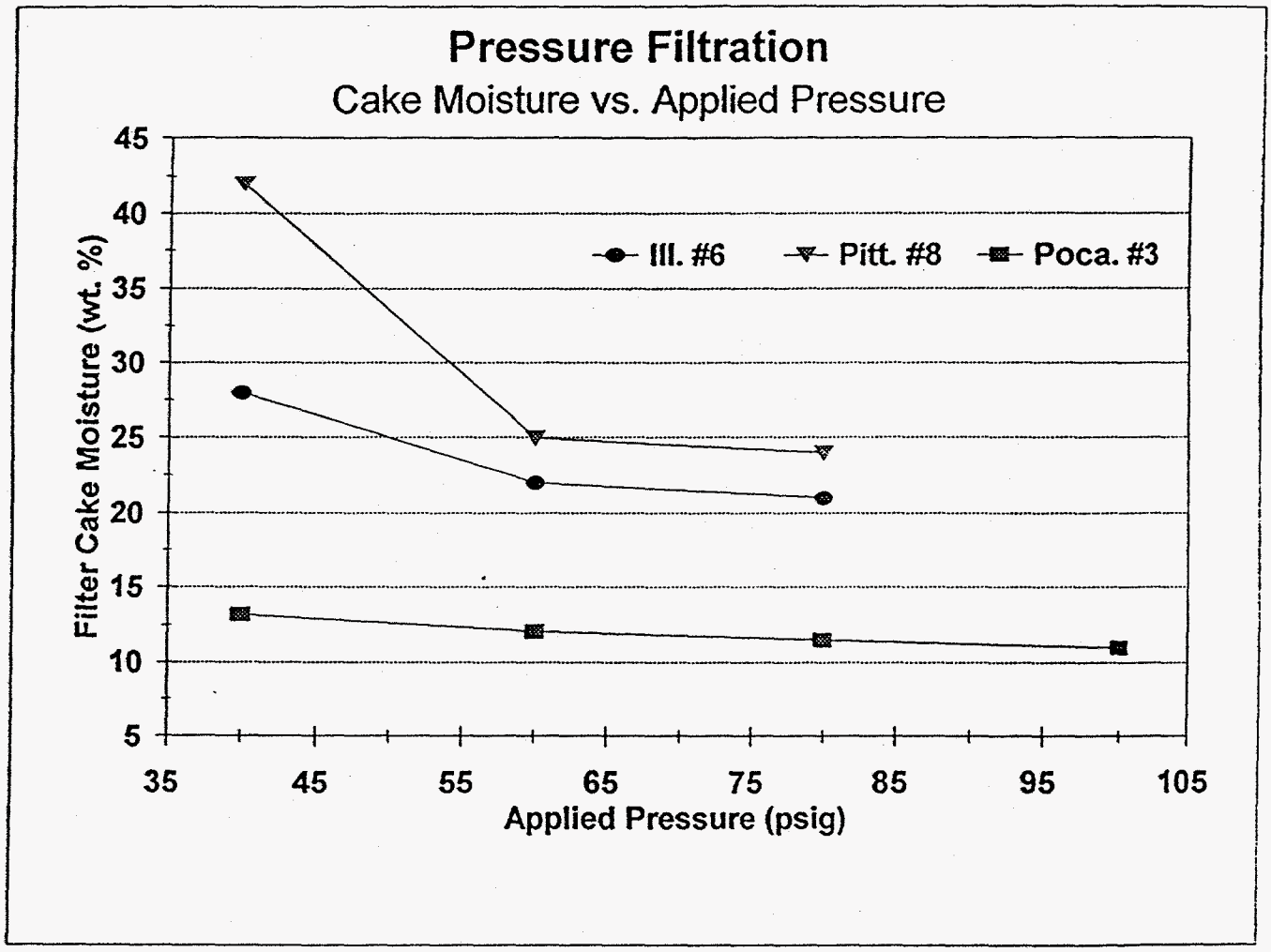

Figure 20. Filter cake moisture versus applied pressure data for the Illinois No. 6, Pittsburgh No. 8 and Pocahontas No. 3 clean coal slurries.

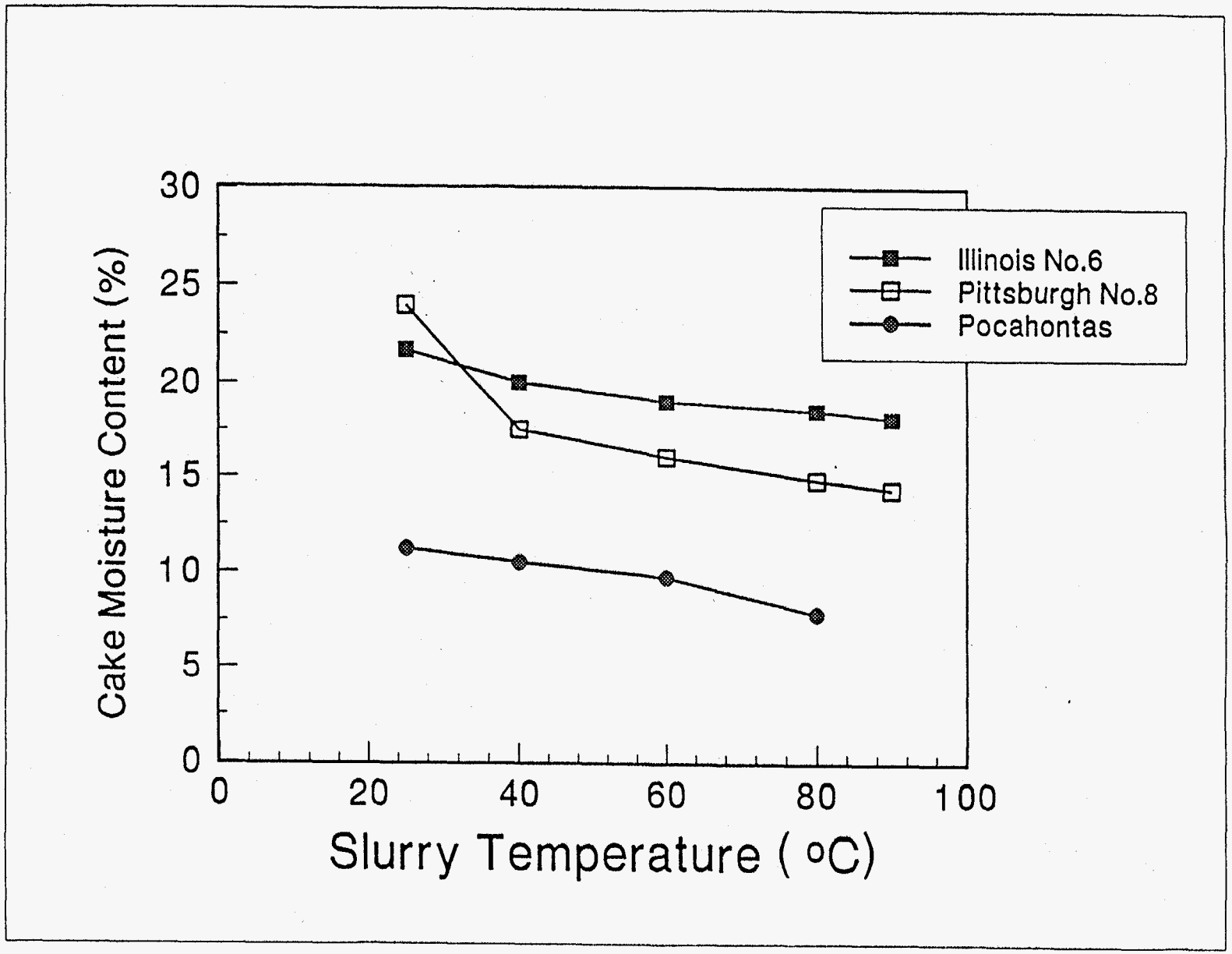

Figure 21. Effect of slurry temperature on filter cake moisture.

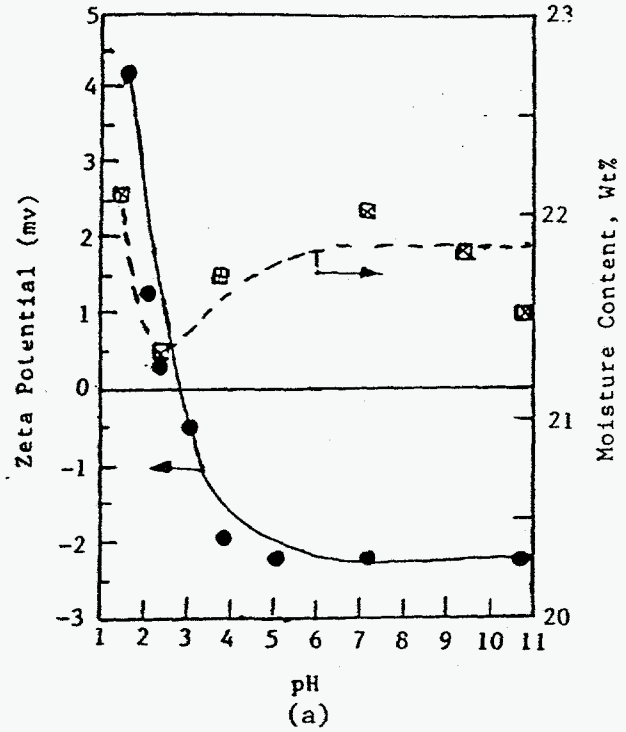

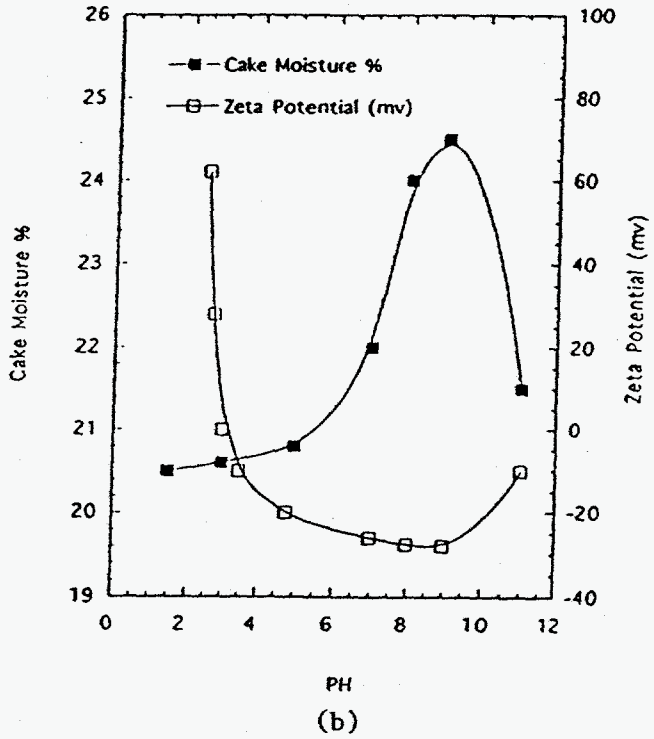

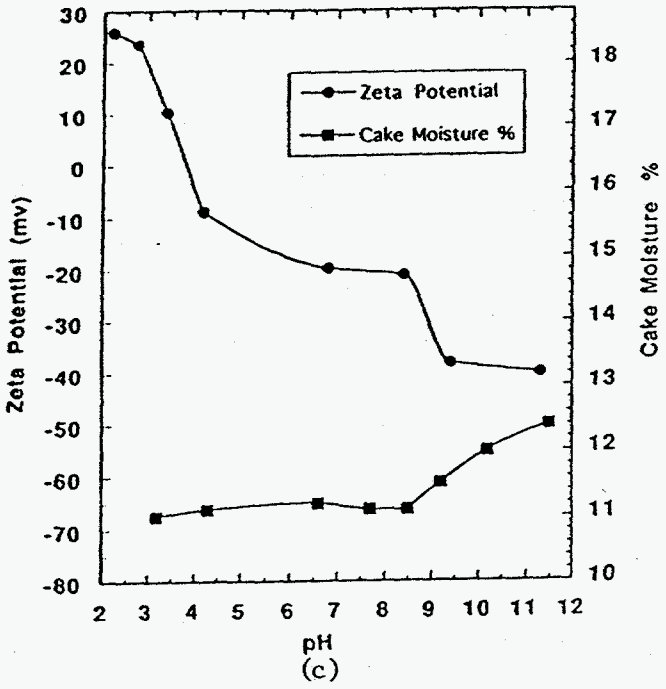

Figure 22. Effect of pH on electrophoretic mobility and filter cake moisture for the (a) Illinois No. 6 coal, (b) Pittsburgh No. 8 and (c) Pocahontas No. 3 clean coal slurries.

filter cake moisture of (a) Illinois, (b) Pittsburgh, and (c) Pocahontas clean coal slurries. Note, that all the three coal slurries show lowering of filter cake moisture around pH 4.0 which is the iso-electric point (IEP) of the coal particles. For Pittsburgh coal, the filter cake moisture increases from 20.5 to 24.5 percent as pH is increased from 4 to 9.5.

Effect of Particle Size:

Particle size plays a very important role in dewatering process. Table XV shows the dewatering data for various size fractions of the three coal slurries. It can be seen from the table that as expected, the finer fractions (minus 200 mesh) have significantly higher moisture than the plus 200 mesh size fractions. These data show that to obtain a low moisture filter cake either classify the material at 200 mesh and filter the +200 mesh and -200 mesh material separately, or, increase the fine particle size by flocculation. Results of these two approaches are described below.

Split Size Dewatering: For this approach, the coal slurry was classified into two different size fractions and each fraction was dewatered separately and the final moisture was calculated by combining the moisture of the both size fractions. Figures 23 and 24 show the results of split size filtration at different split particle sizes for the Pocahontas No.3 and Pittsburgh No.8 coal, respectively. For the Pocahontas No. 3 coal slurry, split size filtration at 100 and 200 mesh provided a 7.5 percent moisture product, a 3.5 percentage point absolute or 31 percent relative moisture reduction over the baseline product moisture of 11 percent. For the Pittsburgh No. 8 coal, split size filtration at 500 mesh yielded a 17 percent moisture product, a 7 percentage point absolute or about 33 percent relative moisture reduction. Even at 200 mesh split size dewatering provided a 20.5 percent product moisture which is about 15 percent improvement in moisture reduction.

Table XV. Cake Moisture of Various Size Fractions of the Illinois No. 6, Pocahontas No. 3, and Pittsburgh No. 8 Coal Slurries

Illinois No. 6 Coal		**Pocahontas No. 3 Coal**		**Pittsburgh No. 8 Coal**	
Size Fraction (mesh)	Cake Moisture %	Size Fraction (mesh)	Cake Moisture %	Size Fraction (mesh)	Cake Moisture %
+60	11.8	28x100	2.5	100x200	4.2
60x100	13.9	28x200	3.3	100x400	6.7
100x200	16.6	28x400	7.2	100x500	7.3
-200	27.0	-100	15.42	-200	24.91
---	---	-200	16.47	-400	25.87
---	---	-400	23.9	-500	27.93
Feed	2.0	Feed	11.0	Feed	24.0

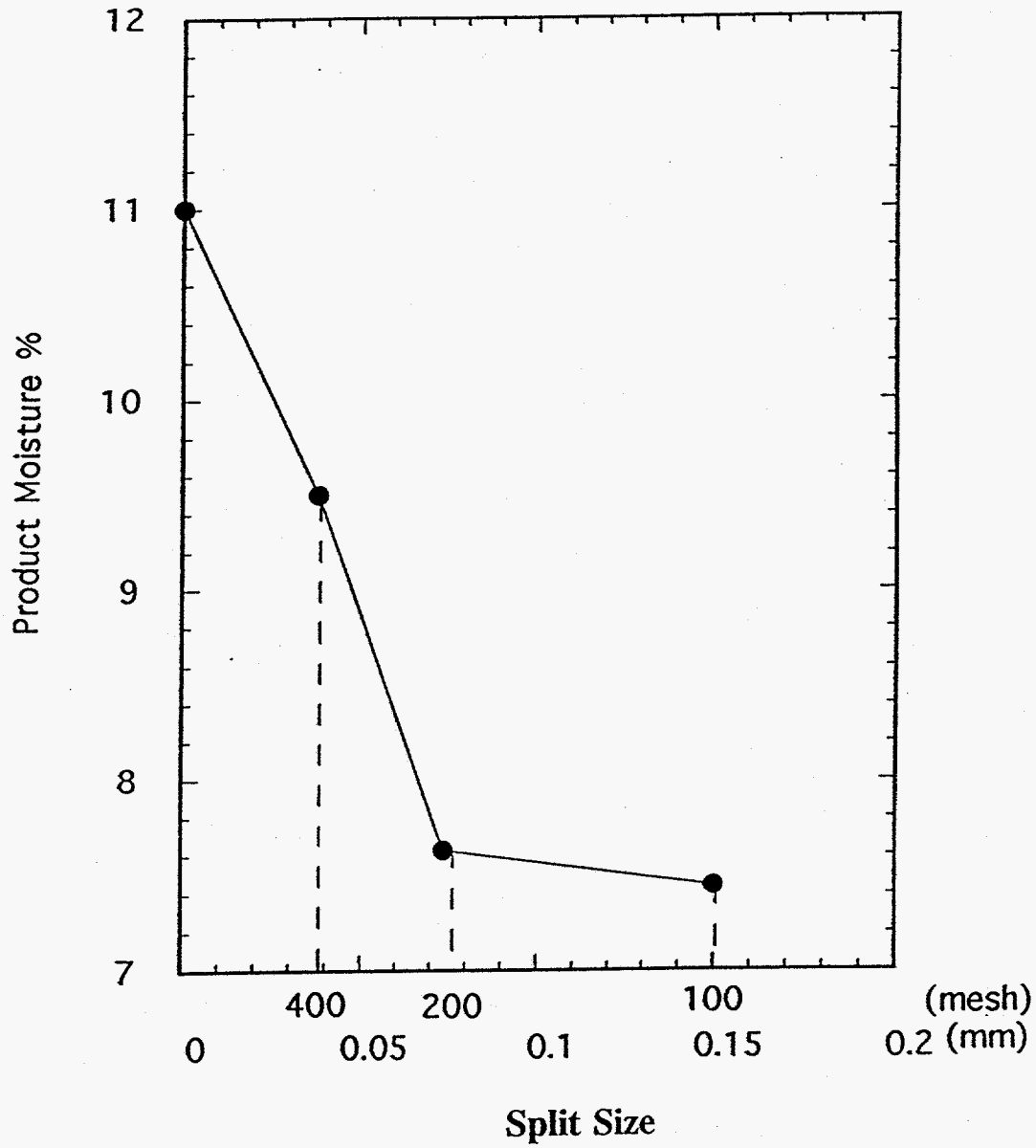

Figure 23. Dewatering data of split size filtration for the Pocahontas No. 3 clean coal slurry.

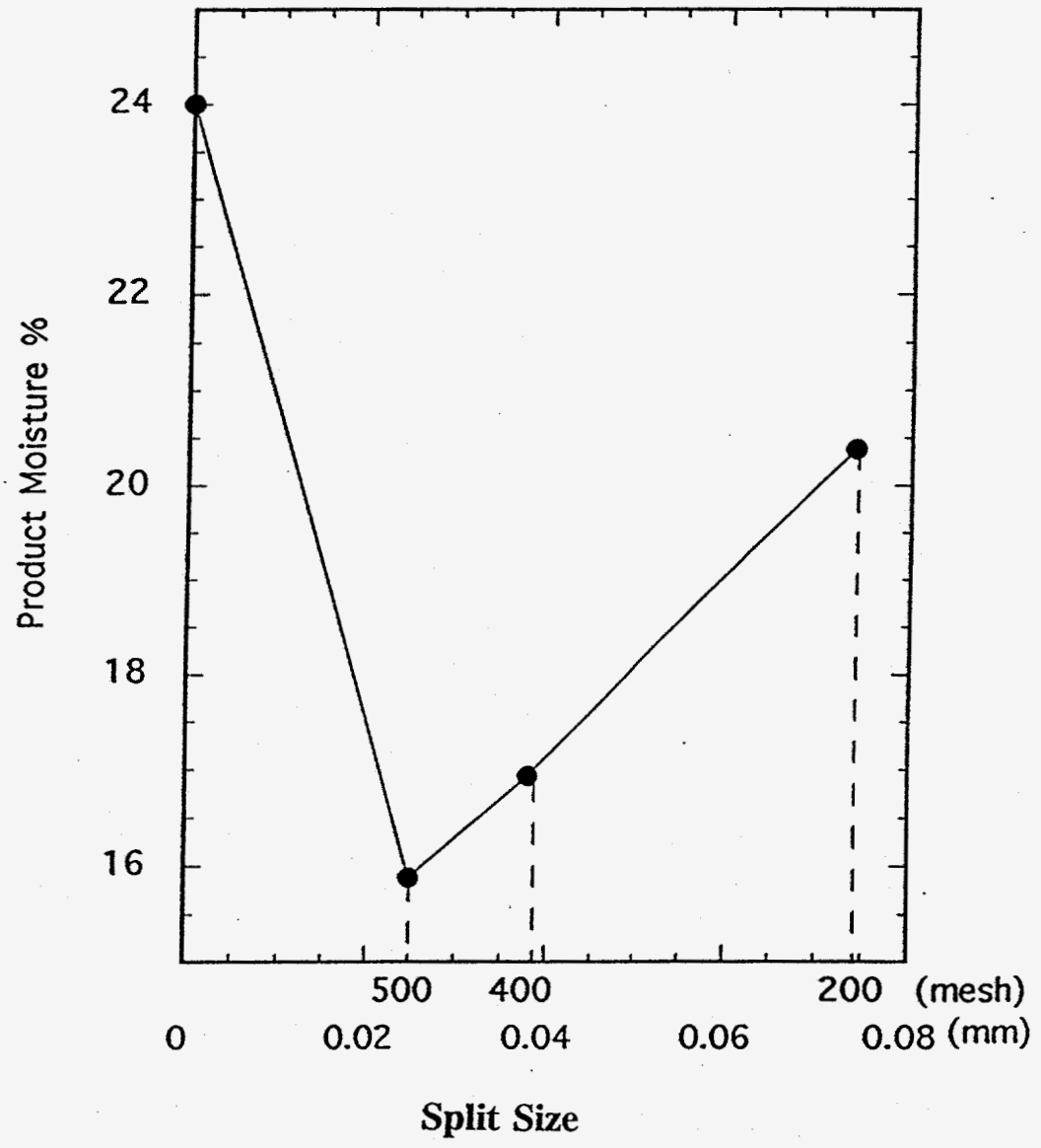

Figure 24. Dewatering data of split size filtration for the Pittsburgh No. 8 clean coal slurry.

The principle of the moisture reduction obtained using the split size filtration could be explained in terms of the particle packing arrangement in a filter cake. The study of systematic packing of uniform spherical particles has given the information that there are six different packing arrangements. Two of them (tight and loose packing) are shown in Figures 25 and 26. In these packing arrangement, each sphere is surrounded by a complex void space, as schematically shown in Figure 26. It is speculated that in a granular particle packing bed, each particle is surrounded by a group of voids which may form the draining channels of water. In this way, a filter cake can be regarded as a porous matrix formed by large particles, in which the voids may be filled by finer particles, water or air. When a cake is formed only by coarser particles, the pores in the cake only are occupied by water and no pores in the cake will be blocked. For a multi-size particle cake, the finer particles and water simultaneously occupy the void spaces formed by coarser particles. The smaller particles in the void spaces will block either completely or partially the void spaces to prevent water from draining out of the cake. The number and diameters of the capillaries in a multi-size particle cake are definitely smaller than in a uniform coarser particle cake.

The cake permeability mainly depends on particle packing arrangement for a coarser particle cake, while the permeability of a multi-size particle cake is mainly determined by the distribution and the amount of finer particles. The moisture of a coarser particle cake is much lower, as compared to a multi-size particle cake. However, there is not much difference in the moisture between multi-size particle cake and finer particle cake because in both cases, cake permeability is principally influenced by finer particles.

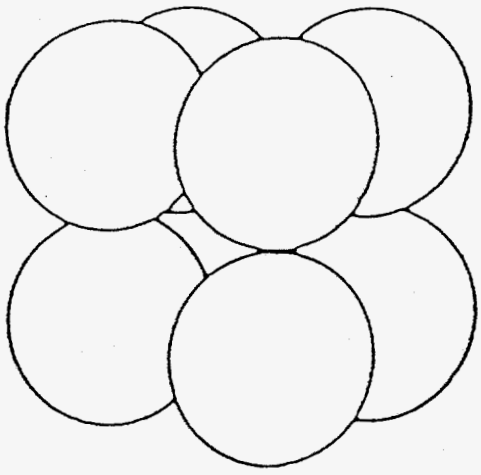

Cubic

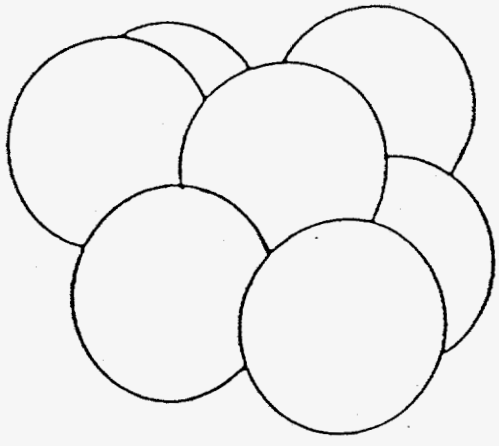

Rhombohedral

Figure 25. Packing arrangement of uniform spheres.

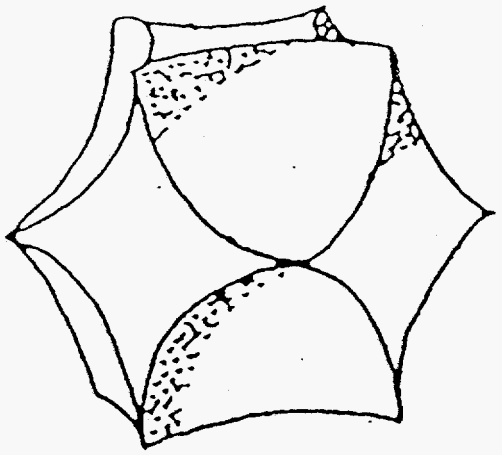

Cubic

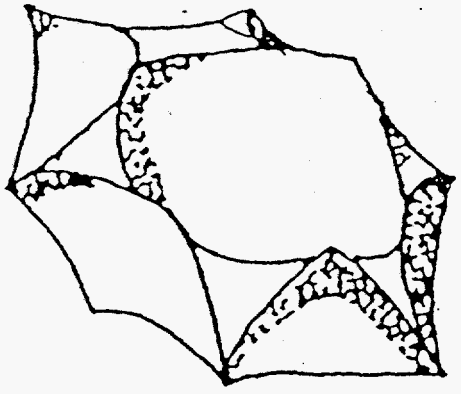

Rhombohedral

Figure 26. Pore spaces in packing of uniform spheres.

Effect of Additives:

Organic flocculants and surfactants are generally used as additives to enhance filtration process. These reagents enhance the filtration process through the modification of the colloidal chemistry properties of the fine coal slurry such as increasing particle sizes, reducing surface tension and surface charge.

Flocculants: Polymeric flocculants are used in many operations for increasing the particle sizes. The principal effect of flocculants is to form "bridges" between particles.[32] This mechanism requires that the flocculant chains be adsorbed from solution onto one particle, and a physical bridge forms between the particles when another particle comes close enough for the extended flocculant chains to be adsorbed onto it. The chain length of flocculants which is directly proportional to the flocculant molecular weight, is an important factor in a flocculation process. Another important factor is the ionic characteristics of the flocculants which controls the adsorption behavior of the flocculants on particles. The addition of flocculants increases particle sizes as well as the filtrate viscosity. The increase of filtrate viscosity is detrimental to the reduction of cake moisture.

The three types of flocculants used in the present study are listed in Table XIV. Figures 27, 28 and 29 show the effect of various types of flocculant dosages on the filter cake moisture for the Illinois, Pittsburgh and Pocahontas clean coal slurries. For the Illinois coal, the anionic flocculant was the most effective providing a 17 percent filter cake at about 120 g/t dosage. For the Pittsburgh and Pocahontas coal slurries, about 60 g/t of the non-ionic flocculant provided filter cakes with about 17.5 percent and 9 percent moisture, respectively.

The relationship between the solution viscosity and flocculant concentration is shown in Figure 30. It can be seen that the solution viscosity increased with flocculant

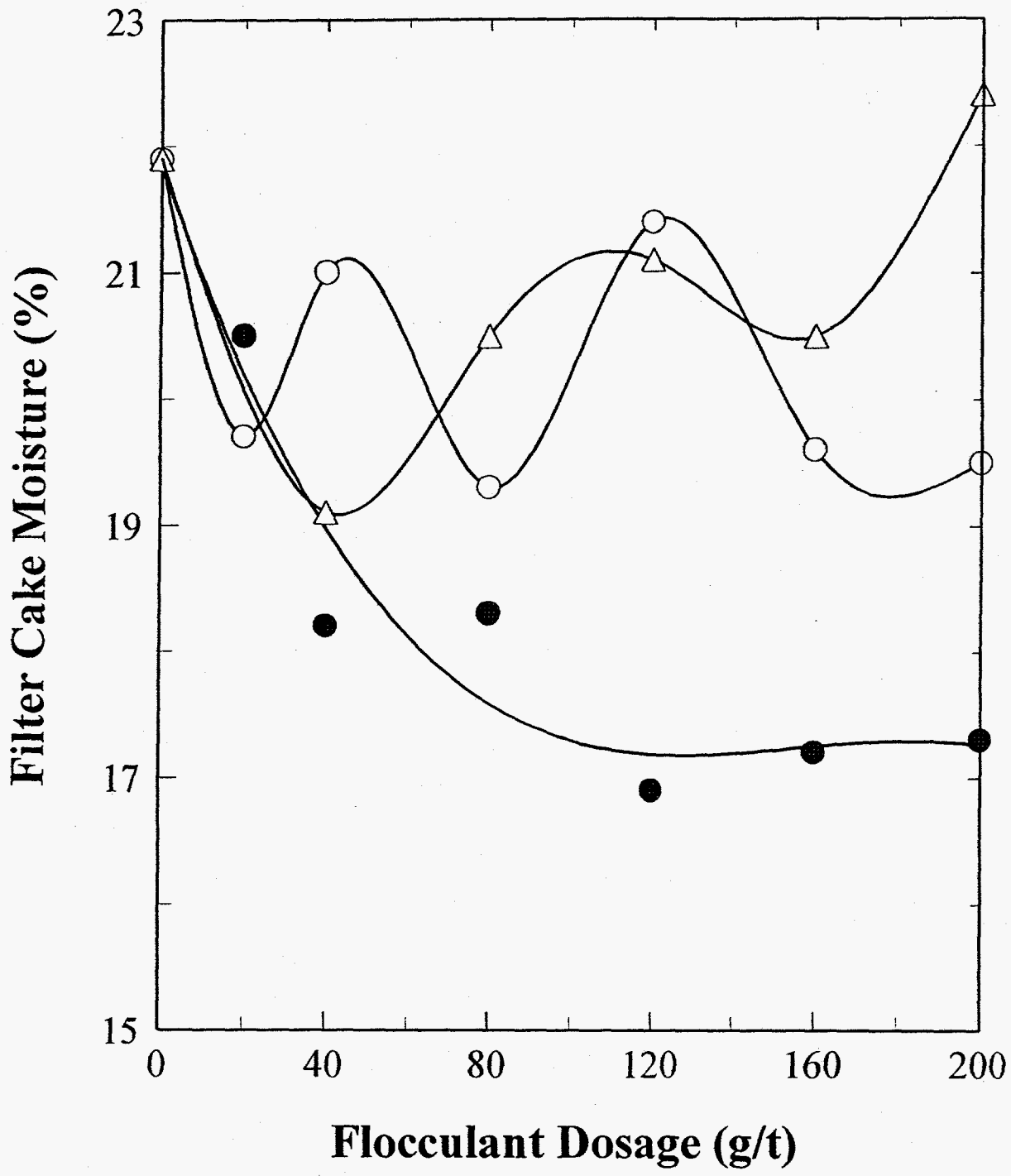

Figure 27. Effect of various flocculants dosage on filter cake moisture of Illinois No. 6 clean coal slurry.

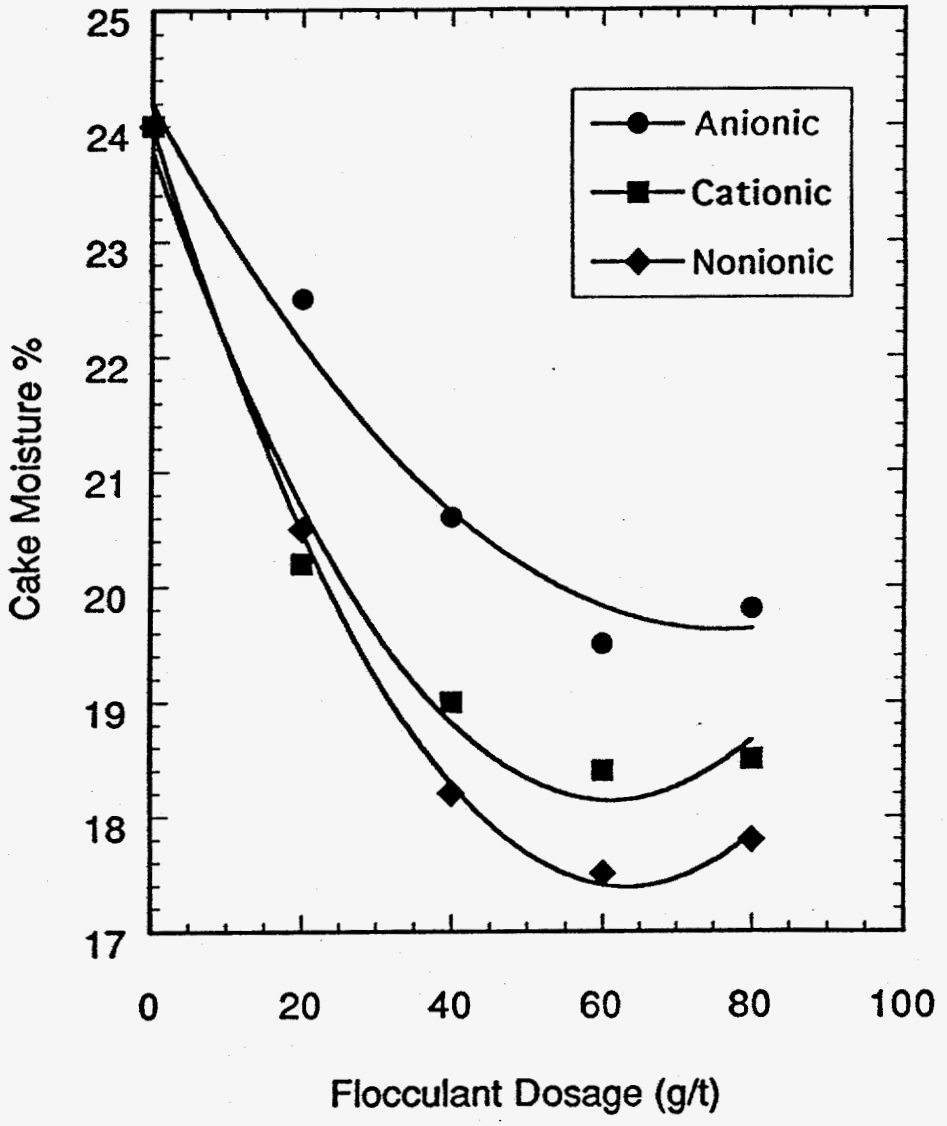

Figure 28. Effect of flocculant dosage on cake moisture for the Pittsburgh No. 8 clean coal slurry.

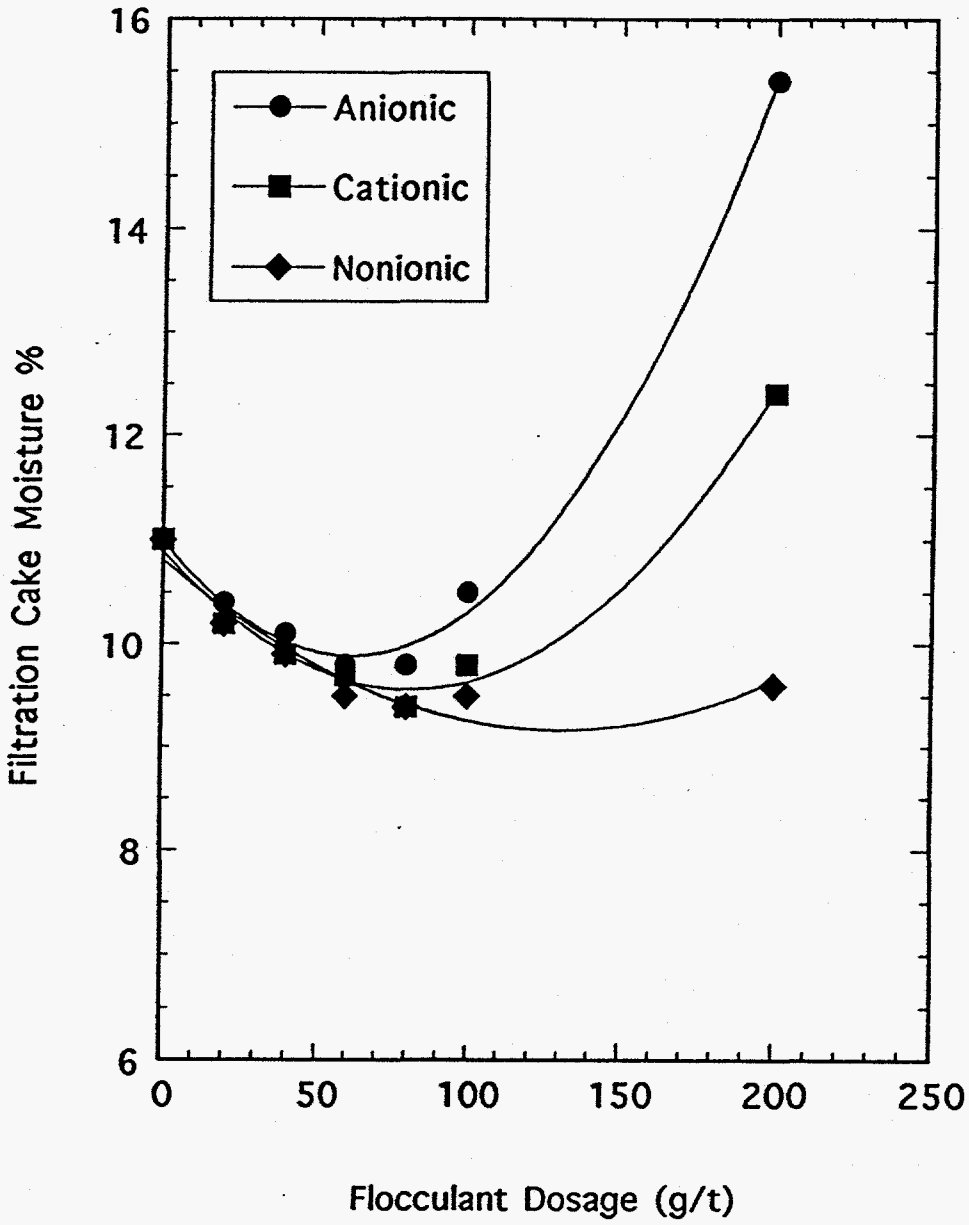

Figure 29. Effect of flocculant dosage on cake moisture for the Pocahontas No. 3 clean coal slurry.

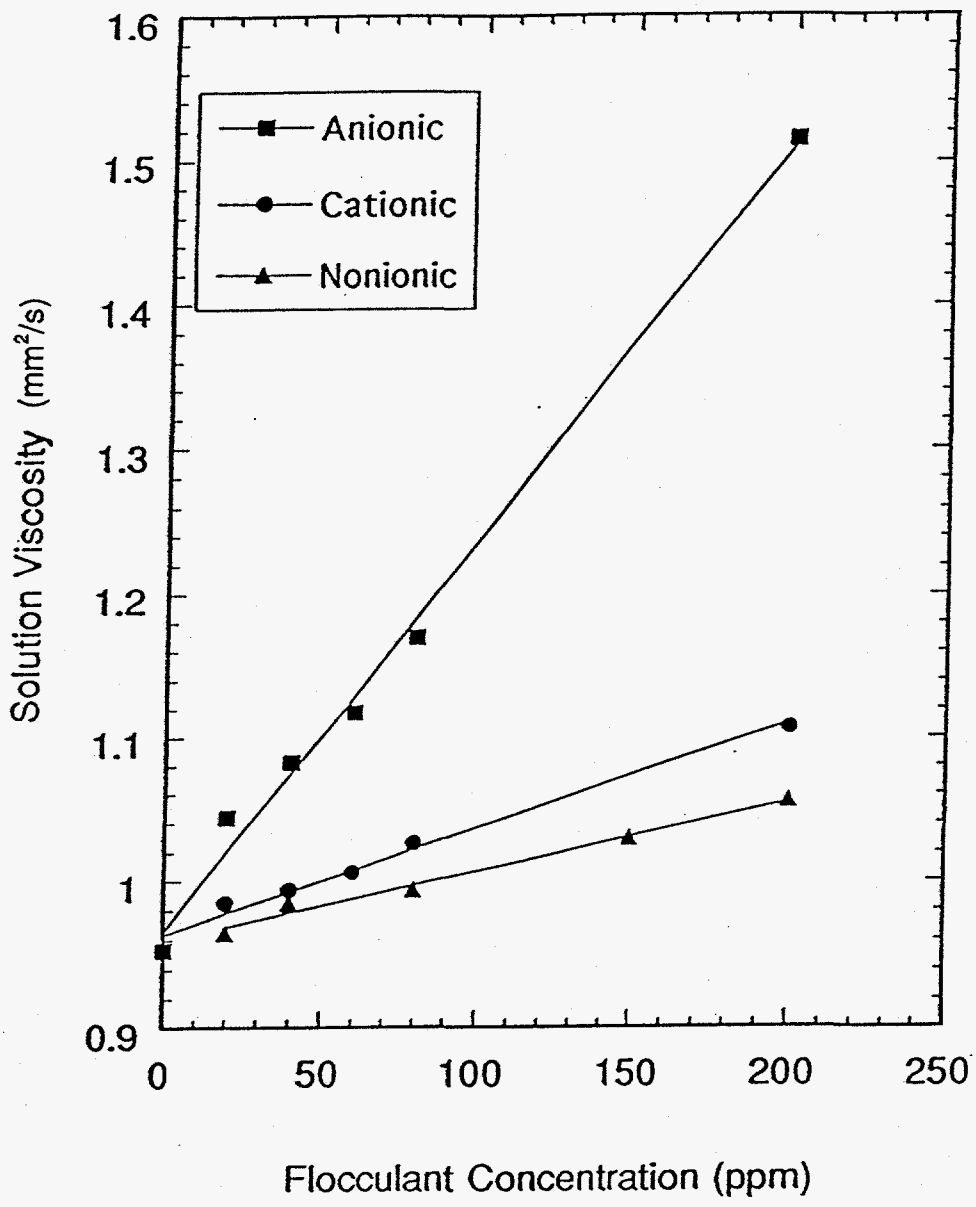

Figure 30. Relationship between flocculant concentration and solution viscosity.

concentration. Thus, in the filtration process, high flocculant dosage lead to the high viscosity of filtrate, which will result in the retention of high moisture on the coal surface. It can also be observed that at the same flocculant concentration, the viscosity of anionic-flocculant solution was higher than those of non-ionic and cationic flocculant solutions. Also, the increase of anionic flocculant concentration caused the solution viscosity to increase very sharply. Therefore, the effect of anionic flocculant on cake moisture was more sensitive to the flocculant dosage in a filtration process.

The effect of the addition of non-ionic flocculants of different molecular weights on cake moisture is shown in Figure 31. The addition of 0.75 million molecular weight flocculant did not reduce the cake moisture because its chain length is not long enough to form suitable size flocs of the fine particles. The additions of 15 million molecular weight and 4-6 million molecular weight flocculant produced the same moisture reduction. However, the optimum dosage of the 15 million molecular weight flocculant was about 40 g/t, whereas for the 4-6 million molecular weight flocculant the optimum dosage was about 70 g/t. In addition, the cake moisture was more sensitive to the dosage of 15 million molecular weight flocculant because the solution of larger flocculant has much higher viscosity than the solution of smaller flocculant. Figure 32 shows the relationships of solution viscosity and concentration of flocculants with various molecular weights. It can be seen that the viscosity of the solution of 15 million molecular flocculant is higher at the same concentration and increases more sharply as flocculant concentration increases.

Surfactants: The general mechanism of enhanced dewatering by surfactants is to reduce the liquid/air interfacial tension, leading to lower capillary retention forces and hence increasing cake drainage under a given pressure drop across the cake.

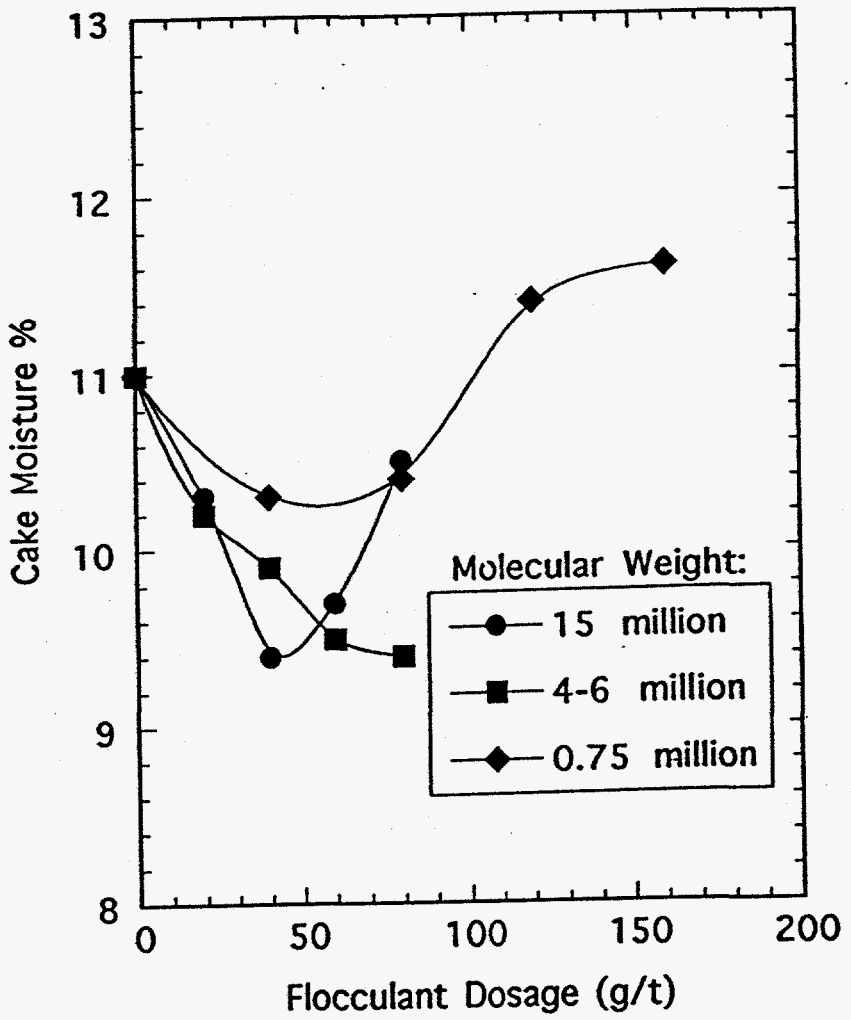

Figure 31. Effect of nonionic flocculant dosage on cake moisture of the Pocahontas clean coal slurry.

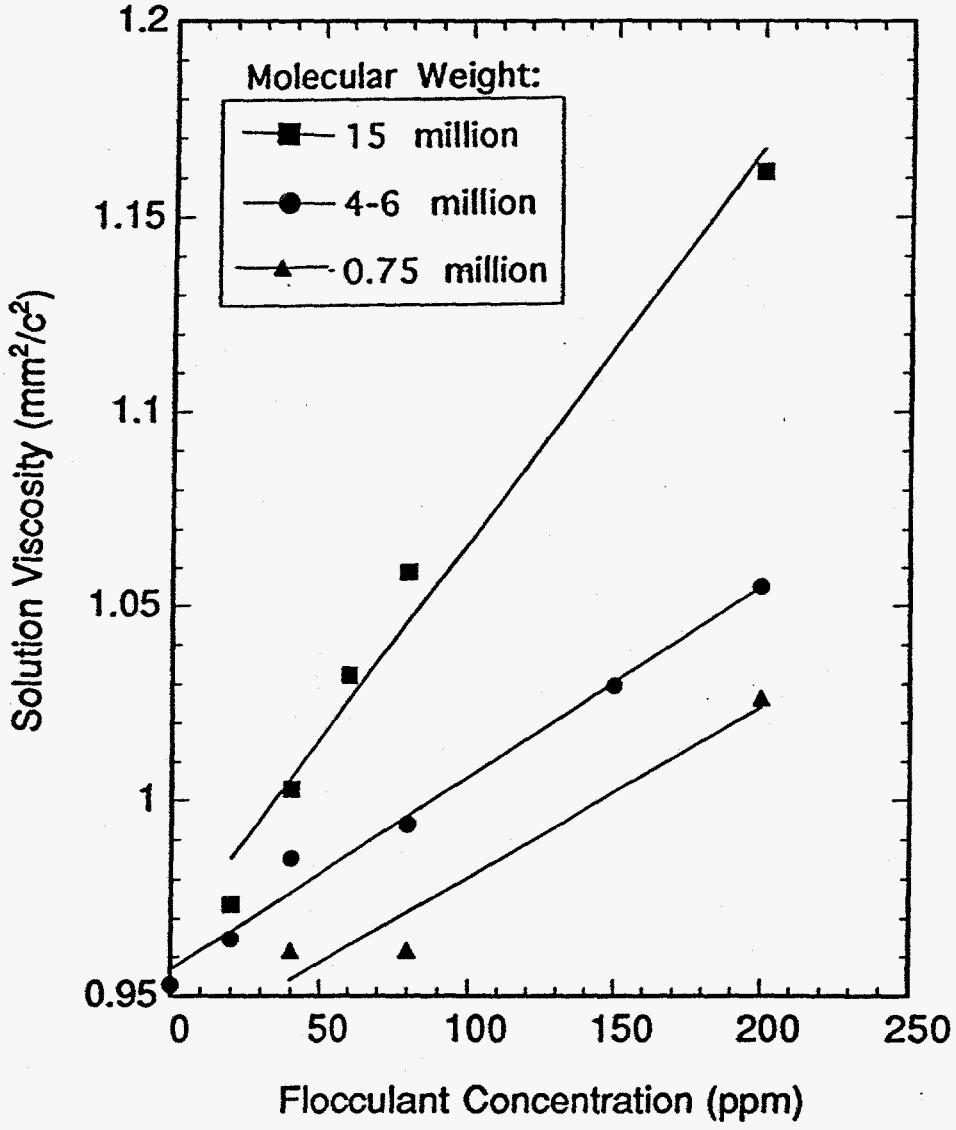

Figure 32. Relationship between nonionic flocculant concentration and its solution viscosity.

The dewatering tests were conducted using three different surfactants, namely, sodium 2-ethyhexyl sulfate (anionic), octyl phenoxy polyethoxy ethanol (nonionic), and cetyl pyridinium chloride (cationic). Table XIII lists the basic information on the three surfactants.

Figure 33 shows the effect of all the three surfactant dosages on filter cake moisture, surface tension values of the original surfactant solution and the filtrate for the Illinois clean coal slurry. These results show that the optimum dosages of nonionic, anionic, and cationic surfactant are 500, 1000, and 1500 g/t, respectively. At these dosages, the filter cake moistures were 18.2, 20.0 and 16.9 percent for the nonionic, anionic, and cationic surfactants, respectively. As can be seen, that the cationic surfactant performed better than the other two surfactants.

The widely accepted mechanism of enhanced dewatering of surfactants is reduction of surface tension of suspension, and adsorption of surfactants from solution onto the coal particles. In order to test which one of these phenomena might be controlling the dewatering process, the surface tension of the original surfactant solution and filtrate were measured. Surface tension was measured by the du Nouy ring method, using Fisher Surface Tensiomat Model 21. The results for surfactant dosage versus surface tension of the surfactant solution and filtrate are also shown in Figure 33. Surface tension of the anionic solution did not change even after it was brought in contact with coal, showing no adsorption on coal surfaces as indicated in Figure 33. In contrast, surface tension of the filtrate from the nonionic and cationic surfactants was substantially higher than the surfactant solution, itself as shown in Figure 33 (b) and (c), respectively. This is a clear indication that the nonionic and cationic surfactants are adsorbing on the coal surface. Figure 33 (b) and (c) for the nonionic and cationic surfactants show that the surface tension of filtrate and the moisture content of the

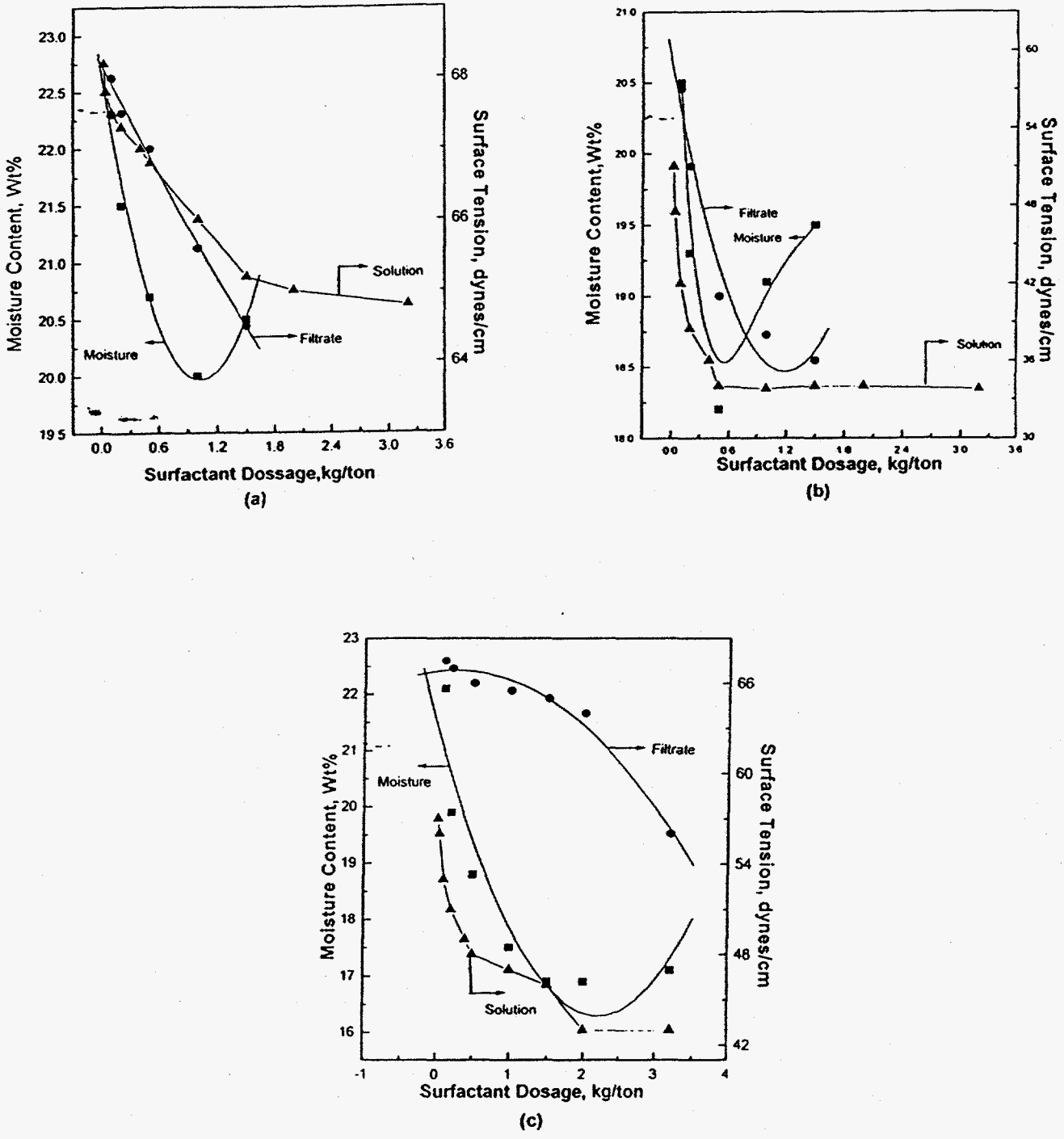

Figure 33. Effect of surfactant dosage on Illinois clean coal slurry filter cake moisture and surface tension of filtration and solution.

dewatered cake decreases with increase in surfactant concentration. However, beyond 0.6 Kg/t of nonionic and 2.5 Kg/t of cationic surfactant concentration the cake moisture begins to increase. Therefore, it is speculated that the effect of the addition of surfactants on the residual filter cake moisture cannot be related directly to the lowering of the liquid-air interfacial tensions. This implies that besides decrease in surface tension, the adsorption of surfactants on coal also plays an important role in changing filtration characteristics.

The effect of surfactant dosage on cake moisture for the Pocahontas No. 3 coal is presented in Figure 34. The addition of the anionic surfactant did not provide any improvement in cake moisture reduction. The reasons may be: (1) the addition of anionic surfactant caused much more foaming; (2) the zeta potential or surface charge on coal surface was negative at the natural pH, which prohibits the adsorption of anionic surfactant onto the coal particle surface. The lowest cake moisture was obtained by adding non-ionic surfactants. During the experiments, it was observed that non-ionic surfactant caused the minimum foaming. Non-ionic surfactant reduced the cake moisture from 11 to 9.7 percent at an optimum dosage of 800 g/t. Overall, surfactants did not profoundly decrease the cake moisture for the Pocahontas No.3 coal.

The effect of surfactant addition on cake moisture for the Pittsburgh No. 8 coal is shown in Figure 35. Cationic surfactant was the most effective among the three surfactants investigated. The addition of 500 g/t cationic flocculant reduced the cake moisture to 19 percent, a 5 percentage point reduction, compared to baseline cake moisture data. The increase of the cationic surfactant dosage from 500 g/t to 6000 g/t provided a cake moisture of 15 percent, which is only a 4 percentage point additional decrease.

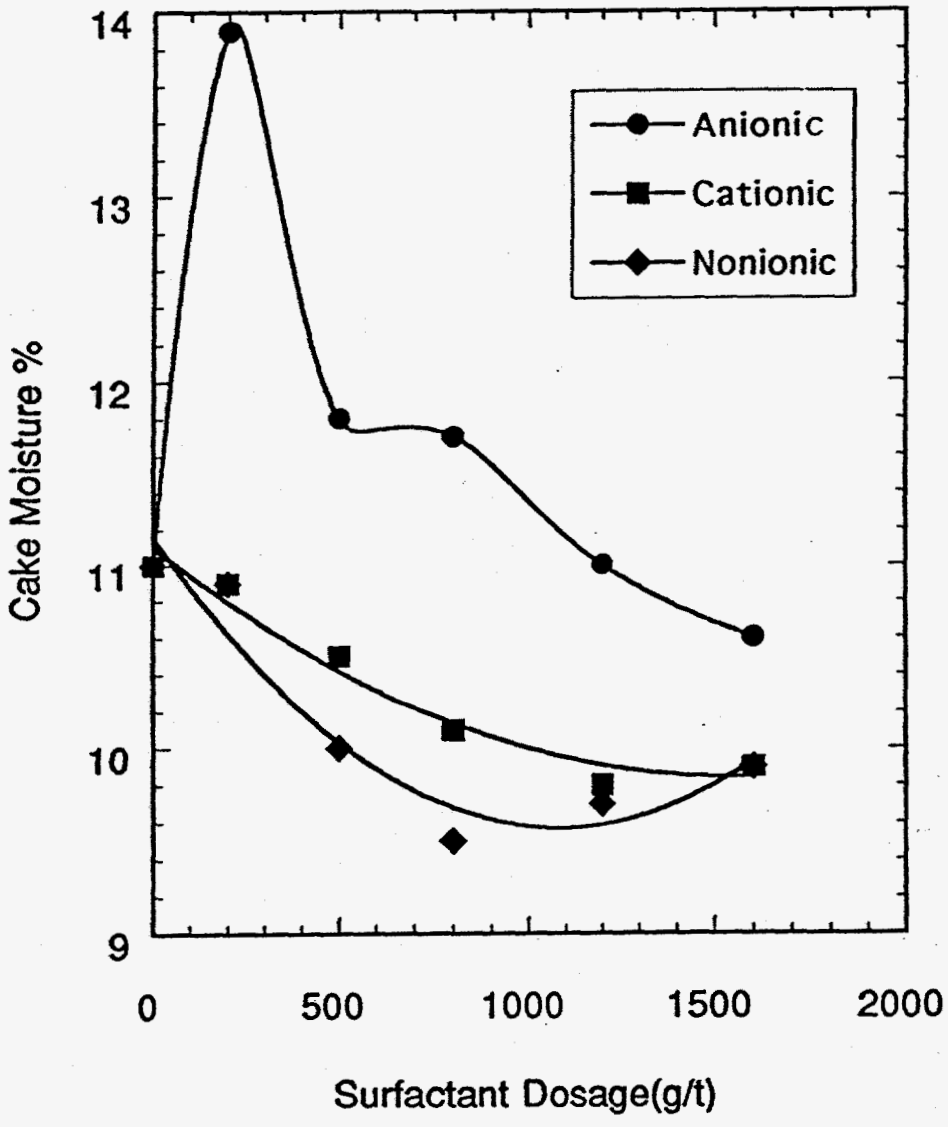

Figure 34. Effect of surfactant dosage on cake moisture of the Pocahontas seam clean coal slurry.

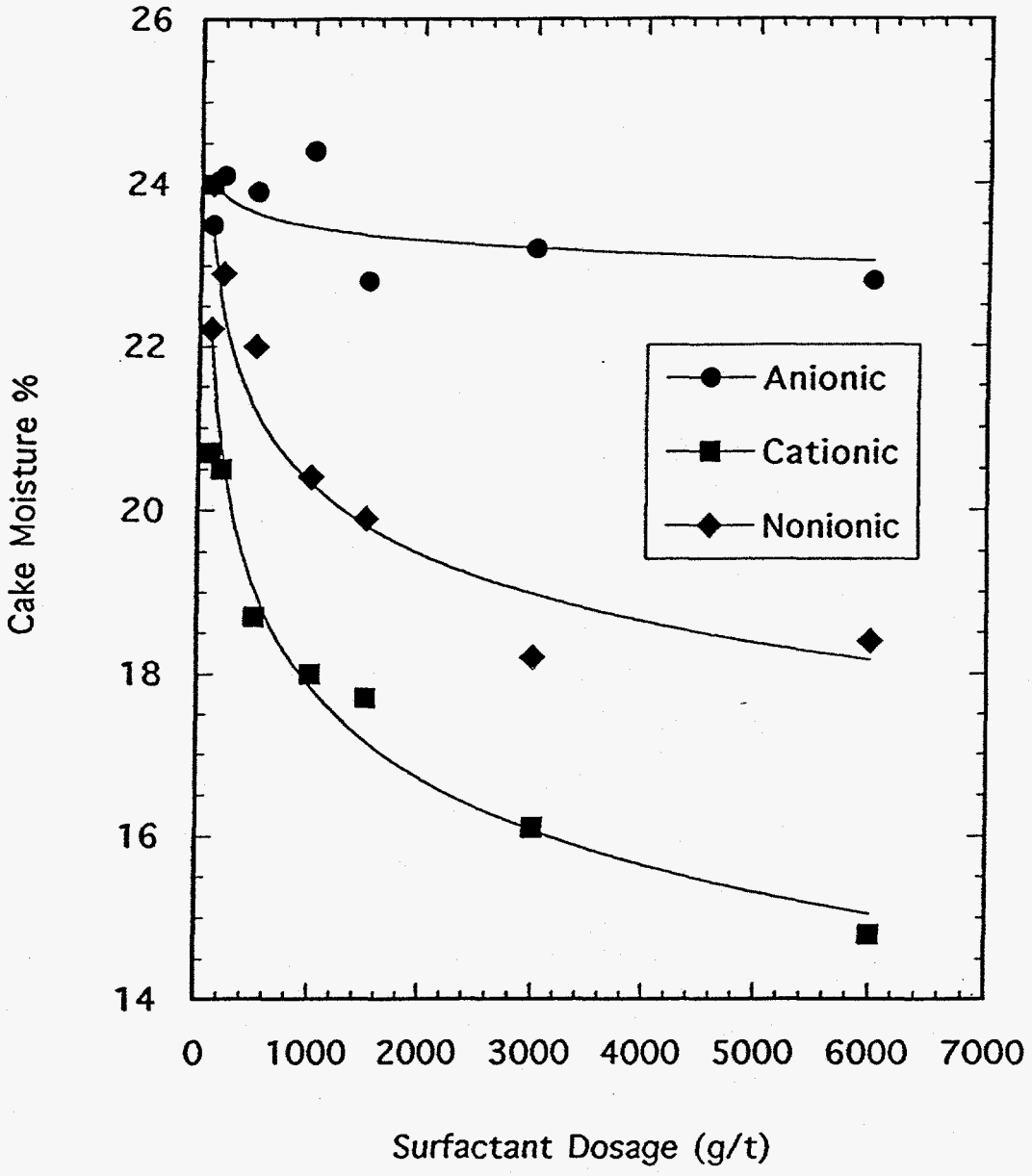

Figure 35. Effect of surfactant dosage on cake moisture of the Pittsburgh seam clean coal slurry.

Combined Use of Flocculants and Surfactants: Figure 36 shows the effect of combined use of flocculant and surfactant on the dewatering of Pocahontas coal slurry. A combination of non-ionic flocculant and non-ionic surfactant produced the best filtration result, decreasing the cake moisture to as low as 7.8 percent. When the flocculants and surfactants, having the same ionic charge, are mixed together, an electrostatic repulsion occurs between the flocculants and surfactants, which may affect the adsorption of additives on the coal surface. When the additives with different kinds of electric charges are used together, they will neutralize each other in the bulk phase. The interaction between non-ionic flocculant/surfactant is weaker than that between anionic/cationic flocculant/surfactant. This may be the reason why the combined use of non-ionic flocculant and non-ionic surfactant gave the largest reduction in cake moisture.

Effect of Metal Ions Addition:

Addition of metal ions such as copper and aluminum ions to a fine particulate improves settling and dewatering of fine particles.[33,34] Most of the metal ions with increasing pH will precipitate out and will coat fine solids increasing its particle size. This has been shown effective for a wide range of particles and metal ions.[33]

The effect of addition of various dosages of copper (Cu^{+2}) and aluminum (Al^{3}) ions as a function of pH on filter cake moisture of the Illinois coal slurry is shown in Figure 37. It can be seen that with Cu^{+2} ions a reduction in filter cake moisture was observed between pH 3.5 and 6 and at pH ~10.0. The two pH corresponds to pH of copper hydroxide precipitation and iso-electric point (IEP) of copper hydroxide.

Figure 38 shows the effect of metal ion dosage on filter cake moisture of Pittsburgh coal slurry. Both Cu^{+2} and Al^{+3} ions provided a five percentage points (or about 25 percent)

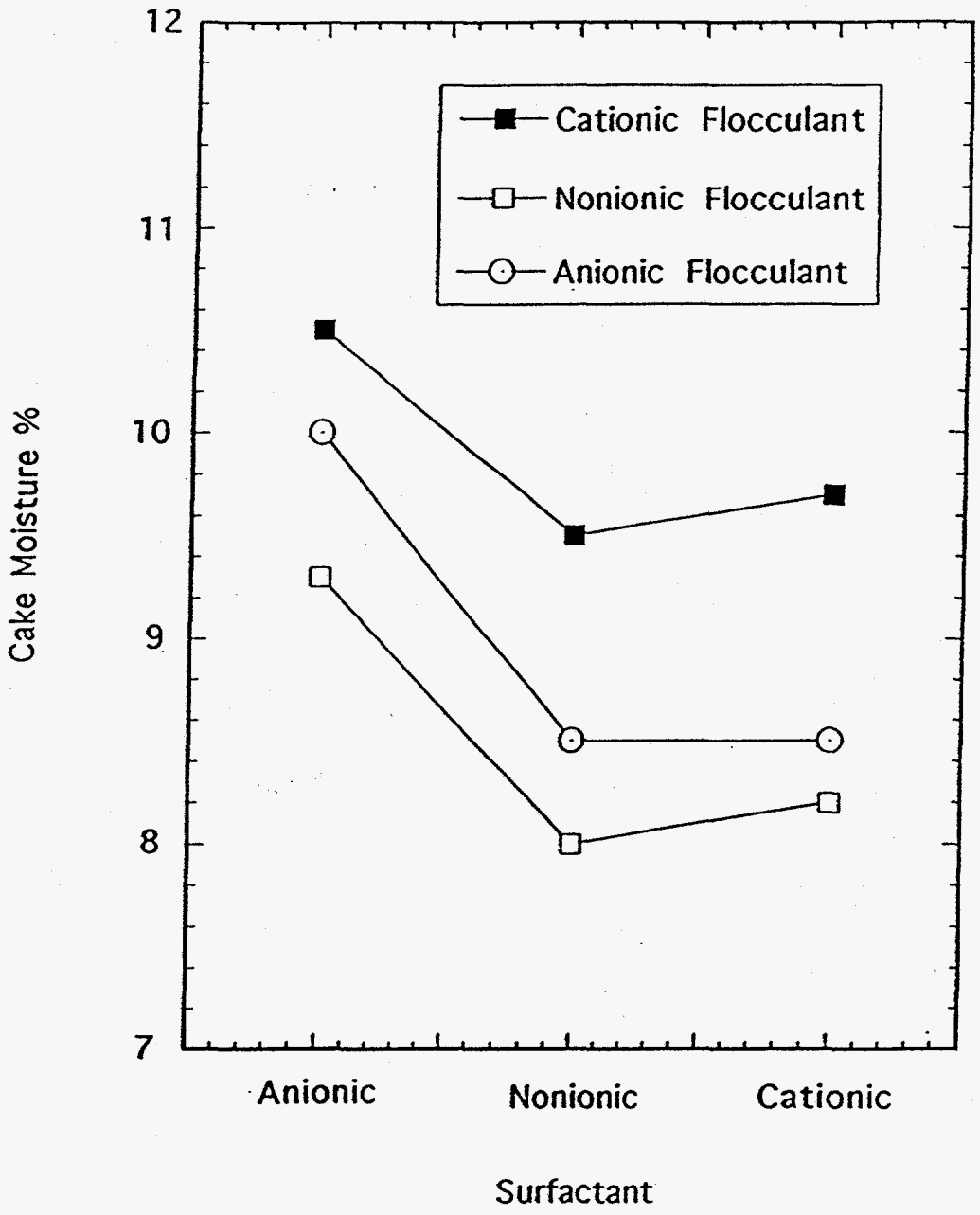

Figure 36. Effect of combined use of flocculant and surfactant on dewatering of the Pocahontas clan coal slurry.

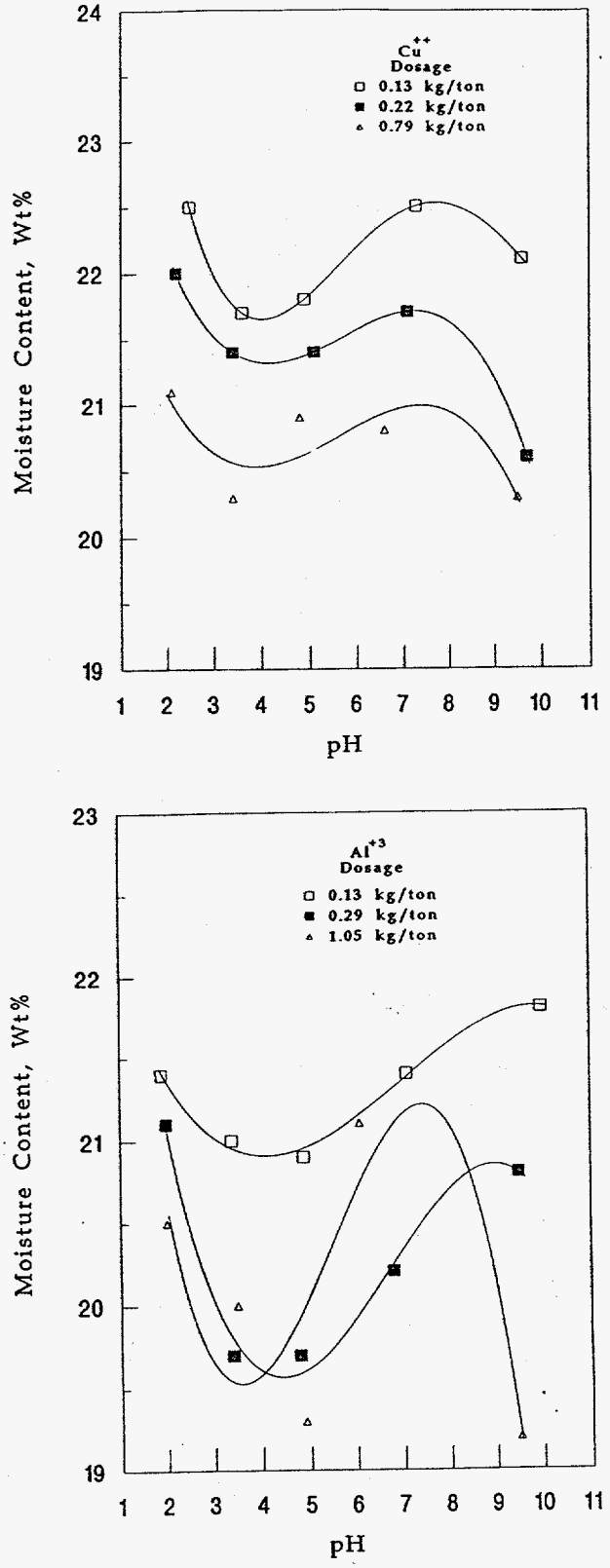

Figure 37. Effect of metal ions addition on filter cake moisture of the Illinois seam clean coal slurry with respect to pH.

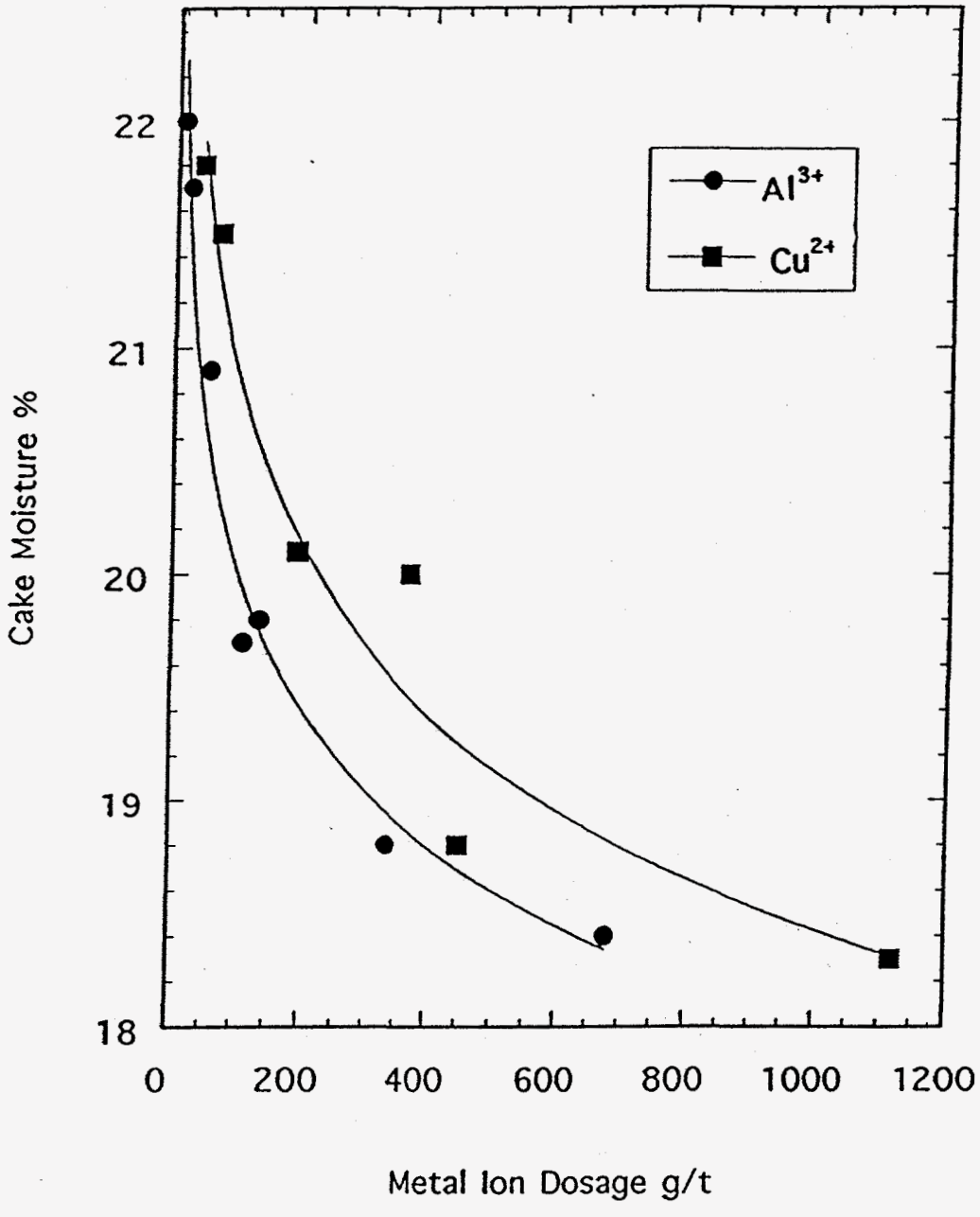

Figure 38. Effect of metal ion dosage on cake moisture of the Pittsburgh seam clean coal slurry.

reduction in the cake moisture. Figure 39 shows the decreasing data for Pocahontas coal in presence of the two metal ions. Note, that in this case, no noticeable reduction in filter cake moisture was observed. As mentioned earlier that metal ions will coagulate only the fine particles. Because of large particle size content of the Pocahontas coal slurry, the metal ions were not effective.

Combined Effect of Metal Ions and Surfactants:

To determine the optimum amount of surfactant needed in combination with metal ions to provide a low moisture filter cake, studies were conducted on varying amounts of surfactants while keeping metal ion dosage constant, i.e., copper (66 mg/liter) and aluminum (40 mg/liter). These metal ion dosages correspond to the lowest moisture content observed in the filter cake as discussed earlier.

Figure 40 illustrates the effect of three different types of surfactants with various metal ions on filter cake moisture for the Illinois coal. With anionic surfactant, there was no noticeable advantage in filter cake moisture reduction with both metal ions since the addition of metal ions alone provides a filter cake containing about 19 percent cake moisture. For the nonionic surfactant, the lowest moisture of 16 percent was achieved with both metal ions. However, the amount of surfactant required was quite high, i.e., 800 mg/liter (3076 g/ton). With the cationic surfactant, the filter cake moisture obtained using copper and aluminum ions reduced to about 16 percent using a surfactant concentration of 100 mg/liter (385 g/ton). However, at higher dosages of surfactant, the addition of surfactant alone was more effective to remove the cake moisture than that of combination of metal ions and surfactant.

Figure 41 shows the dewatering data Pittsburgh No. 8 coal slurry in presence of metal ions and three different surfactants. With anionic surfactant, no noticeable improvement in

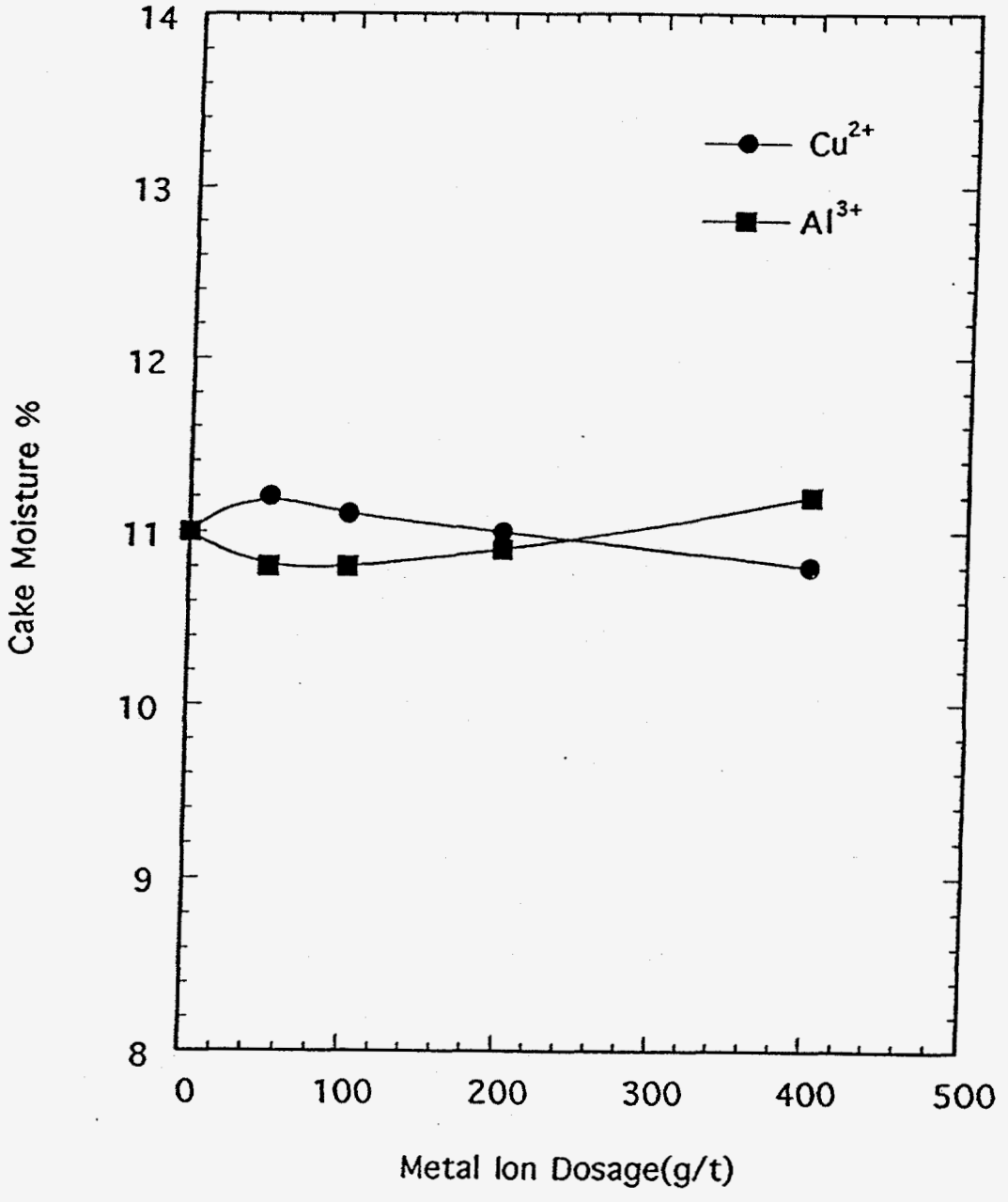

Figure 39. Effect of metal ion dosage on cake moisture of the Pocahontas seam clean coal slurry.

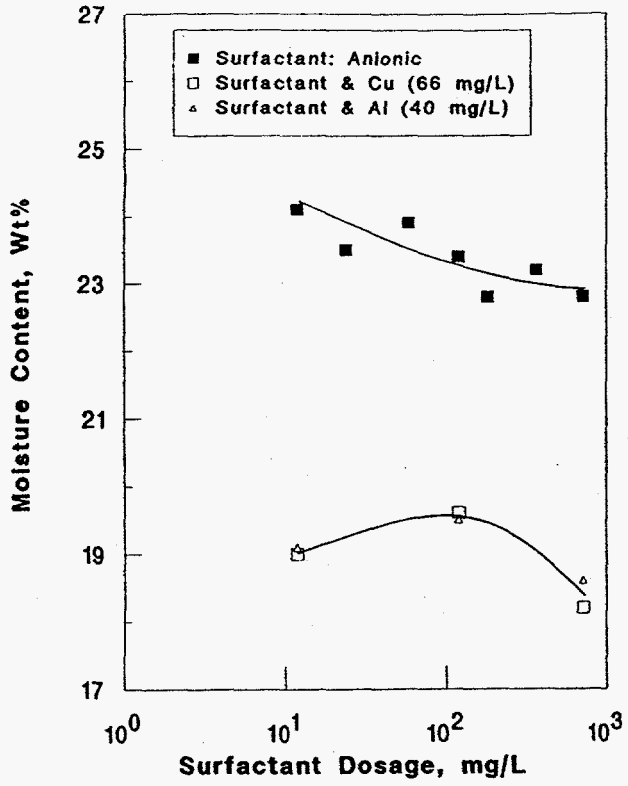

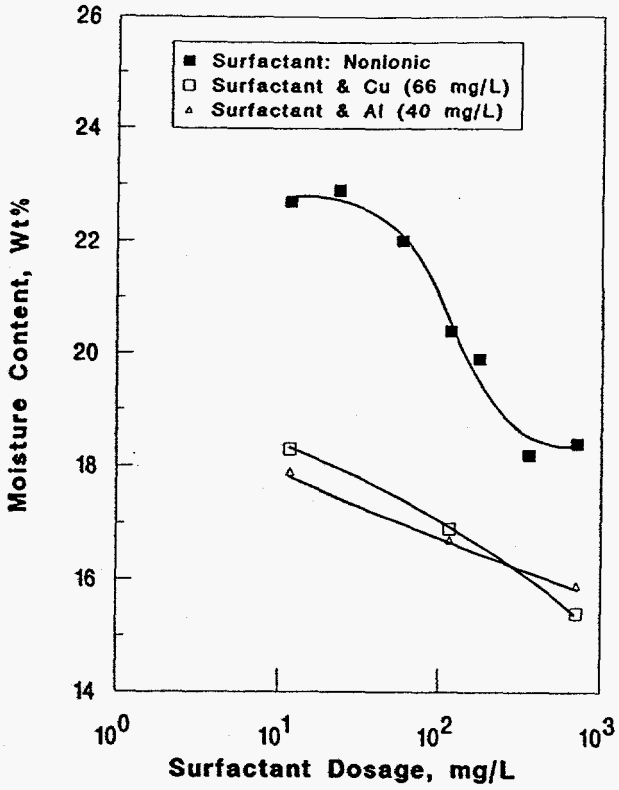

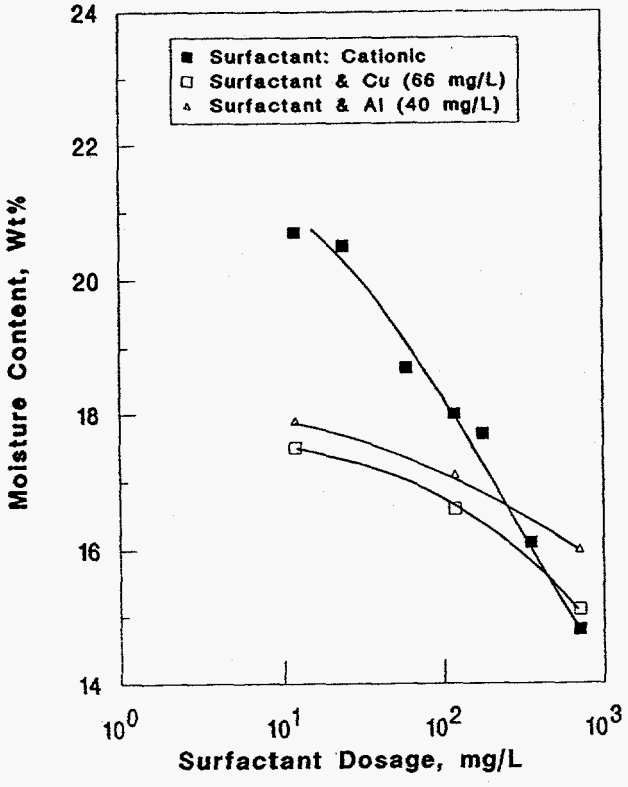

Figure 40. Combined effect of metal ions and surfactant on cake moisture of the Illinois seam clean coal slurry.

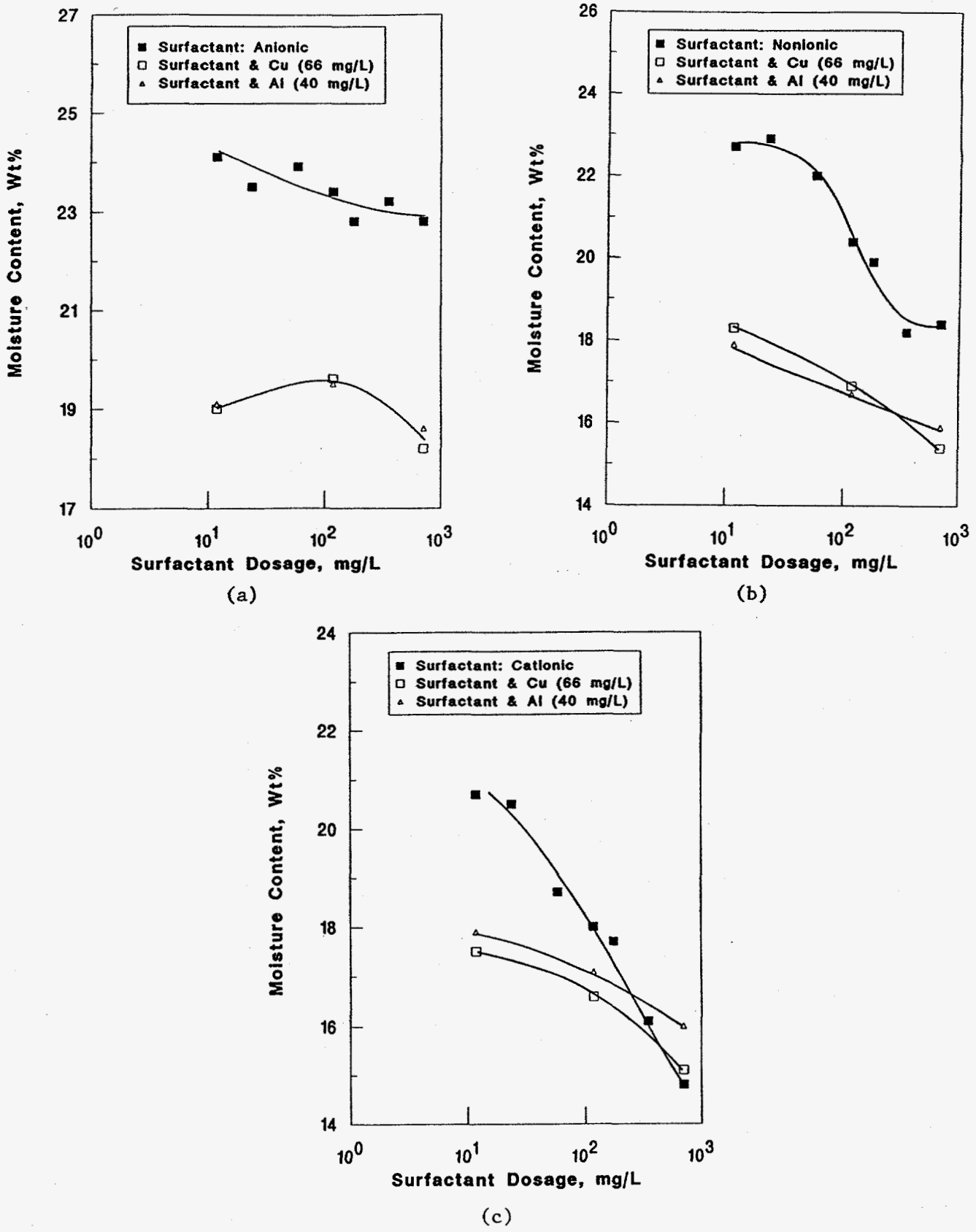

Figure 41. Effect of combining metal ions with different surfactant dosages on filter cake moisture of the Pittsburgh seam clean coal slurry.

filter cake moisture reduction was obtained. Since the addition of metal ions alone provided a filter cake containing about 19 percent cake moisture. For the nonionic surfactant, the lowest moisture of 16 percent was achieved with both the metal ions. However, the amount of surfactant required was 800 mg/liter (7000 g/t). With the cationic surfactant, the filter cake moisture obtained using copper and aluminum ions reduced to about 16 percent using a surfactant concentration of 100 mg/liter (900 g/t). These data clearly indicate that combining metal ions with an anionic or cationic surfactant improves dewatering of fine coal.

Effect of Filtration Medium and Support:

Effect of Medium Support: Perforated plates are conventionally used as filtration medium supports. The open area of the perforated plate is much smaller than the geometric area of the filter medium. The effective filtration area is also much smaller than the medium geometric area when a perforated plate is employed. In this study, a modification was made by inserting a piece of 30 mesh opening screen between the perforated plate and filtration medium, as shown in Figure 42. Springs were placed between the sieving screen and the perforated plate to separate them in order to make the effective filtration area as large as possible. The filtration results obtained using the conventional medium support and the modified support are compared in Table XVI. The data in the table shows that the modified medium support produced a moisture reduction ranging from 2 to 5.2 percentage point, depending on the particle size. It can be seen that for the Pocahontas No.3 coal, the cake moisture of the plus 400 mesh size fraction is reduced by 5.6 percentage points (from 7.2 to 1.6 percent), while the cake moisture of the minus 400 mesh size fraction is reduced by 3 percentage points (from 23.9 to 20.9 percent). The effect of medium support on the cake moisture for coarser size fraction is more significant than for the finer size fraction.

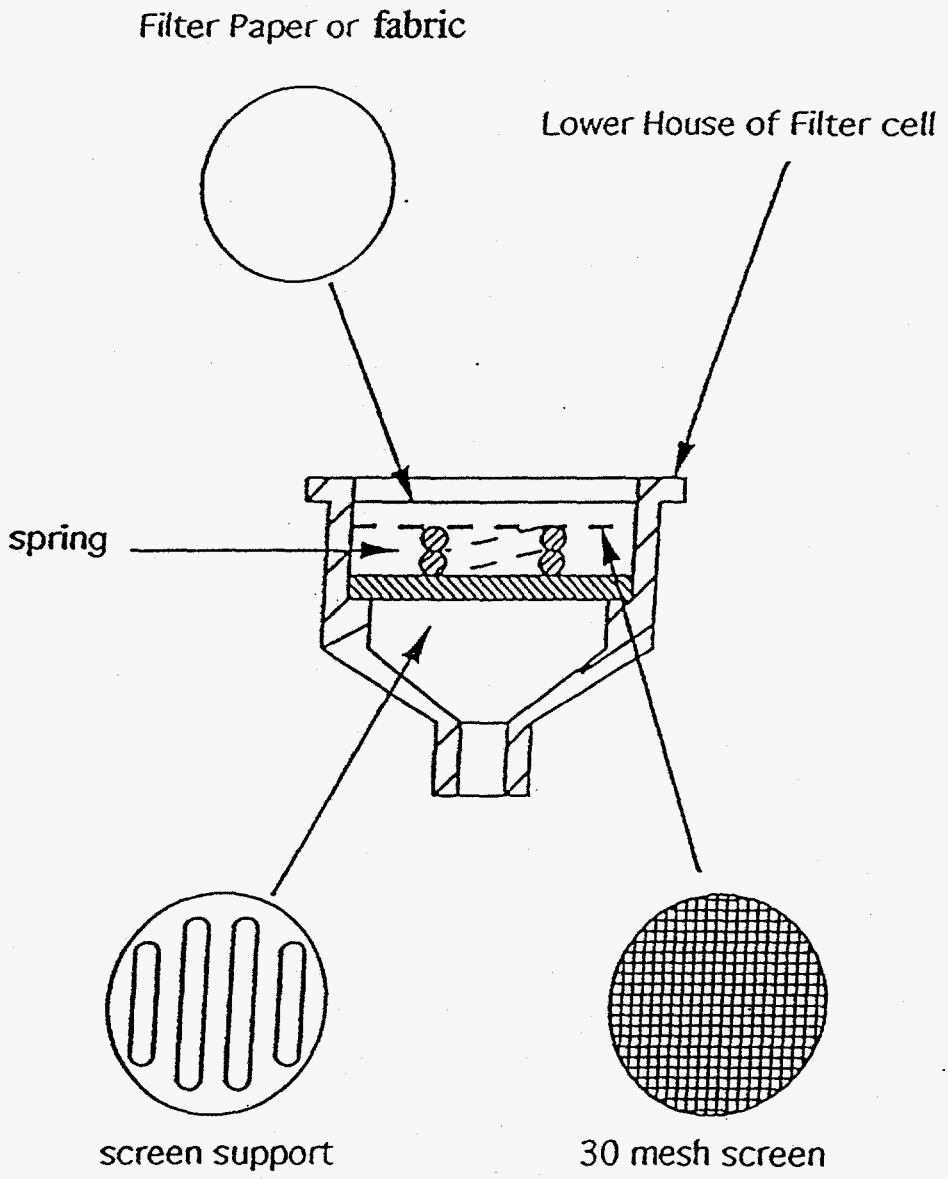

Figure 42. Schematic diagram of the modified filtration medium support.

Table XVI. Effect of Medium support on Cake Moisture of Various Size Samples of Pocahontas Coal Slurry

Sample Name	Particle Size (mesh)	Filtration Condition	Cake Moisture	
			Conventional Support	Modified Support
Pocahontas No.3	28×400	P=80psi,Time=2 min. Thickness=1.4 cm	7.2	1.6
	-28	P=80psi,Time=2 min. Thickness=1.4 cm	11.2	9.2
	-400	P=80psi,Time=2 min. Thickness= 1.4 cm	23.9	20.9

The enhancement obtained by using the modified support could be explained in terms of the capillary model. According to the capillary filtration model, a filter cake is considered as a bundle of tortuous capillaries with various diameters and the outlets of the capillaries are located at the bottom of the cake. If the filtration medium is directly on a perforated plate, some of the capillary outlets may be blocked by the imperforate area of the perforated plate support, which will obstruct the flow of water from capillaries. The water in the capillaries obstructed must travel horizontally to the nearest hole. The flow of water in horizontal direction is minimum due to very low pressure drop. When the filtration medium is put on a screen instead of a perforated plate, the capillary water is not blocked due to the larger opening area.

Effect of The Combination of Medium and Support: A comparison of the effect of the combination of filter medium (paper and fabric) with medium support (conventional and modified) for the Pittsburgh No. 8 coal is shown in Figure 43. Among the four combinations, the fabric/modified medium support produced the lowest cake moisture and

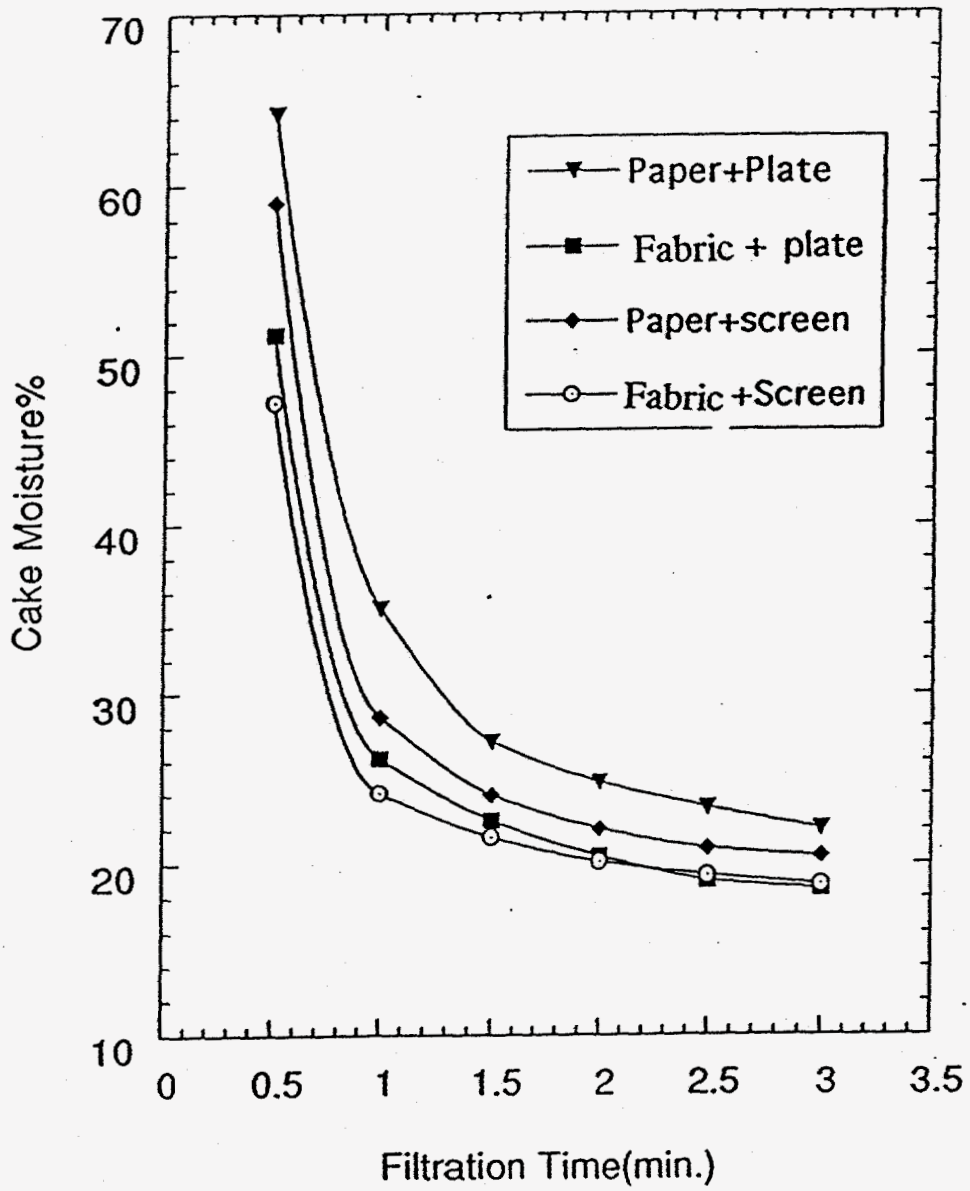

Figure 43. Effect of filtration medium and medium support on dewatering of Pittsburgh seam clean coal slurry.

dramatically reduced the filtration time. The highest cake moisture is obtained from the filter paper with the conventional support. The average filtration rate in the first 30 seconds for the various combination of medium and medium support is shown in Table XVII. Note that compared to the conventional support, the modified support increased filtration rate by 25 percent using the paper and 11 percent using a fabric filter medium.

Table XVII. Filtration Rate In First 30 Seconds for the Pittsburgh No.8 Coal.

Filtration Medium + Support	Filtration Rate (g/s)	Relative Filtration Rate
Paper + Conventional Support	1.67	1.00
Paper + Modified Support	2.09	1.25
Fabric + Conventional Support	2.21	1.32
Fabric + Modified Support	2.46	1.47

Combined Use of Various Dewatering Enhancement Methods

Tables XVIII and XIX show the dewatering data obtained utilizing addition of 60 g/t of a non-ionic flocculant (MW=4-6 m) and using modified fabric filter, medium support and split size filtration for the Pittsburgh No. 8 coal and Pocahontas No. 3 coal slurry, respectively. Note that for the Pittsburgh No. 8 coal, the combined enhancement dewatering approach produced filter cakes of 10.5 to 14.3 percent moisture, a 13.5 to 9 percentage point total absolute moisture reduction over the baseline data of 24 percent moisture. This represents a 40 to 56 percent of relative moisture reduction in the filter cake. Similarly, for the Pocahontas No. 3 coal slurry, the combined enhancement approach provided filter cake with 4.8 to 7.1 percent moisture, a 6.15 to 3.8 percentage point of total absolute moisture

Table XVIII. Result of Combined Enhancement Methods for the Pittsburgh No. 8 Coal (Filter Cloth; Modified Support; Split Size Filtration; 60 g/t Nonionic Flocculant for the Finer Size Fractions)

Split Size (mesh)	Size Fraction (mesh)	% Wt.	Cake Moisture
200	100×200	21.8	1.3
	200×0	78.2	17.9
	Composite	100	14.28
400	100×400	46.6	1.6
	400×0	53.4	18.96
	Composite	100	10.87
500	100×500	57.7	2.6
	500×0	42.3	21.2
	Composite	100	10.47

(The baseline cake moisture obtained without using any enhancement approach was 24%)

Table XIX. Result of Combined Enhancement Methods for the Pocahontas No.3 Coal (Filter Cloth; Modified Support; Split Size Filtration; 80 g/t Nonionic Flocculant for the Finer Size Fractions)

Split Size (mesh)	Size Fraction (mesh)	% Wt.	Cake Moisture
100	28×100	49.8	1.01
	100×0	50.2	13.2
	Composite	100	7.13
200	28×200	67.1	1.4
	200×0	32.9	15.59
	Composite	100	6.06
400	28×400	78.0	1.6
	200×0	22.0	16.4
	Composite	100	4.85

(The baseline cake moisture obtained without using any enhancement was 11%)

reduction over the baseline of 11 percent moisture. This represents 35 to 56 percent of relative moisture reduction.

Task III - Pilot Plant Testing:

The hyperbaric filter pilot plant testing was conducted at two CONSOL Inc. preparation plants processing the Pittsburgh No. 8 (a high volatile A rank) and Pocahontas No. 3 (a low volatile rank) coals. A photograph of the Andritz mobile pilot scale hyperbaric filter (HBF) test unit used for the study is shown in Figure 44. The pressure chamber has one disc filter which is composed of 20 hollow segments, each covered with a filter cloth (Figure 45). The disc diameter is 1.4 m with a filter area of 2 m^2 (22 sq. ft.). Coal slurry is pumped into a filter tub (50 percent disc submergence) where the level is controlled by sensors.

Cake forms on the filter segments that are submerged in the slurry (Cake Formation Zone). A motor rotates the disc so that the cake emerges from the slurry into the Cake Dewatering Zone. The time allowed for cake formation and cake dewatering is controlled by a fixed and slotted disc previously referred to as the "control disc."

Before the last segment re-submerges, air is "snap" blown from inside the segment causing the cake to fall off of the filter segment and into the discharge chamber. After a fill time of approximately one (1) minute, the top gate closes and the discharge chamber is vented to the atmosphere. The bottom gate opens and the cake is discharged from the HBF. The bottom gate then closes and the discharge chamber repressurizes to begin another cycle. Figure 46 shows the pilot plant operation in progress at one of the CONSOL Inc. mines.

<u>Pittsburgh No. 8 Seam Preparation Plant Tests</u>:

Three feed materials were tested, namely, a 28x0 mesh filter feed, a 100x0 mesh flotation product, and a 100x0 mesh deslimed (classified) product. Table XX lists the HBF

Figure 44. Andritz hyperbaric pilot filter unit.

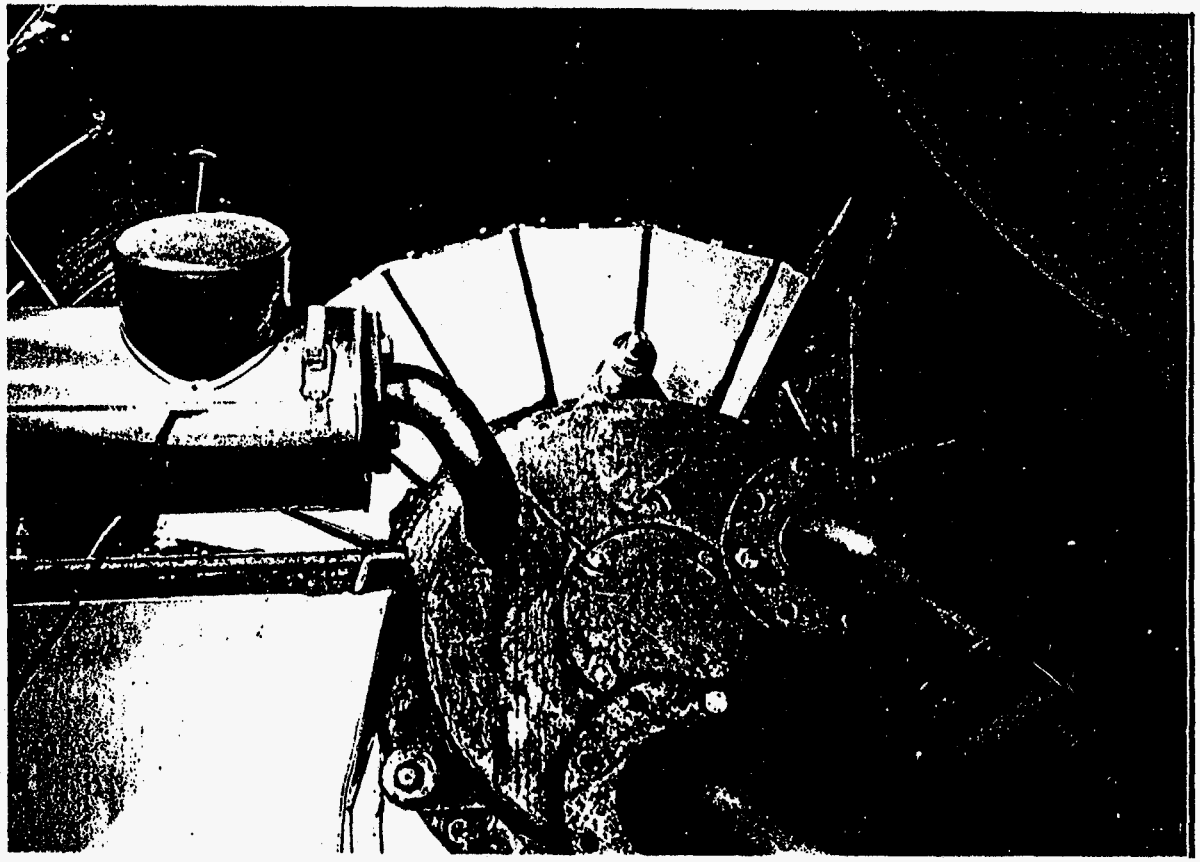

Figure 45. The filter disc inside the hyperbaric unit.

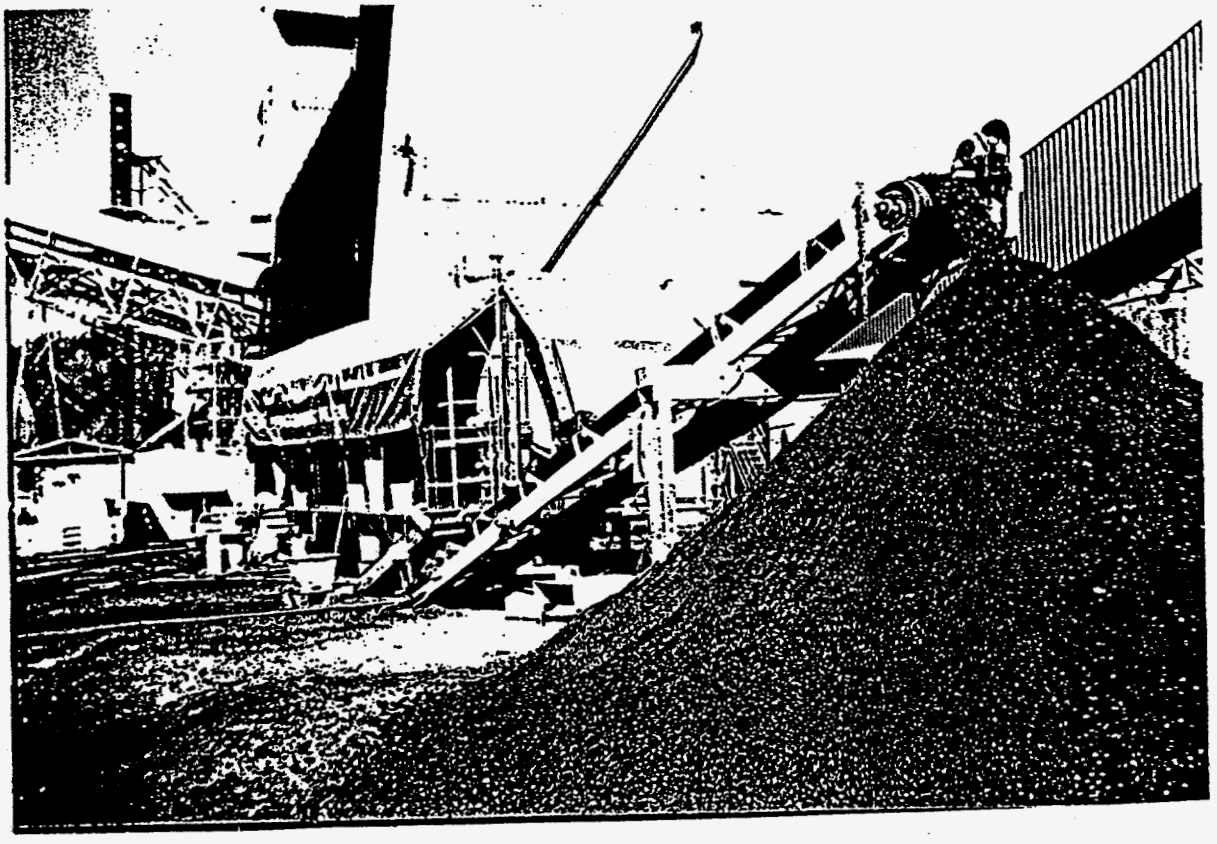

Figure 46. HBF pilot-scale test in progress.

pilot-scale tests conducted with the Pittsburgh No. 8 seam clean coal slurry using various parameters and reagents.

A. Filter Feed Material:

The filter feed material consisted of 28x0 mesh size which included classifying cyclone underflow and froth flotation concentrate.

Figure 47 shows the effect of applied pressure on filter cake moisture, solids throughput, and air consumption. Note, that the filter cake moisture decreases from 21.0 percent to 16.0 percent as the pressure increases from 0.7 bar to 5 bar. The solids throughput also increased from 500 to 1020 Kg/m^2-h (104 to 211 lb/ft^2-h) with increasing pressure, however, at 5 bar pressure it showed a significant decline. The air consumption stays nearly constant at about 170 Nm^3/t (90 cfm/t), except at 2 bar pressure. The observations for air consumption at 2 bar and solids throughput at 5 bar don't follow expected trends.

The cake formation angle (CFA) is an important parameter for the hyperbaric filter. Figure 48 shows the effect of cake formation angle using 5 bar pressure on filter cake moisture, solids throughput and air consumption. It is interesting to note that the filter cake moisture and solids throughput increased with increasing CFA from 55° to 165°, and the air consumption on a per ton basis showed a decline. Based on the above-mentioned data, it can be concluded that for the Pittsburgh No. 8 seam filter feed material 3.5 bar pressure and 165° CFA were the most favorable HBF filtration conditions providing about 17.5 percent moisture filter cake with solids throughput of 1020 Kg/m^2-h (211 lb/ft^2-h) and air consumption of 170 Nm^3/t (90 cfm/t).

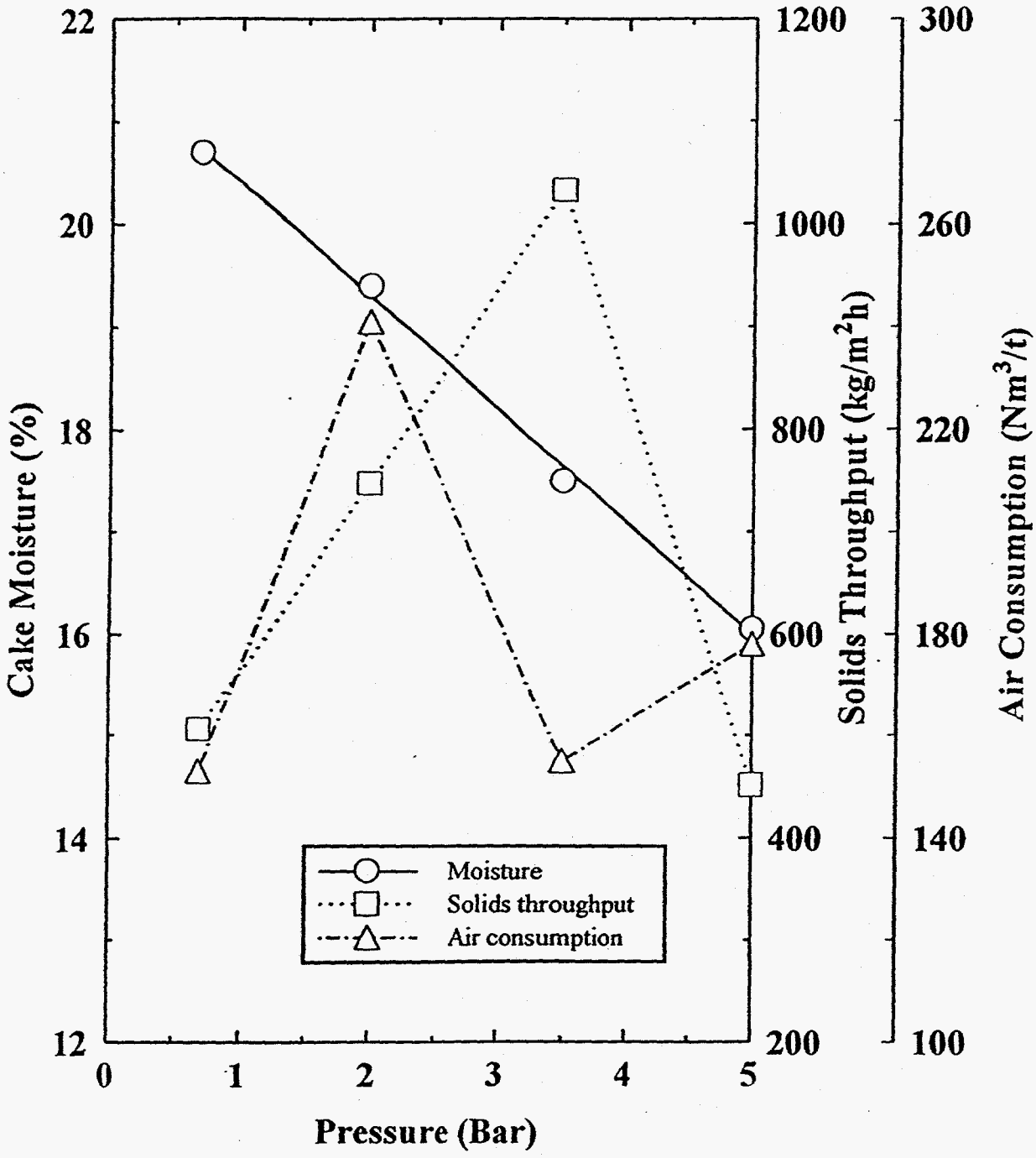

Figure 47. The effect of applied pressure on filter cake moisture, solids throughput and air consumption for the Pittsburgh seam 28x0 mesh filter feed (CFA = 85°, RPM = 0.5).

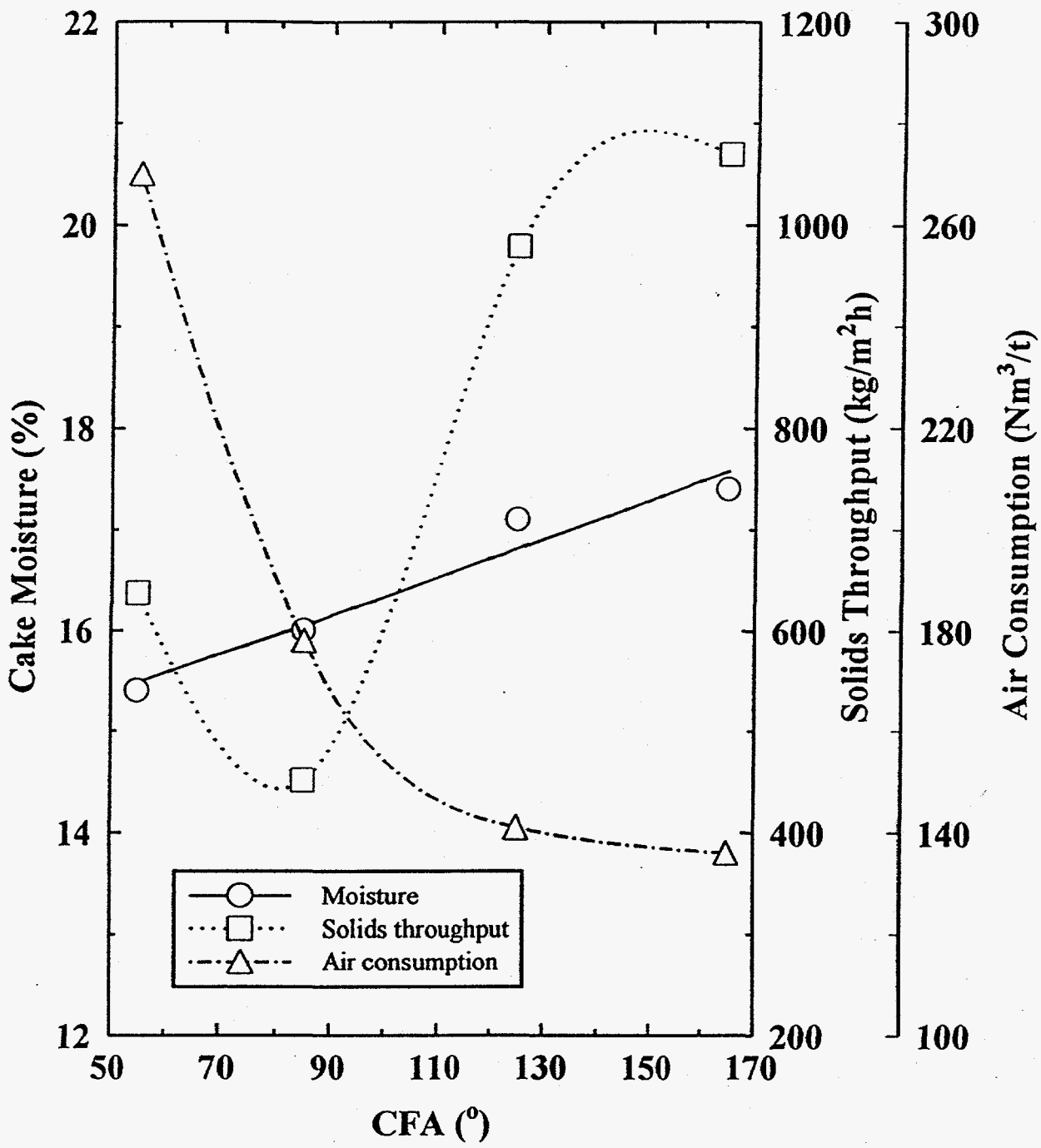

Figure 48. The effect of cake formation angle (CFA) on filter cake moisture, solids throughput and air consumption for the Pittsburgh seam 28x0 mesh feed (pressure = 5 bar).

Table XX. List of the Pilot Scale Hyperbaric Filter Tests Conducted Using Pittsburgh No. 8 Seam Clean Coal Slurry

---

A. FILTER FEED MATERIAL[a]

1. Statistical Parametric Evaluation (15 Tests)
2. Anionic Floc (8 Tests)
3. Cationic Floc (6 Tests)
4. Cationic Surfactant (6 Tests)

B. FROTH FLOTATION PRODUCT[b]

1. Statistical Parametric Evaluation (15 Tests)
2. Pressure Variation (4 Tests)
3. Anionic Floc (5 Tests)
4. Cationic Coagulant (6 Tests)
5. Cationic Surfactant (5 Tests)
6. Other (1 Test)

C. CLASSIFIED FROTH FLOTATION PRODUCT

1. Size, Pressure, and Solids Content Variation (6 Tests)
2. Anionic Floc (2 Tests)
3. Coagulant (4 Tests)

---

[a]28x0 mesh
[b]100x0 mesh

Effect of addition of an anionic (Nalco 9810) flocculant dosage on dewatering of the filter feed at 3.5 bar and 5 bar pressure is shown in Figures 49 and 50, respectively. Using 3.5 bar pressure, both the filter cake moisture and solids throughput increases with increasing flocculant dosage. However, the air consumption first declined from 230 Nm^3/t to 140 Nm^3/t and then increased to 240 Nm^3/t with increasing flocculant dosage. At 5 bar pressure, the filter cake moisture decreased from 18.2 to 15.8, and air consumption decreased from 377 Nm^3/t to 141 Nm^3/t (200 cfm/t to 75 cfm/t) as the flocculant dosage is increased to 11 g/t. Increasing flocculant dosage to 19 g/t increased the moisture content, air consumption and solids throughput. This type of behavior was commonly seen with addition flocculant which is due to the formation of large size flocculated material. Effect of a cationic flocculant (Nalco 8856) dosage on dewatering of the filter feed is shown in Figure 51. Again, the dewatering results are very similar to that obtained with anionic flocculant (Nalco 9810). The addition of flocculant to the feed material was detrimental to the filter cake moistures, which could be due to the entrapped moisture in the flocs.

Figure 52 shows the effect of addition of cetyl pyridinium chloride (CPC), a cationic surfactant, on dewatering of filter feed. It shows a marginal reduction in filter cake moisture with increasing surfactant dosage.

The dewatering data on the filter feed material indicated that the hyperbaric filter operating at 5 bar pressure will provide a product containing about 16 percent moisture. Addition of flocculant or surfactant was not effective in lowering the moisture content of the filter cake.

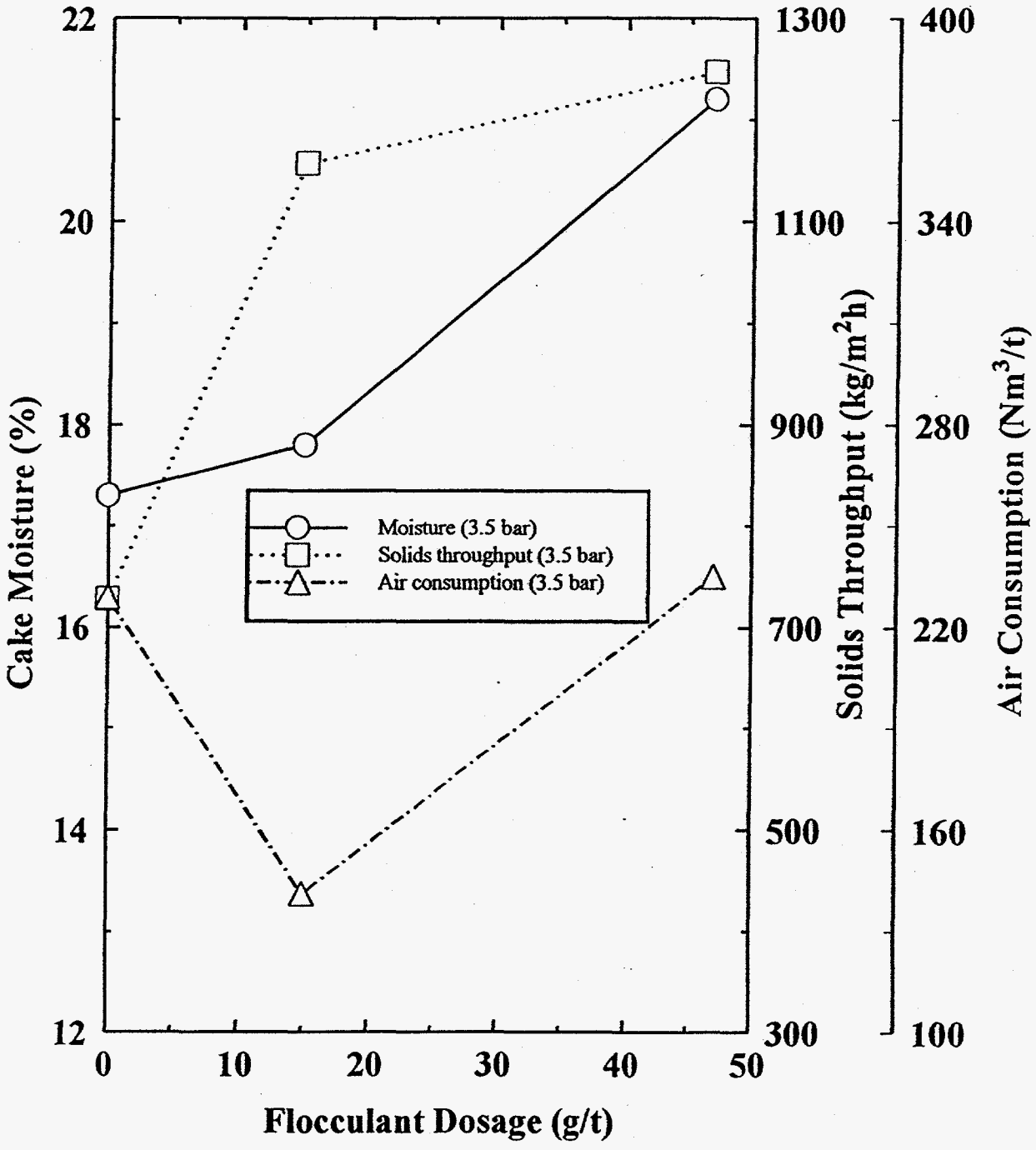

Figure 49. The effect of anionic flocculant (Nalco 9810) dosage on dewatering of the Pittsburgh seam filter feed material (CFA = 85°, pressure = 3.5 bar).

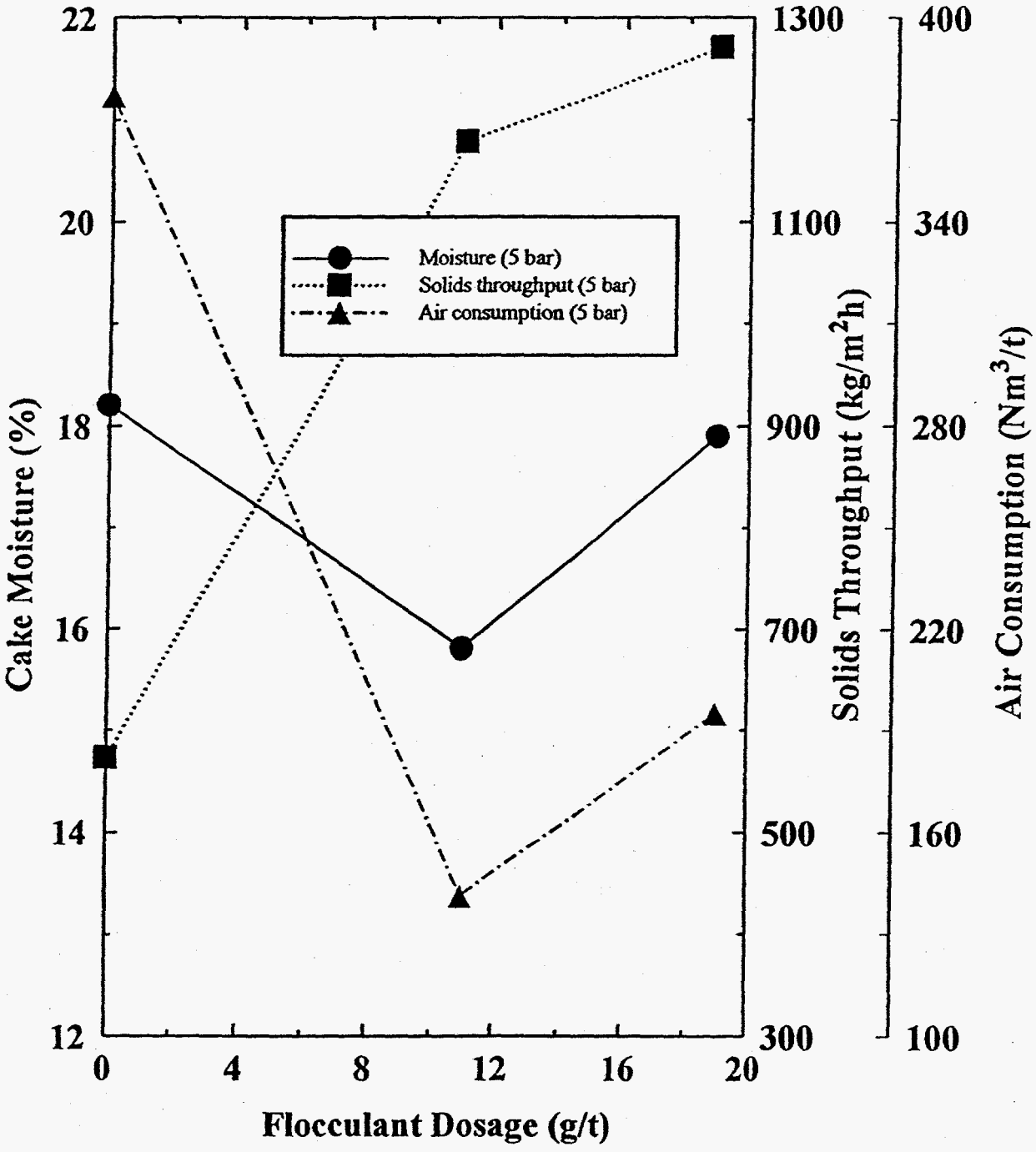

Figure 50. The effect of the anionic flocculant dosage on dewatering of the Pittsburgh seam filter feed material (CFA = 85°, pressure = 5 bar).

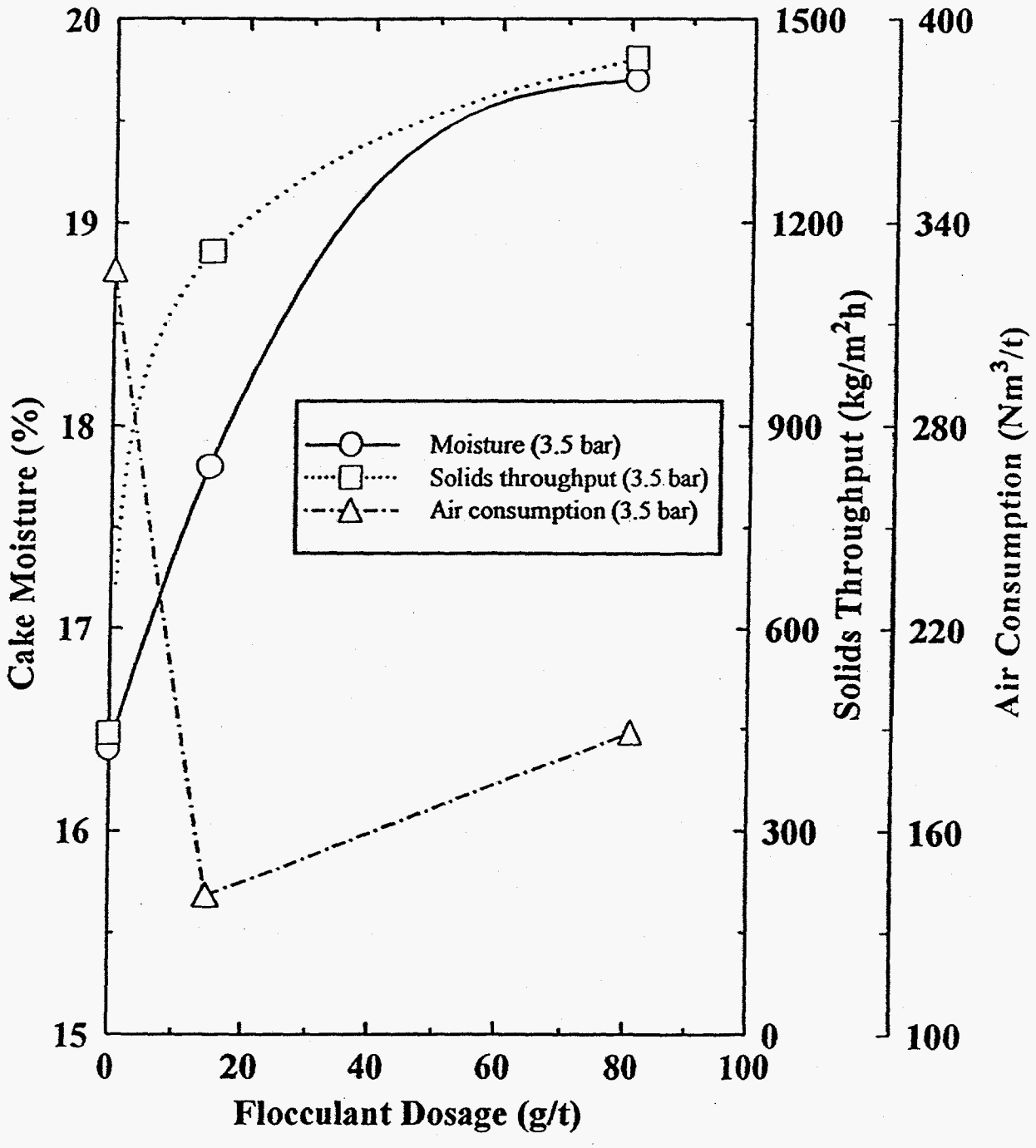

Figure 51. The effect of the cationic flocculant (Nalco 8856) dosage on dewatering of the Pittsburgh seam filter feed (pressure = 3.5 bar).

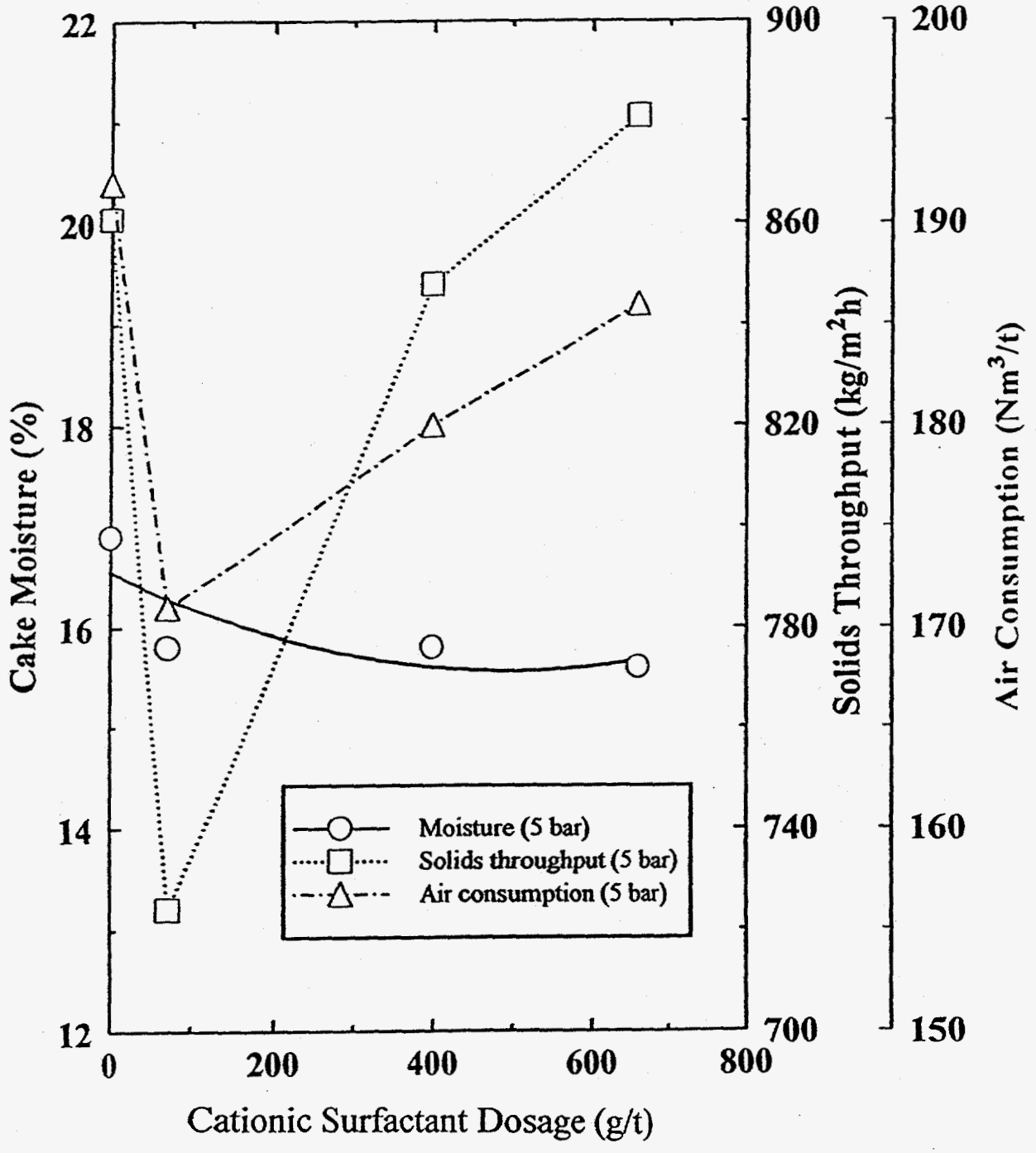

Figure 52. The effect of the cationic surfactant dosage on dewatering of the Pittsburgh seam filter feed (pressure = 5.0 bar).

B. Pittsburgh Coal Froth Flotation Product:

The 100x0 mesh HBF feed was the fine clean coal concentrate generated in the flotation circuit. The effect of applied pressure on dewatering of the froth product is shown in Figure 53. The filter cake moisture decreased from 29.7 to 22 percent as the applied pressure increased from 0.7 to 5.8 bar. The solids throughput increases from 200 to 500 Kg/m^2-h (41.4 to 103 lb/ft^2-h) as pressure increased from 0.7 to 1.5 bar; with a further increase in applied pressure no significant change in solids throughput was observed. An increase in air consumption from 75 Nm^3/t (40 scfm) to 380 Nm^3/t (202 scfm) was observed when pressure increased from 0.7 to 2.7 bar, however further increase in pressure to 5.8 bar reduced the air consumption to 177 Nm^3/t (98 scfm/t). The lower air consumption at higher 5.8 bar pressure could be due to tight compaction of filter cake closing all the capillaries. The effect of cake formation angle (CFA) on dewatering of froth product is shown in Figure 54. It shows that using 3.5 bar pressure 85° CFA provided a 20.5 percent moisture filter cake. Increasing CFA provided higher filter cake moisture. The solids throughput was largest (727 Kg/m^2-h or 150 lb/ft^2-h) and air consumption was lowest (208 Nm^3/t or 110 cfm/t) at high (165°) CFA. These data suggest that for the Pittsburgh No. 8 froth product, a high CFA of 165° at 3.5 bar pressure will provide about 24 percent moisture filter cake.

The effects of a cationic coagulant (Nalco 8856) dosage on dewatering of froth product at 3.5 bar pressure is shown in Figures 55. This figure shows that using a 3.5 bar pressure and 120 g/t of the flocculant provided a filter cake with 21.4 percent moisture with the air consumption of 239 Nm^3/t (127 cfm/t) and solids throughput of 675 Kg/m^2-h (140 lb/ft^2-h).

Figures 56 and 57 show the effect of an anionic flocculant (Nalco 9810) dosage on dewatering of the froth product using 3.5 and 5.0 bar pressure, respectively. Both these

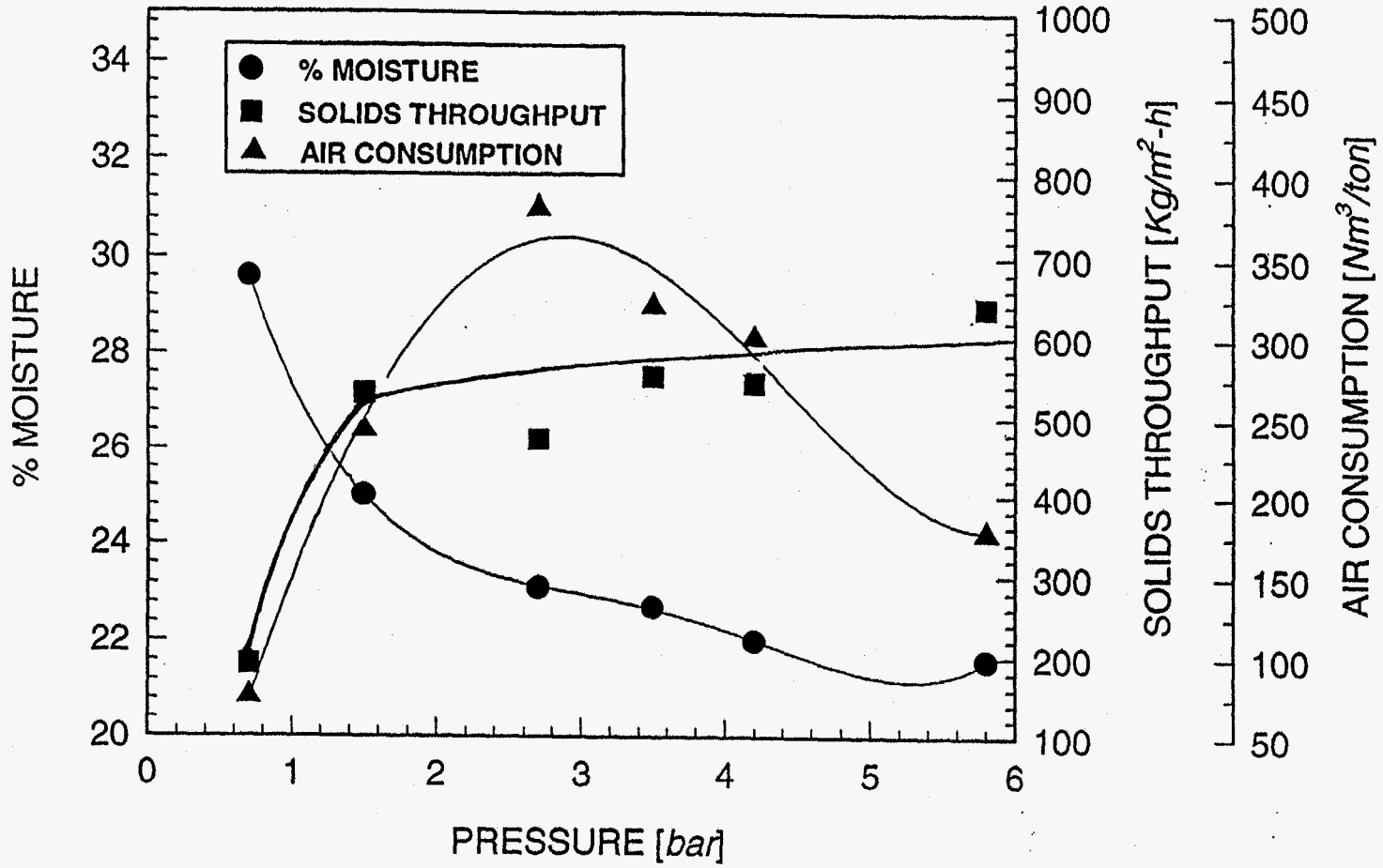

Figure 53. The effect of applied pressure on dewatering of the Pittsburgh seam froth product (CFA = 125°).

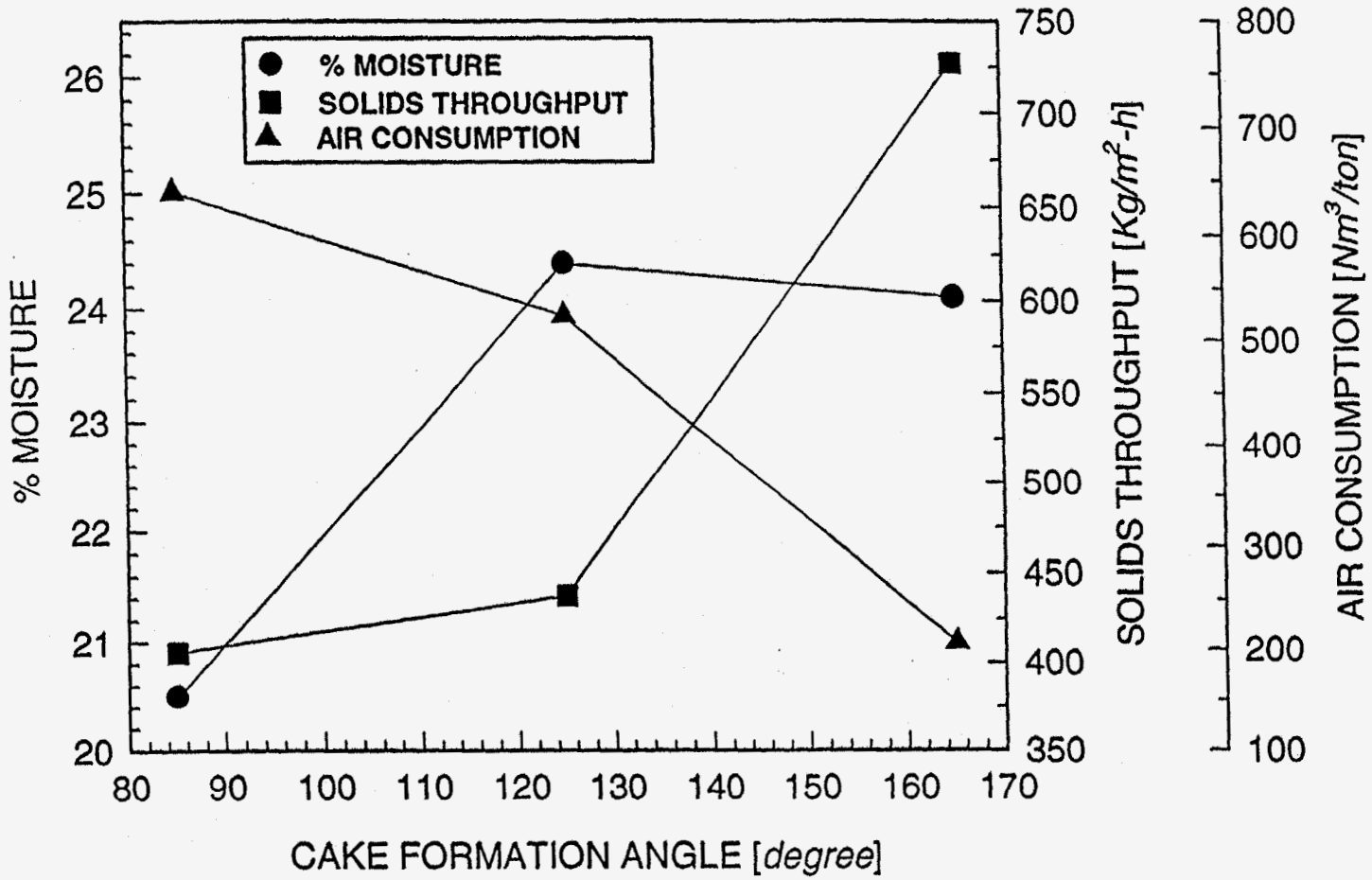

Figure 54. The effect of cake formation angle (CFA) on dewatering of the Pittsburgh seam froth product (pressure = 3.5 bar).

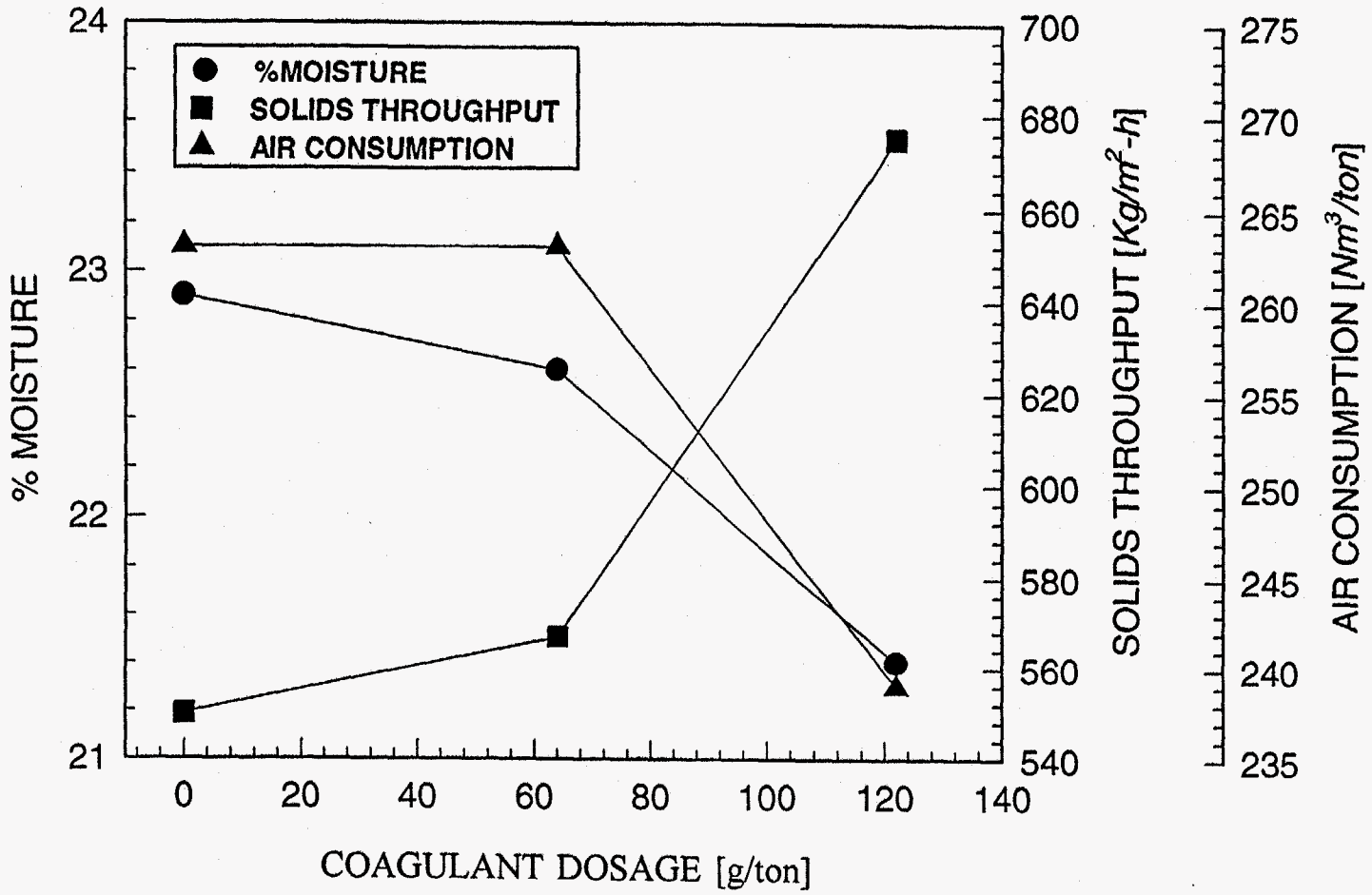

Figure 55. The effect of cationic coagulant (Nalco 8856) dosage on dewatering of the Pittsburgh seam froth product (CFA = 165°, pressure = 3.5 bar).

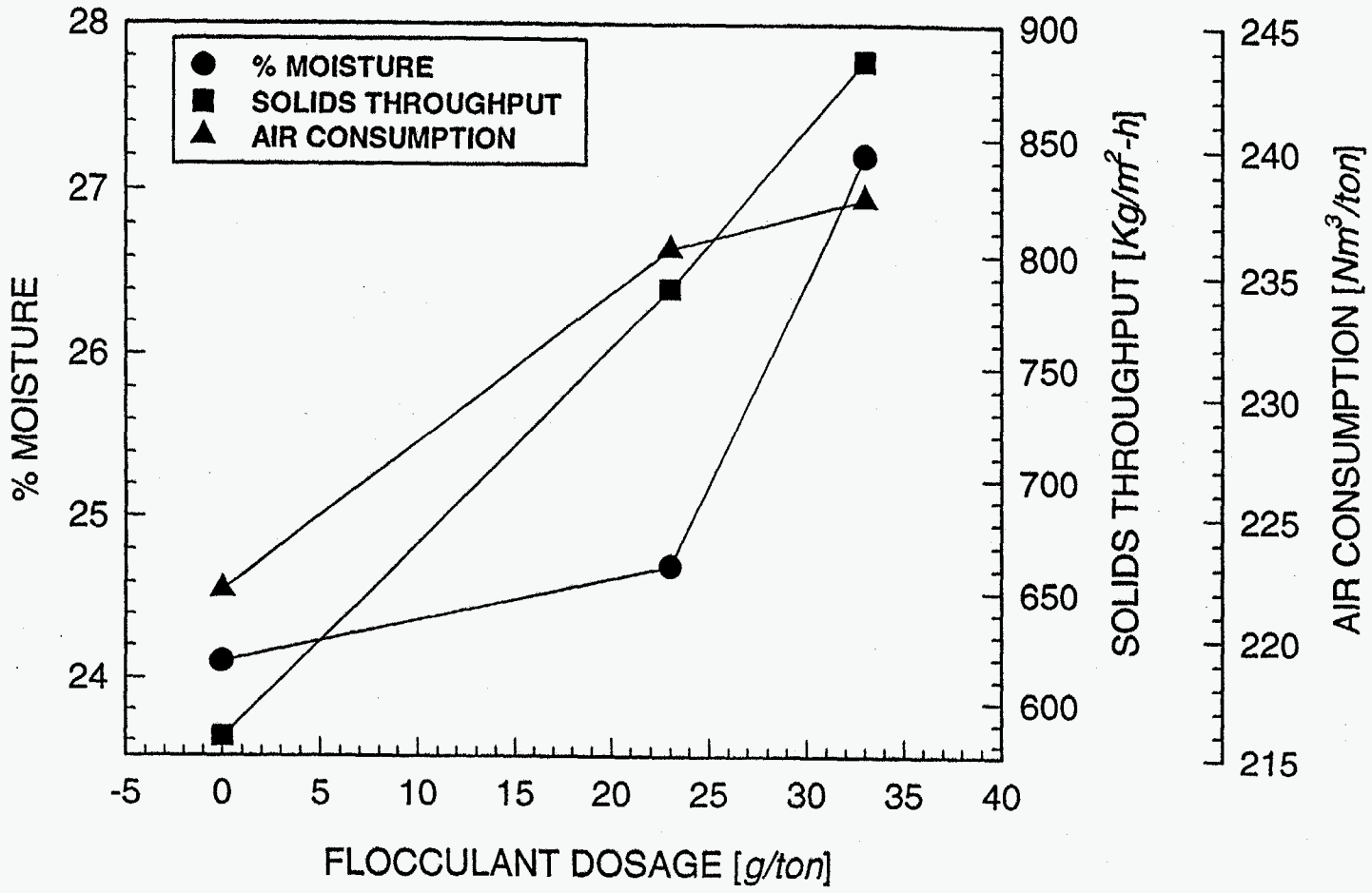

Figure 56. The effect of anionic flocculant (Nalco 9810) dosage on dewatering of the Pittsburgh seam froth product (CFA = 165°, pressure = 3.5 bar).

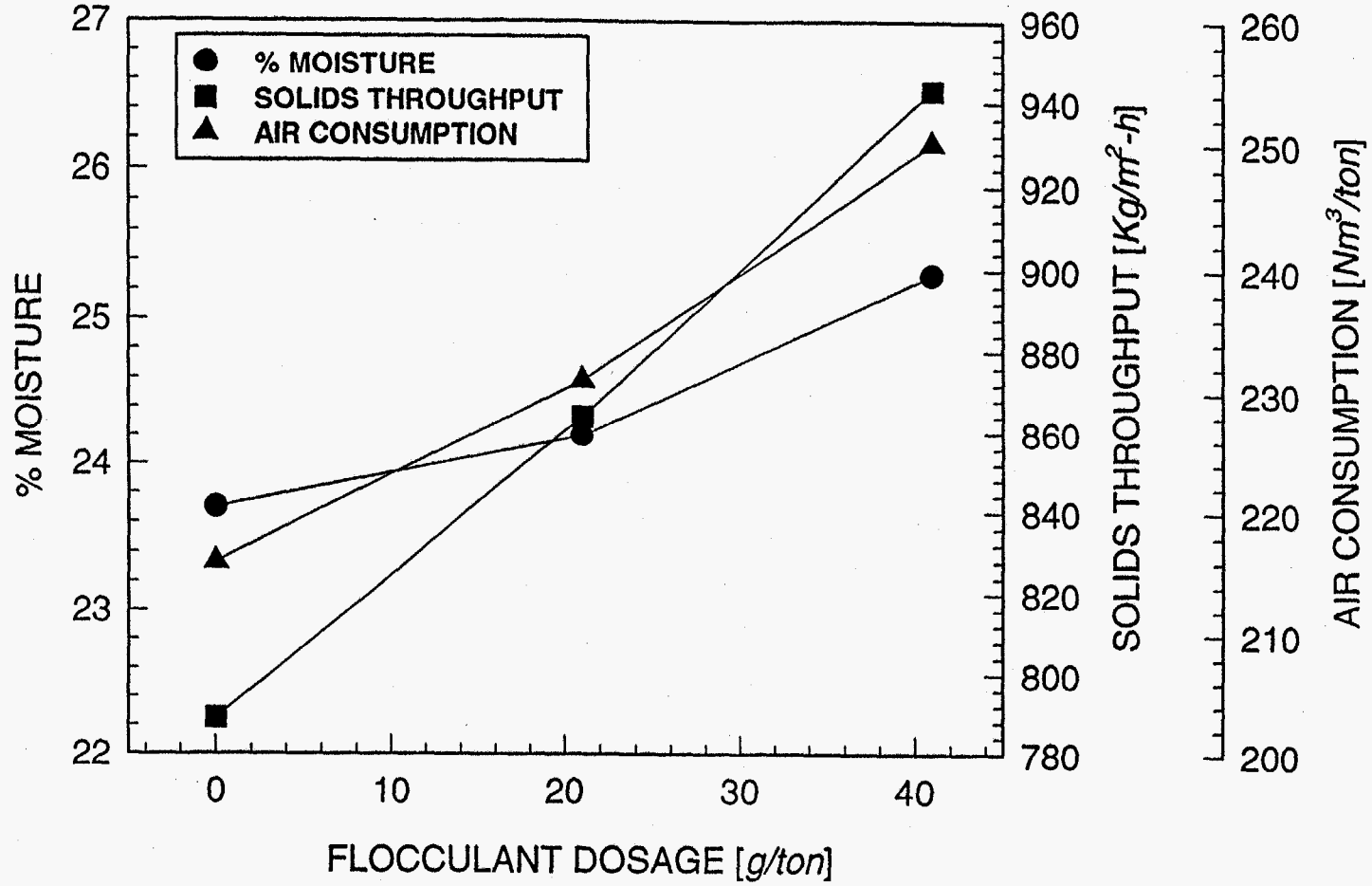

Figure 57. The effect of the anionic flocculant dosage on the dewatering of the Pittsburgh seam froth product (CFA = 165°, pressure = 5.0 bar).

figures show that with increasing flocculant dosage all the three resulting parameters, i.e., filter cake moisture, solids throughput and air consumption, increased linearly with flocculant dosage. These data showed that addition of flocculant was detrimental to filter cake moisture.

Effect of a cationic surfactant (1-hexyl cetyl pyridinium chloride) dosage on dewatering of the froth product using 3.5 and 5.0 bar pressures, is shown in Figures 58 and 59, respectively. These data show that the cationic surfactant was effective in lowering the filter cake moisture from 24 to 21 percent, at about 800 g/t dosage of the reagent. The data obtained using 5.0 bar pressure showed similar moisture reduction, using 800 g/t of the surfactant, however, solids throughput at 5.0 bar pressure was 711 Kg/m^2-hr (147 lb/ft^2-h) compared to 539 Kg/m^2-h (111 lb/ft^2-h) obtained at 3.5 bar pressure.

In the laboratory dewatering studies, it was shown that classifying the flotation feed at 200 or 400 mesh and filtering the oversize and undersize material separately and on combining the filtered product, the final moisture was significantly lower. At the Pittsburgh seam coal preparation plant, a 4-in. diameter cyclone was used for classifying the froth product by varying inlet feed pressure. Only the cyclone underflow was utilized for dewatering tests. Table XXI list the dewatering data of the deslimed froth feed conducted using 3 bar and 5 bar pressures. Note, that the filter cake moisture obtained using the two different pressures were very similar. Also note, that the classified slurries obtained using various the cyclone feed inlet pressure showed an increase in filter cake moisture from 21.6 to 24.6 percent as the feed inlet pressure to the cyclone increased from 10 psi to 20 psi. Particle size distribution of the classified material showed D_{50} of 35 μm compared to D_{50} of 24 μm for the unclassified feed slurry. Addition of flocculants did not provide any improvement in filter cake moisture, however, it did improve solids throughput.

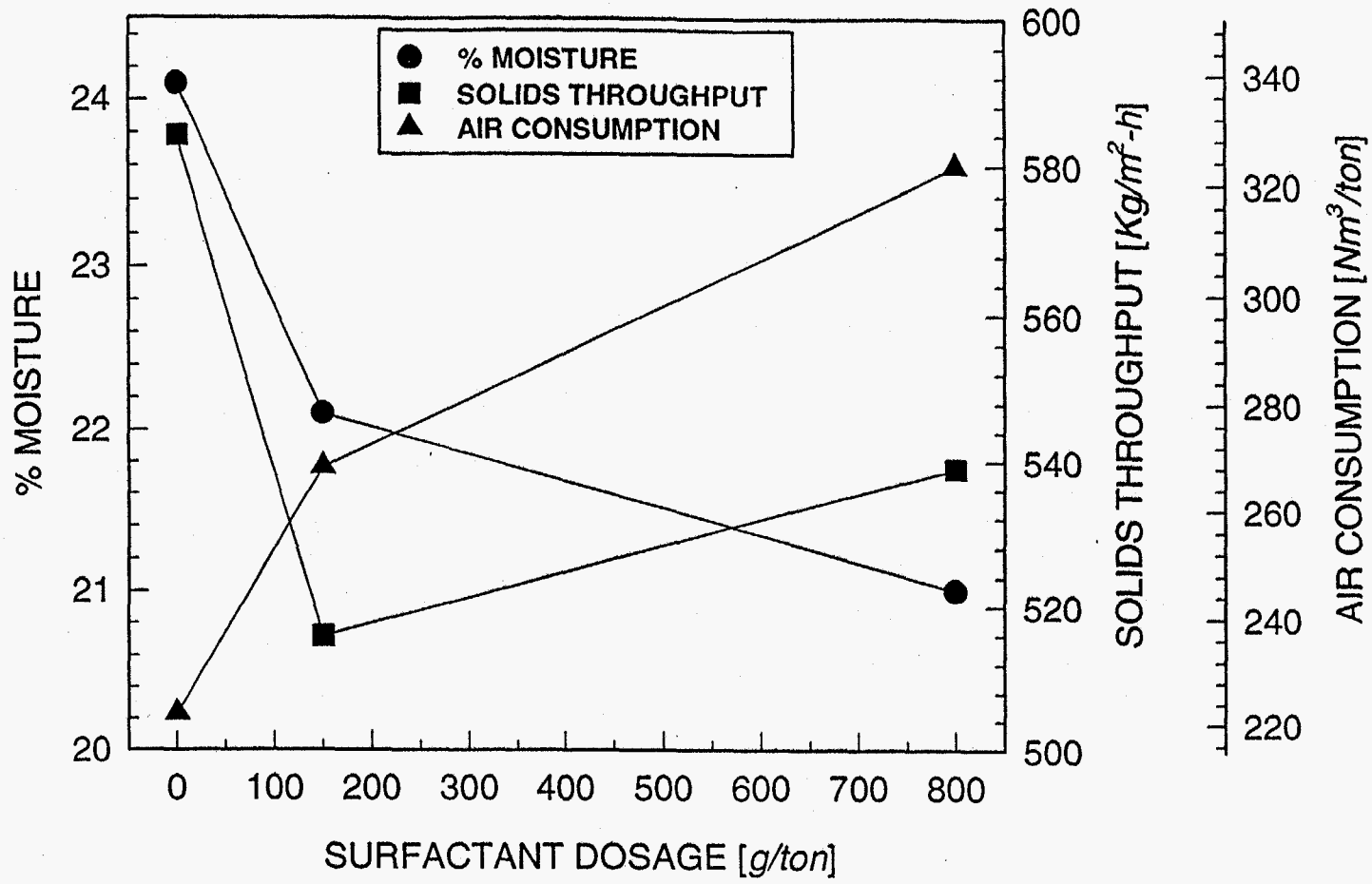

Figure 58. The effect of a cationic surfactant (Cetyl Pyridinium Chloride) dosage on dewatering of the Pittsburgh seam froth product (pressure = 3.5 bar).

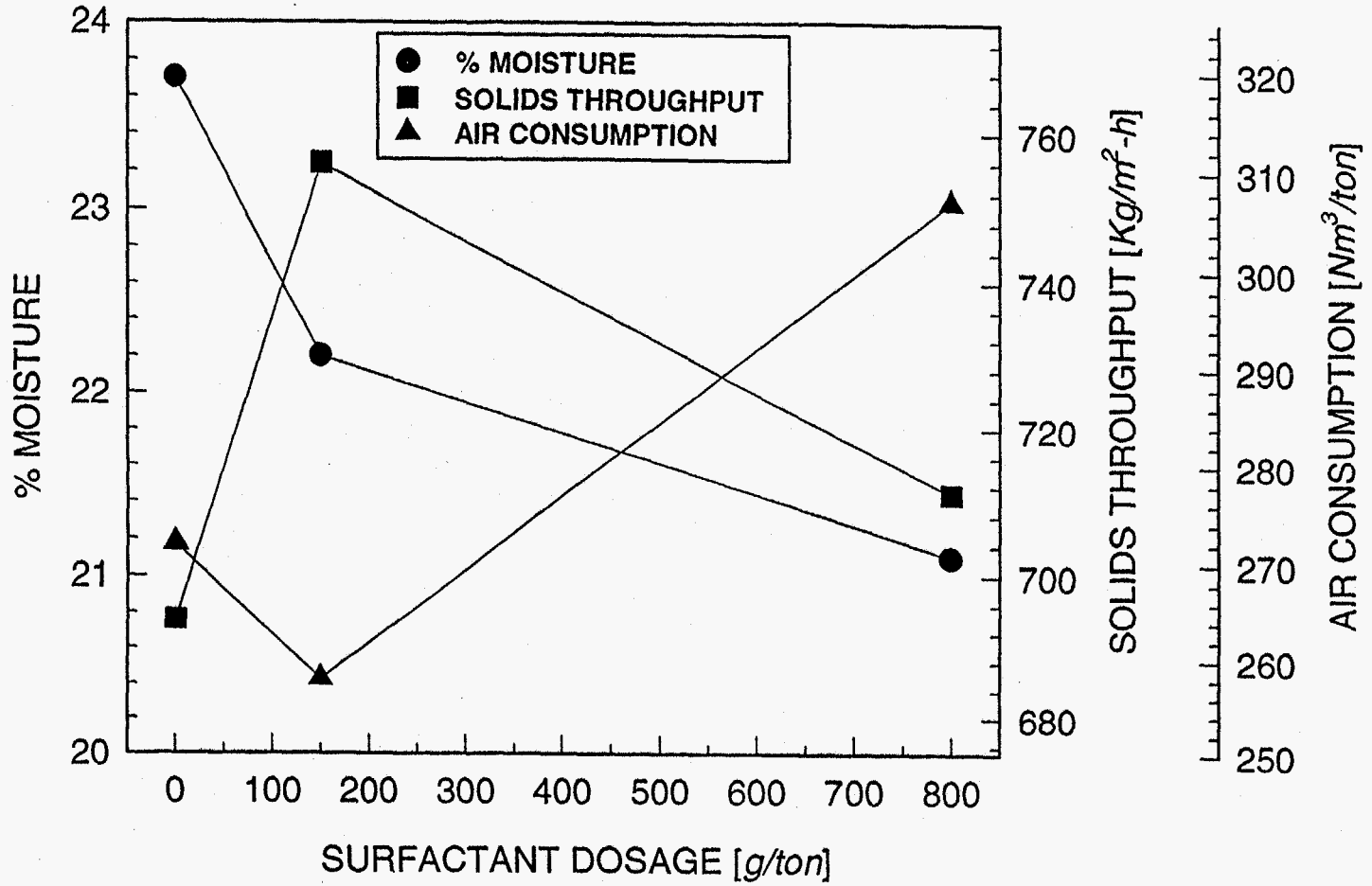

Figure 59. The effect of the cationic surfactant (CPC) dosage on dewatering of the Pittsburgh seam froth product (pressure = 5.0 bar).

Pocahontas No. 3 Preparation Plant Tests:

Particle size distribution of the Pocahontas No. 3 flotation product is shown in Table XXII. Note, that about 50 weight percent of particles are coarser than 100 mesh and only 24 percent are finer than 325 mesh. The ash content of clean coal slurry was 4.72 percent. Table XXIII lists test conditions utilized for the pilot plant tests with the Pocahontas product.

Figure 60 shows the effect of various pressure on dewatering of the Pocahontas No. 3 flotation product. It shows that increasing pressure from 2 to 5 bar the filter cake moisture decreased from 15.3 to 14.3 percent; solids throughput increased from 937 to 1368 Kg/m^2-h (194 to 283 lb/ft^2-h); and air consumption decreased from 123 to 57 Nm^3/t (65.4 to 30 scfm/t). Note, lowering of air consumption with increasing air pressure. This could be filter cake capillaries by fine particle present in this coarse size product.

The effect of cake formation angle (CFA) on dewatering of the flotation concentrate using 5 bar pressure is shown in Figure 61. It shows that the filter cake moisture and solids throughput increased and air consumption decreased with increasing CFA. A 55° CFA was selected for the rest of the studies as it provided a low moisture filter cake.

The effect of anionic and cationic surfactant dosage is shown in Figures 62 and 63, respectively. The addition of anionic surfactant did not show any change in the moisture content of filter cake, but it was detrimental to solids throughput and air consumption. The addition of cationic surfactant lowered filter cake moisture from 13.4 to 12.4 percent as the surfactant dosage increased form 0 to 380 g/t. With increasing surfactant dosage solids throughput decreased from 1446 to 964 Kg/m^2-h (299 to 199 lb/ft^2-h), and air consumption increased from 104 to 121 Nm^3/t (55 to 65 scfm/t).

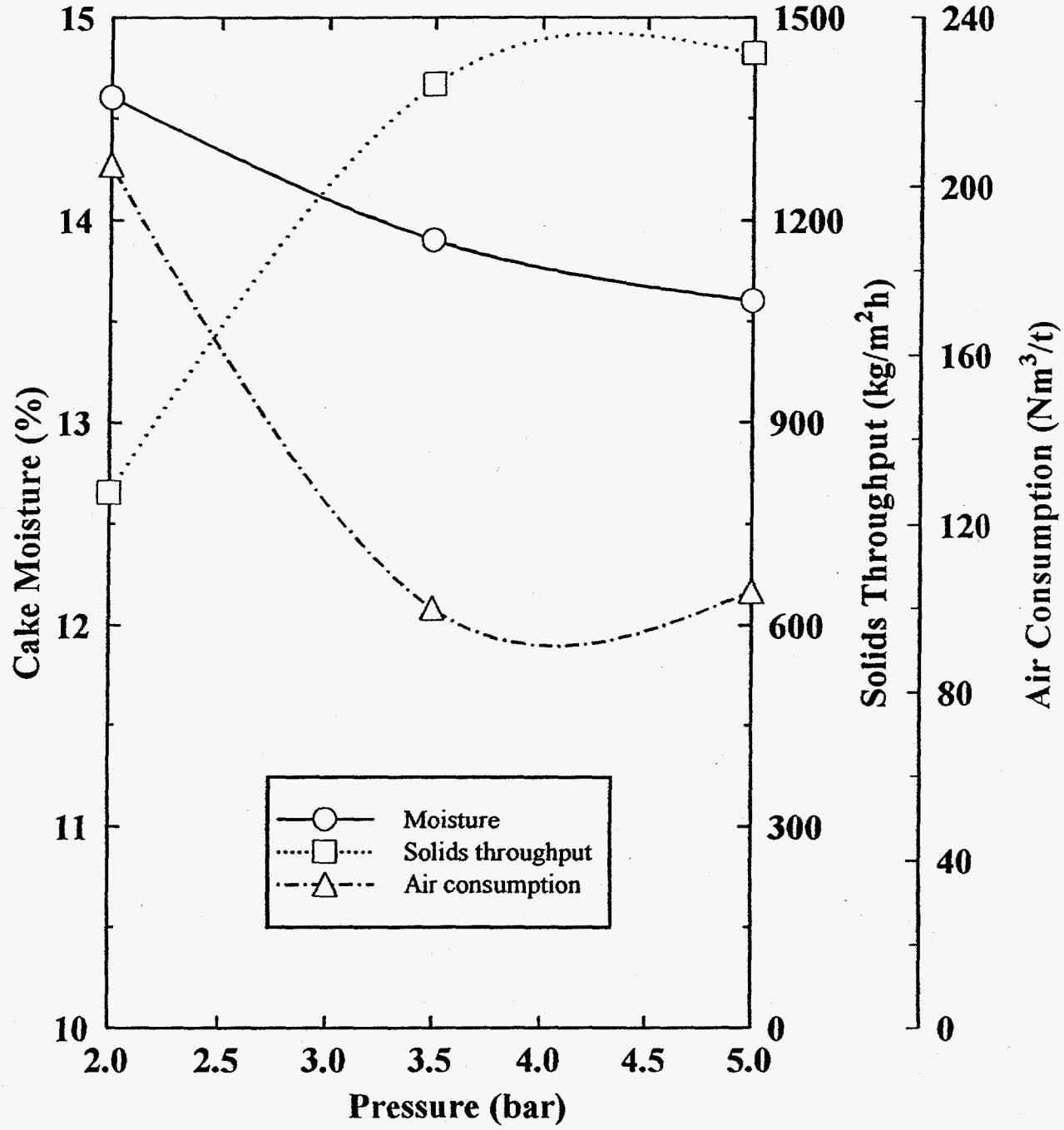

Figure 60. The effect of applied pressure on dewatering of the Pocahontas seam froth product (CFA = 55°).

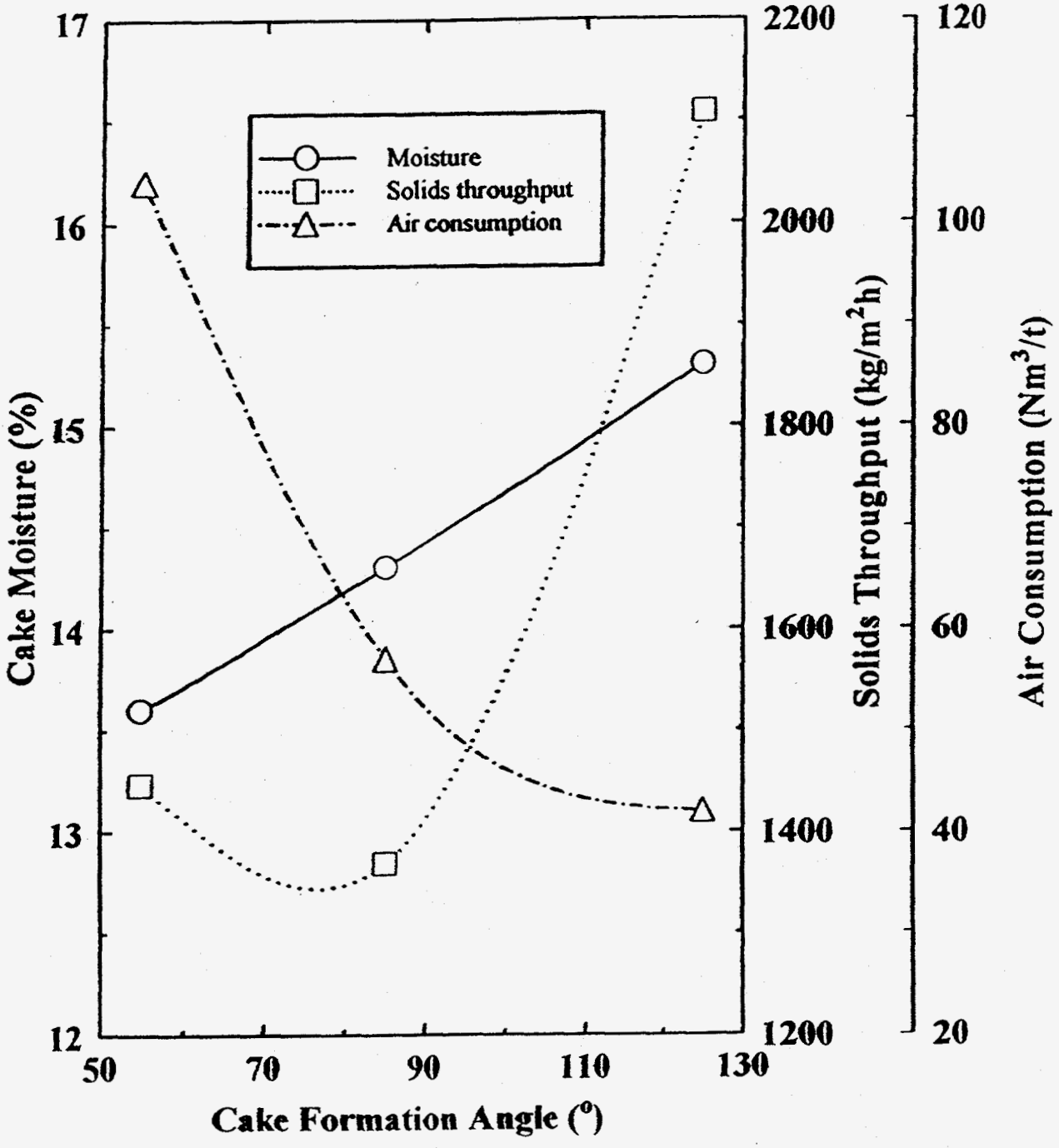

Figure 61. The effect of CFA on dewatering of the Pocahontas seam froth product (pressure = 5.0 bar).

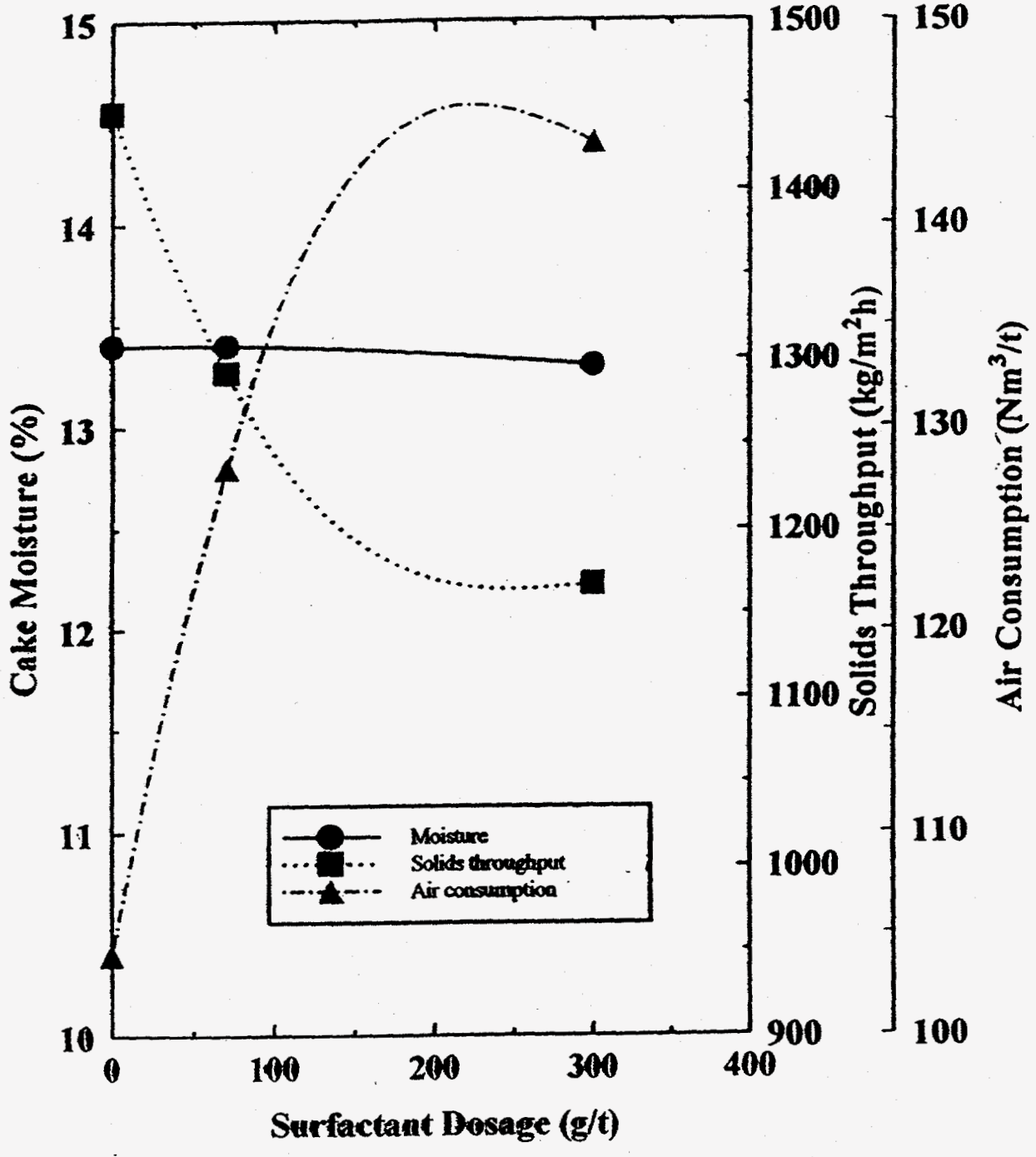

Figure 62. The effect of anionic surfactant (2-ethylhexyl sulfonate) dosage on dewatering of Pocahontas seam froth product (CFA = 55°, pressure = 5.0 bar).

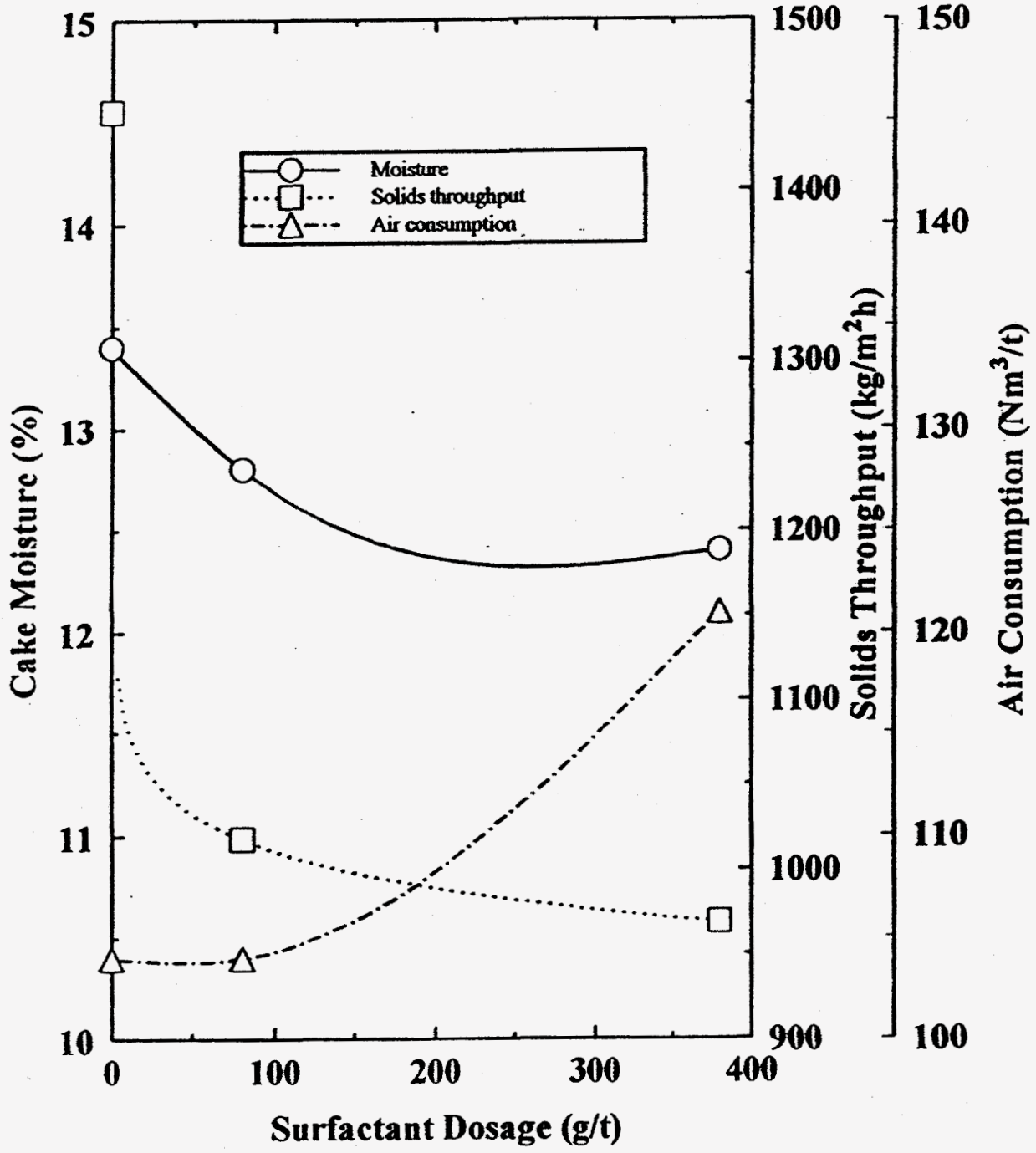

Figure 63. The effect of cationic (CPC) dosage on dewatering of Pocahontas seam froth product (CFA = 55°, pressure = 5 bar).

Table XXI. Dewatering Data of Deslimed Pittsburgh No. 8 Froth Flotation Product

Cyclone Feed Pressure (psi)	Reagent (g/t)	Filter Cake Moisture (%)	Solids Throughput (Kg/m^2-h)	Air Consumption (Nm^3/t)
		Pressure - 3.0 bar		
10	--	21.6	623	265
15	--	22.1	642	297
20	--	24.4	722	184
20	Nalco 8856, 170 g/t	22.8	779	204
20	Nalco 9810, 20 g/t	23.1	823	251
		Pressure - 5.0 bar		
10	--	21.6	674	264
15	--	23.0	723	258
20	--	24.6	676	215
20	Nalco 8856 (170 g/t)	22.3	823	291
20	Nalco 9810 (20 g/t)	22.1	927	221

Table XXII. Particle Size Distribution of Pocahontas No. 3 Flotation Product

Size (mesh)	Weight %	Cum. Weight %	Cum. Weight
28	4.87	4.87	4.87
28x48	20.73	25.60	25.60
48x100	25.60	51.20	51.20
100x200	17.47	68.67	68.67
200x325	7.73	76.40	76.40
-325	23.60	100.00	100.00
Head Ash	4.72%		

Table XXIII. List of Pilot Scale Dewatering Tests Conducted at the Pocahontas No. 3 Mine

A. Filter Feed

1. Experimental Design (15 Tests)
2. Anionic Flocculant Addition (5 Tests)
3. Cationic Surfactant Addition (5 Tests)
4. Anionic Surfactant Addition (5 Tests)
5. Other (1 Test)

B. Classified Filter Feed

1. Size, Pressure and Solids Content (5 Tests)
2. Anionic Surfactant and Cu^{+2} Ions (5 Tests)

Effect of addition of an anionic (Nalco 9810) flocculant dosage on dewatering of the flotation concentrate at 3.5 bar and 5.0 bar pressure is shown in Figures 64 and 65, respectively. Note, that in both cases, addition of flocculant increases filter cake moisture and solids throughput.

Deslimed Product:

A few dewatering tests were conducted on classifying cyclone deslimed material. Table XXIV tests the dewatering data on the deslime feed. Note, that deslime feed either mixed with or without reagents did not show any difference in the filter cake moisture. Even at high 5 bar pressure the filter cake moisture reduction was very small.

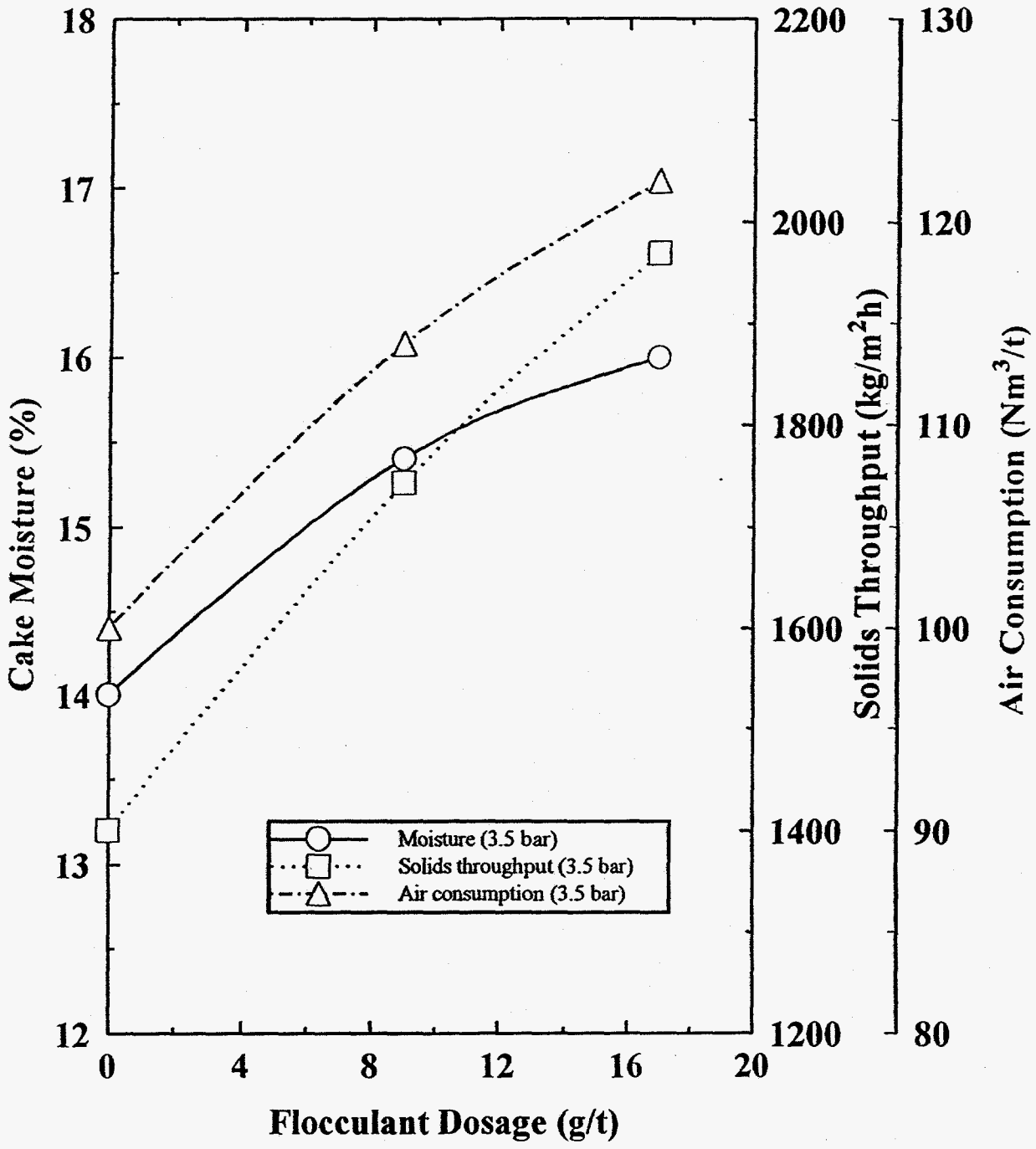

Figure 64. Effect of anionic flocculant (Nalco 9810) dosage on dewatering of Pocahontas seam froth product (CFA = 55°, pressure = 3.5 bar).

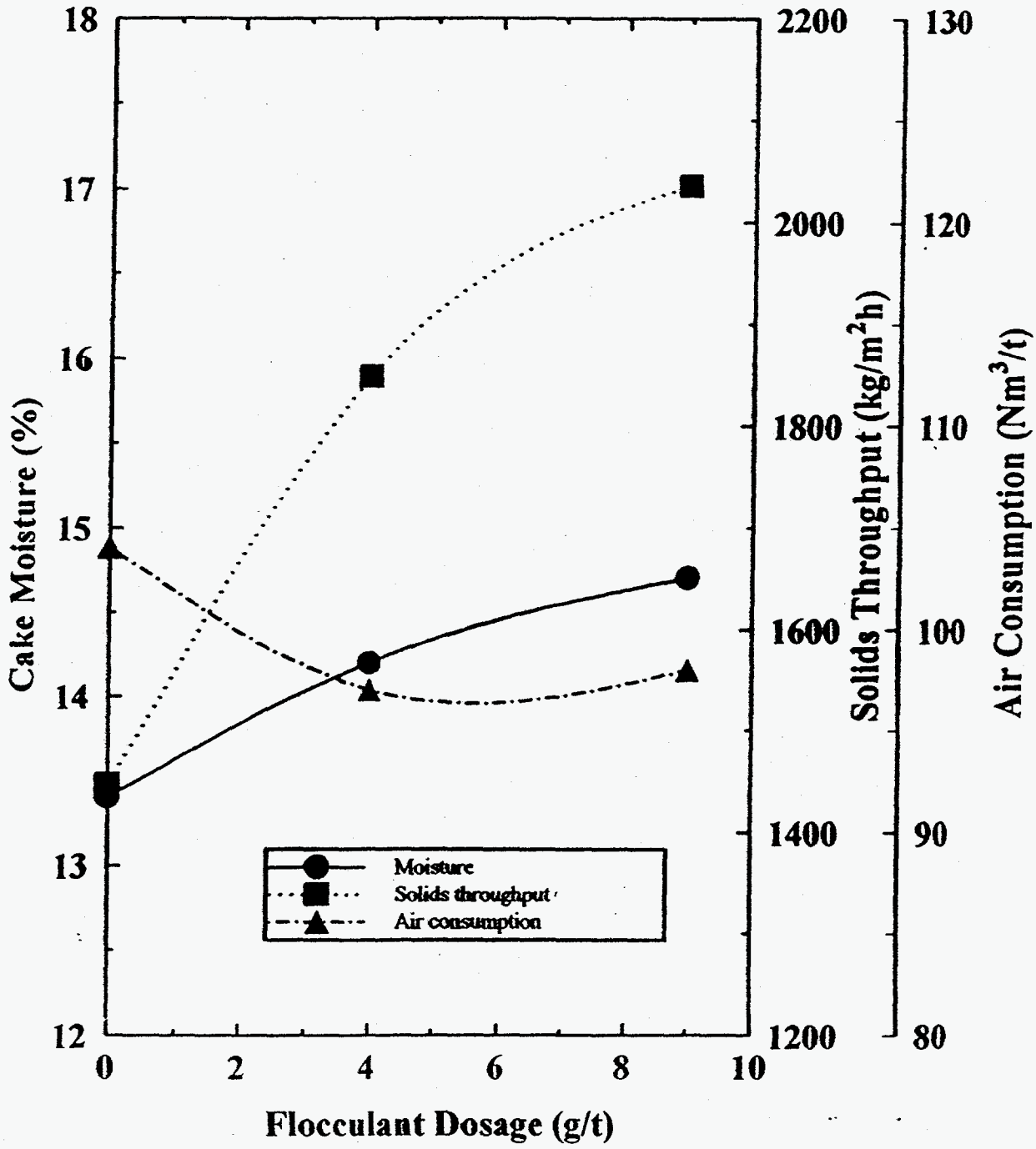

Figure 65. Effect of the anionic flocculant dosage on dewatering of Pocahontas seam froth product (CFA = 55°, pressure = 5 bar).

Table XXIV. Dewatering Data of the Deslimed Pocahontas No. 3 Flotation Product (CFA-85°, Pressure - 3.5 bar)

Reagents		Filter Cake	Solids	Air
Cu^{+2} (g/t)	Anionic Surf. (g/t)	Moisture (%)	Throughput (Kg/m^2h)	Consumption (Nm^3/t)
--	--	13.6	1389	70
--	--	13.9	2056	55
40	90	13.9	1104	140
40	270	13.7	1039	157
40*	90*	13.3	1242	125
40*	220*	13.1	1142	150

*5 bar pressure

SUMMARY

Generalized models for continuous hyperbaric filtration have been developed using the classical model for constant pressure filtration as a starting point. Specific models have been developed and evaluated for:

- cake formation and filter capacity
- cake dewatering: residual saturation and air consumption

Emphasis has been placed on the role of cake structure in the filtration process. Since detailed analysis of cake structure is only possible *post priori*, and by no means simple even then, we have concentrated primarily on the use of simplified structure models in which the pore structure in the cake is predicted from a knowledge of the characteristics of the feed particles.

It has been shown that the simplest structure model, in which pores are treated as a set of uniform capillaries with a single effective circular radius, cannot uniquely represent a pore size distribution. The distribution of pore sizes has a dominant effect on fluid (water or air) flow through the cake and on residual moisture content. Pore shape is also important but its effects appear to be less significant than those of size distribution. Our evaluation of shape effects suggest that it is probably reasonable, in most cases, to combine size and shape effects into a single distribution of effective pore radii.

Materials such as clean coal do not generally form compressible filter cakes, yet measured flow resistances show some attributes (e.g., pressure effects) of compressible cakes. We have proposed a binary packing model in which the finest particles in the feed (which may often be subject to agglomeration) form an inner, open-structured and potentially compressible layer within the main cake structure. Pressure effects and the role of flocculants, etc., can be ascribed to modifications of this layer.

While the major objective of this research program has been to investigate mechanical dewatering by hyperbaric filtration, the possible role of evaporation has also been evaluated. Based on a simplified model for evaporative dewatering, it has been concluded that this mechanism probably plays a negligible role under normal (i.e., ambient temperature) conditions. It could, however, be a principal mechanism at elevated temperatures, e.g., in steam filtration.

The laboratory dewatering study results for the Illinois No. 6, Pittsburgh No. 8, and Pocahontas No. 3 clean coal slurries are summarized in Figures 66, 67 and 68, respectively. For the Illinois slurry, the vacuum filtration provided a 24.8 percent moisture; whereas high pressure (60 psi or 4 bar) filtration provided 21.8 percent moisture filter cake. Addition of

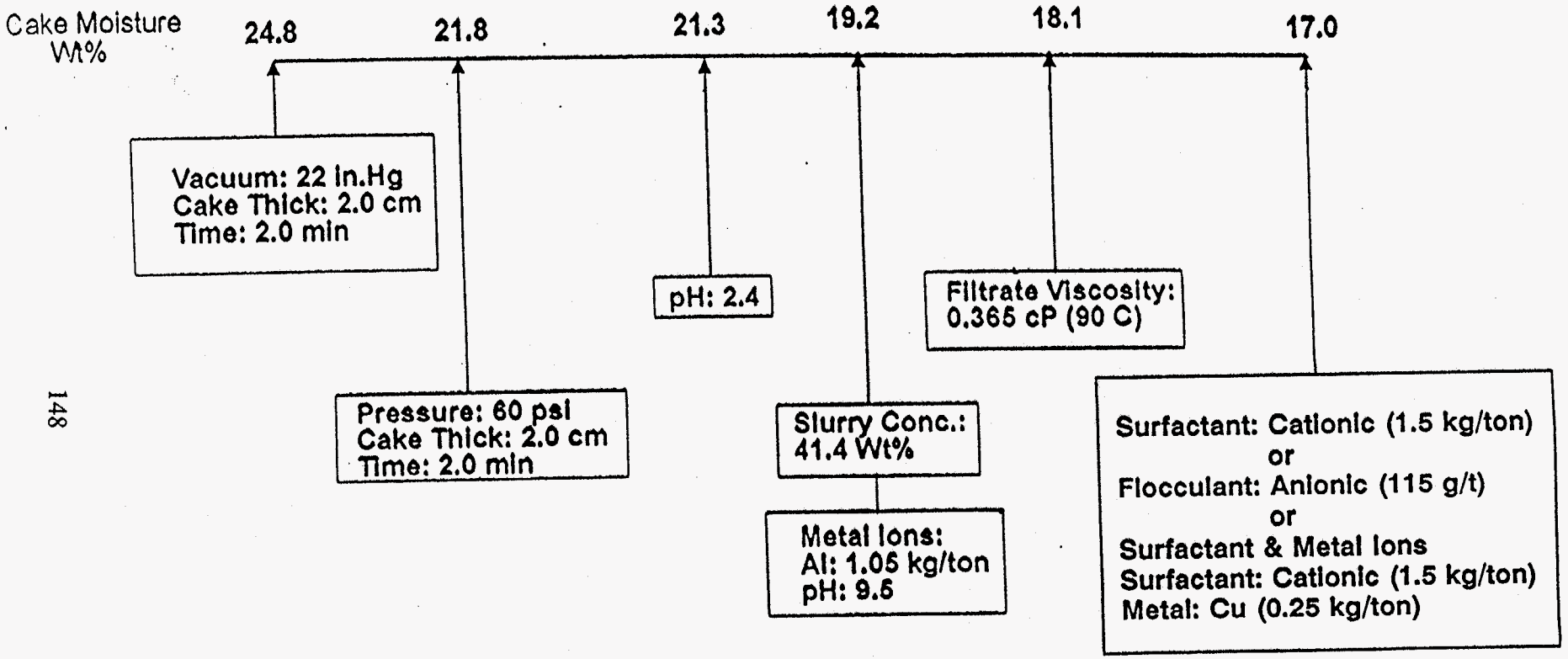

Figure 66. Summary of laboratory dewatering results for the Illinois No. 6 seam froth product.

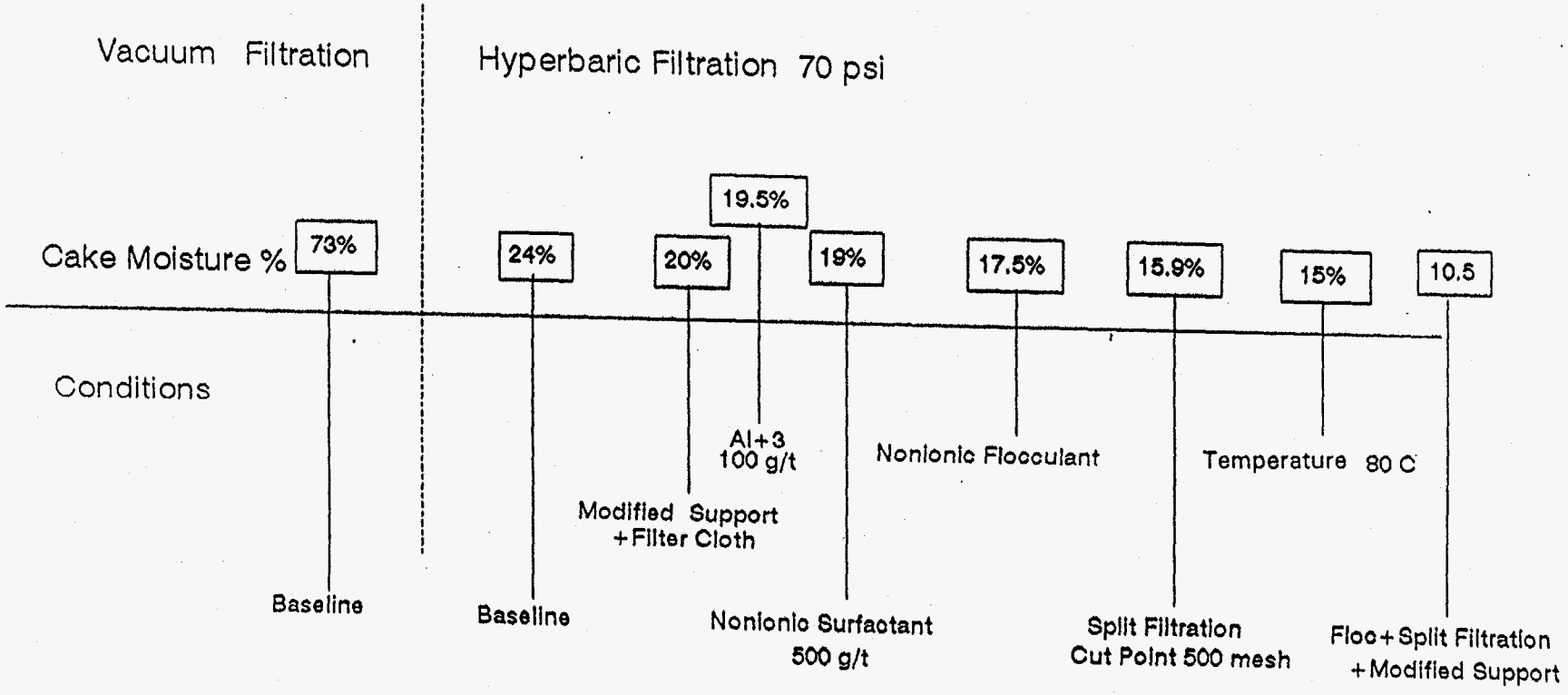

Figure 67. Summary of laboratory dewatering results for the Pittsburgh No. 8 seam froth product.

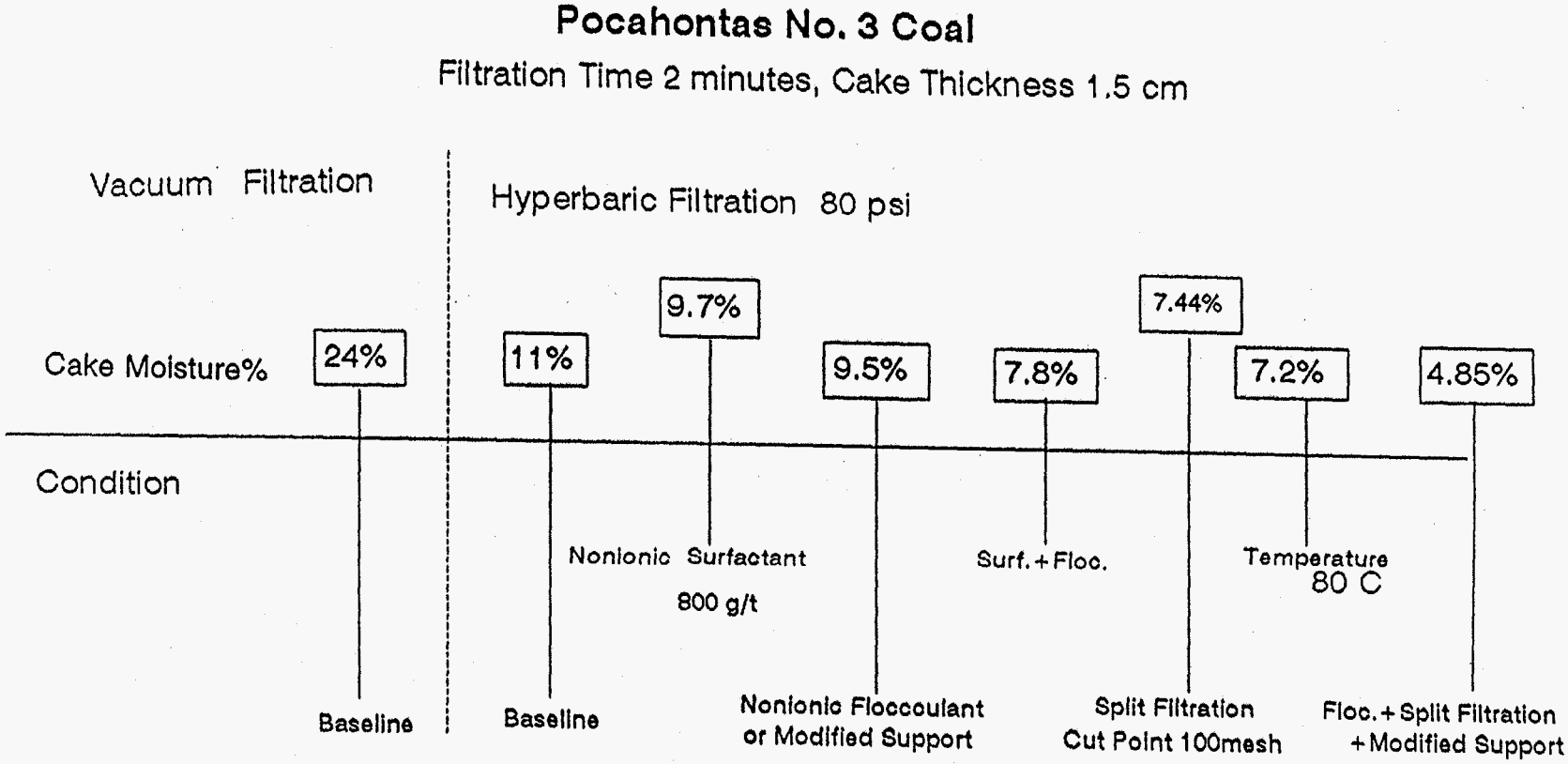

Figure 68. Summary of laboratory dewatering results for the Pocahontas No. 3 seam froth product.

either 115 g/t of an anionic flocculant, or 1.5 Kg/ton of a cationic surfactant provided the lowest 17 percent moisture in the filter cake, which is about 20 percent relative moisture reduction over that obtained with high pressure filter without addition of reagents and 31 percent relative moisture reduction over the filter cake moisture obtained using the vacuum filter.

For the Pittsburgh No. 8 coal slurry (Figure 67), the vacuum filter produces a 73 percent moisture product due to the very fine size particles, while the hyperbaric filter using 70 psi (4.8 bars) pressure reduces the moisture to 24 percent. The combined use of various types of enhancement approaches such as split size, addition of a flocculant and the modified filter support reduces the moisture to 10.5 percent. The final moisture reduction achieved is 56 percent over the baseline moisture obtained using the hyperbaric filtration alone. For the Pocahontas No. 3 coal slurry (Figure 68), vacuum filtration provides a 24 percent moisture product, which is close to that obtained in the preparation plants processing the Pocahontas No. 3 coal. Hyperbaric filter using 80 psi (5.5 bar) pressure reduces the moisture to 11 percent which is more than 50 percent relative moisture reduction. The use of the combined dewatering enhancement approaches (addition of a flocculantl, split size and modified filter support) reduces the moisture to as low as 4.85 percent, which is a 56 percent relative moisture reduction over the baseline moisture obtained using the hyperbaric filter and an 80 percent relative moisture reduction over the filter cake moisture obtained using the vacuum filter.

The HBF pilot-scale data can be summarized as follows:

- For the Pittsburgh No. 8 filter feed material, the HBF using 5 bar pressure and 165° cake formation angle will provide 16 percent moisture filter cake.

- Addition of flocculants increased the filter cake moisture. Addition of cationic surfactant showed only marginal reduction in filter cake moisture.
- For the Pittsburgh No. 8 froth flotation product, using 3.5 bar pressure and 85° CFA provided 20.5 percent moisture.
    - Addition of flocculant increased the moisture content of filter cake and increased solids throughput.
    - Using 800 g/t of the cationic surfactant lowered the filter cake moisture from 24 percent to 21 percent.
    - Desliming the feed using a cyclone provided 21.6 percent filter cake moisture.
- For the Pocahontas No. 3 flotation product, 5 bar pressure and 55° CFA provided filter cake with 13.5 percent moisture.
    - Addition of flocculant increased the filter cake moisture.
    - Addition of about 380 g/t of the cationic surfactant lowered the filter cake moisture from 13.4 to 12.4 percent.
    - Desliming of feed did not provide any reduction in moisture of the filter cake.

In general, the HBF was effective in providing about 20 percent moisture filter cake for the ultrafine clean coal product. For the coarser size clean coal product HBF was effective in providing filter cake with about 13 percent moisture.

A comparison of the laboratory and pilot-scale testing is given below.

Comparison of Lab and Pilot-Scale Results
for the Pittsburgh No. 8 and Pocahontas No. 3 Seam Froth Flotation Products

Seam	Pittsburgh #8	Pocahontas #3
Lab Results		
Pressure, psi	60-70	70-80
Presssure, bar	4.2-4.8	4.8-5.5
Cake Thickness, (cm)	1.5	1.4
Cake Moisture, (%)	24	11-12
Pilot-Scale Results		
Pressure, (psi)	60.9	72.5
Pressure, (bar)	4.2	5
Cake Moisture, (%)	22-23	14
Throughput, ($Kg/m^2.h$)	103	283
Air Consumption, (scfm/tph)	202	30
Air Consumption, Nm^3/t	380	57

These data show that the testing parameters identified and results obtained in the laboratory were very close to that obtained in the pilot-scale studies.

The mathematic model developed and applied to real system showed that the predicted versus the actual moisture content of filter cakes obtained at various pressures were very close. Similarly, the air consumption value in general were close to predicted value. However, model was unable to explain lower air consumption usage for coarser particle compared to high air consumption by fine particle filter cake.

RECOMMENDATIONS

Based on the results obtained for the project, the following recommendations are offered:

- Hyperbaric filter pilot plant tests should be conducted with column flotation product which has an average particle size of 25 microns.
- Continuous hyperbaric filter tests should be conducted at a mine for 7 to 15 days to obtain technical and economic data.
- Studies should be conducted to understand the higher air consumption with finer size compared to coarser size material.

REFERENCES

1. Harrison, C.D. and J.R. Cavalet, "High-G Centrifuge Test Results -- Fine Coal Dewatering", SME Meeting, Albuquerque, NM, Oct. 17 (1985).
2. Tschamler, H. and E. Ruiten, "Physical Properties of Coals", Chemistry of Coal Utilization, (Lowry, H., Ed.), John Wiley, pp. 35 (1963).
3. Parekh, B.K. and A.E. Bland, "Fine Coal and Refuse Dewatering - Present State and Future Consideration", Flocculation and Dewatering (B.M. Moudgil and B.J. Scheiner, Eds.), Engineering Foundation, pp. 383-398 (1989).
4. Dosoudil, M., "Continuous Pressure Filtration in the Coal Industry", Coal Prep '87, Lexington, KY (1987).
5. Smith, L. and T. Durney, "Proof of Concept and Performance Optimization of High Gravity Batch Type Centrifugal Dryer for Dewatering of Fine Coal", Final Report DOE Contract No. DE-AC22-89PC88885 (1991).
6. Barbulesclu, A., "The Shoe Rotary Press", Recent Advances in Solid/Liquid Separation, Battelle Press (1986).
7. Vickers, F., "The Treatment of Fine Coal", Colliery Guardian (1982).
8. Muralidhara, H.S., N. Senapati, and R.B. Beard, "A Novel Electro-acoustic Process for Fine Particle Suspensions", Advances in Solid/Liquid Separation, Battelle Press, Columbus, OH (1986).
9. Wakeman, R.J., "Cake Dewatering", Liquid-Solid Separation, L. Savarovsky (Ed.), Butterworth, London, pp. 297-306 (1977).
10. Keller, D.V., G.J. Stelma, and Y.M. Chi, "Surface Phenomena in the Dewatering of Coa' EPA 600/7-79-008 (1979).

11. Gala, H.B., S.H. Chiang, J.W. Klinzing, J.W. Tierney, and W.W. Wen, "Effect of Surfactant Adsorption on the Hydrophobicity of Fine Coal", Proc. of International Conference on Coal Science, pp. 260-263 (1983).

12. Silverblatt, C.E. and D.A. Dahlstrom, "Moisture Content of a Fine Coal Filter Cake", Ind. Eng. Chem. 46, pp. 1201-1207 (1954).

13. Nicol, S.K., "The Effect of Surfactants on the Dewatering of Fine Coal", Proc., Aust. Inst. Min. Metall. 260, pp. 37-44 (1976).

14. Pearse, M.J. and A.P. Allen, "The Use of Flocculants and Surfactants in the Filtration of Mineral Slurries", Filtration and Separation, 20, pp. 22-27 (1983).

15. Wang, S.S. and M.E. Lewellyn, U.S. Patent 4,153,549 (1979).

16. Wang, S.S. and M.E. Lewellyn, U.S. Patent 4,097,390 (1978).

17. Quinn, J.E., L.S. Wittenbrook, and C.E. Donogan, U.S. Patent 4,156,649 (1979).

18. Gray, V.R., "The Dewatering of Fine Coal", J. Inst. Fuel, 31, pp. 96-108 (1958).

19. Dolina, L.F. and U.S. Kominski, Coke and Chemistry, UUUR, No. 10, p. 16 (1971).

20. Rosen, M.J., "Relationship of Structure Properties in Surfactant III. Adsorption at Solid-Liquid Interface from Aqueous Solution", J. Am. Oil Chem. Soc. 52, pp. 431-435 (1975).

21. Brooks, G.F. and P.J. Bethell, "The Development of a Flotation/Filtration Reagent System for Coal", Proc. of 8th Intl. Coal Prep. Cong., Paris (1976).

22. Ehlert, G.W., "Hyperbaric Pressure Filtration: Innovation Technology for Dewatering Fines", Coal Prep '91, Lexington, KY, pp. 185-198 (1991).

23. Wen, W.W., H. Cho, and R.P. Killmeyer, "The Simultaneous Use of a Single Additive for Coal Flotation Dewatering and Cake Hardening", Processing and Utilization of High Sulfur Coals V, B.K. Parekh and J.G. Groppo (Eds.), pp. 237-249 (1993).

24. Wilson, W.W., "Ultrafine Coal Single Stage Dewatering and Briquetting Process", ICCI Project No. 94-1/1.1A-2P (1994).

25. Chiang, S.H. and D. He, "Filtration and Dewatering: Theory and Practice", Fluid/Particle Separation Journal.

26. Klotz, K., "Zur Laminarstronmung in einem rohr mit der Querschnittsform eines Kreibogendreiecks", Zeitschrift fuer Angewandte Mathematik and Mechanik, Vol. 67, No. 6, pp. 249-256 (1987).

27. Neese, Th. and M. Fahland, "Model Calculations for Porosity, Pore Size Distribution and Flow Resistance in Filter Cakes", Aufbereitungs Technik, Vol. 35, No. 3, pp. 117-124 (1994).

28. Adamson, A.W., "Physical Chemistry of Surfaces", 5th Ed., Pub. J. Wiley and Sons, NY (1990).

29. Rootare, H.M., J.M. Powers, and R.G. Craig, J. Dental Res, Vol. 58, p. 1097 (1979).

30. McCabe, W.L., J.C. Smith, and P. Harriott, "Unit Operations of Chemical Engineering", 5th Ed., McGraw-Hill, Inc. (1993).

31. Wakeman, R.J., Filtration Post-Treatment Process, Elsevier (1975).

32. Ruethrwein, R.A. and D.W. Wad, "Principles of Flocculation Using Polymers", Soil Science, 73, p. 485 (1952).

33. Parekh, B.K., "The Role of Hydrolyzed Metal Ions in Charge Reversal and Flocculation Phenomena", Ph.D. Thesis, The Pennsylvania State University (1979).

34. Groppo, J.G., "The Role of Metal Ions and Surfactants in the Dewatering of Ultra-Fine Clean Coal", Ph.D. Thesis, University of Kentucky (1992).

LIST OF SYMBOLS

Roman

A = area of cross section of cake

A_f = area of cross section for the fines in the fines/coarse bed

A_{ijk} = area of arched triangle

A_l = area of liquid surface per unit area of cake element

c = mass of solids in cake per unit mass of liquid in filtrate

c_f = mass fraction of solids in filtrate

c_s = mass fraction of solids in feed

c_v = mass of solids per unit volume of liquid in filtrate

f_e = fraction of cycle available for evaporation

$f_0(r)$ = number distribution of pore radii

$f_0(R)$ = number distribution of dimensionless pore radii

$f_0(x)$ = number distribution of particle sizes

$f_3(x)$ = volume distribution of particle sizes

$F_3(x)$ = cumulative particle size distribution given by the Schuhmann function

g_{ik} = functional form given by equation 22

G_{ijk} = shape factor as defined by equation 21

J_n = net flux of water due to evaporation

J_r = relative removal rate of water

k_a = permeability of cake to air

k_e = evaporation rate constant

k_p = constant to relate pore radius to particle radius defined by equation 74

k_w = permeability of cake to water

k_t = tortuosity factor

K = permeability of cake

K_m = medium permeability

K_r = relative permeability (k_a/k_w)

K_s = Schuhmann size modulus

K_1 = constant given by equation 102

K_2 = constant given by equation 103

K_3 = constant given by equation 104

m_w = viscosity of water

m_{sc} = mass of dry solids in cake

m_{wf} = mass of liquid collected in filtrate

M = moisture content of cake

M_w = molecular weight of water

n = number of triangular pores for an equivalent hydraulic radius r_h

n_m = concentration of vapor in gas (moles/cc)

n_{mo} = equilibrium vapor concentration

n_{mI} = vapor concentration of incoming gases

N = rotational speed of disk filter

N_p = total number of pores

p = applied pressure

p_c = pressure drop across coarse bed only

p_{cap} = capillary pressure across a curved interface

p_f = pressure drop across fines/coarse bed

p_{ijk} = perimeter of arched triangle

$\overline{P}$ = mean pressure across cake

Q_a = volume flow rate of air across unit cross section of cake

Q_d = volumetric flow rate through a distributed pore system

Q_f = volume fraction of fine particles with $x < x_f$

Q_{rel} = relative flow rate through a distributed pore system relative to a single pore of radius r_h

Q_s = volumetric flow rate through a single pore of radius r_h

Q_{st} = volume flow rate of air across a unit cross section of cake expressed at a standard pressure

Q_w = volumetric flow rate of water across area of cross section A of cake

Q_{wd} = volumetric flow rate during cake dewatering

Q_{wf} = volumetric flow rate during cake formation

Q_o = volumetric flow rate through a pore of unit radius

r = pore radius

r_c = critical radius of curvature defined by equation 69

r_e = evaporation rate

r_h = mean hydraulic radius

r_{max} = maximum radius of all pores in cake

r_{min} = minimum radius of all pores in cake

r_s = radius of curvature of curved interface of liquid at contact with solid

R = dimensionless pore radius defined by equation 70

R_a = air consumption relative to cake throughput (defined by Equation 87)

R_g = gas constant

R_s = solids throughput per unit area of cake

S = residual cake saturation

S_v = specific surface area of bed

S_{vc} = specific surface area of coarse particles (x>xf)

S_{vf} = specific surface area of fine particle (x<xf)

t = time

t_d = displacement time

t_f = cake formation time

T = cycle time

T_o = temperature

u = superficial gas velocity

$\bar{v}$ = mean flow velocity of fluid in cake

V_c = cake volume

V_f = bulk volume of fines

V_p = total pore volume per unit cake thickness

V_{sf} = solid volume of fines

V_w = volume of water flowing across area of cross section A in time t

V_{wc} = volume of liquid in saturated cake

V_{wf} = volume of water passing into filtrate during cake formation

x = particle diameter

x_f = cut-off particle size

$y_{ij} = x_i/x_j$

z = thickness of an element of cake

Greek

α = specific cake resistance

$\bar{\alpha}$ = average specific cake resistance

α_b = overall specific cake resistance for a non-uniform binary packing model

α_m = filter medium resistance

α_{rel} = specific cake resistance relative to a single pore of radius rh

α_{Rel} = specific cake resistance for a non-uniform binary packing model relative to a uniformly packed bed

γ = interfacial tension of liquid

ε = average bed porosity

ε_c = porosity of the coarse particle bed

ε_f = porosity of fine particle bed

θ = contact angle between liquid and solid

θ_a = dewatering angle

θ_d = water displacement angle

θ_f = cake formation angle

λ = cake thickness

λ_c = thickness of the coarse particle bed only

λ_e = effective pore length (across bed) related to bed thickness through a tortuosity factor, k_t

λ_f = thickness of the fines layer in the coarse bed

λ_m = medium thickness

μ_a = viscosity of air

μ_w = viscosity of water

ρ_s = density of solid particles in cake

ρ_w = density of water

σ = standard deviation for $f_0(r)$

ϕ_i = functional form given by equation 24